UiT
NORGES
ARKTISKE
UNIVERSITET

Department of pharmacy

Development of self-eliminating linkers for drug conjugates

—

Silje Lillemark Nergård

Master thesis in Pharmaceutical sciences, May 2018

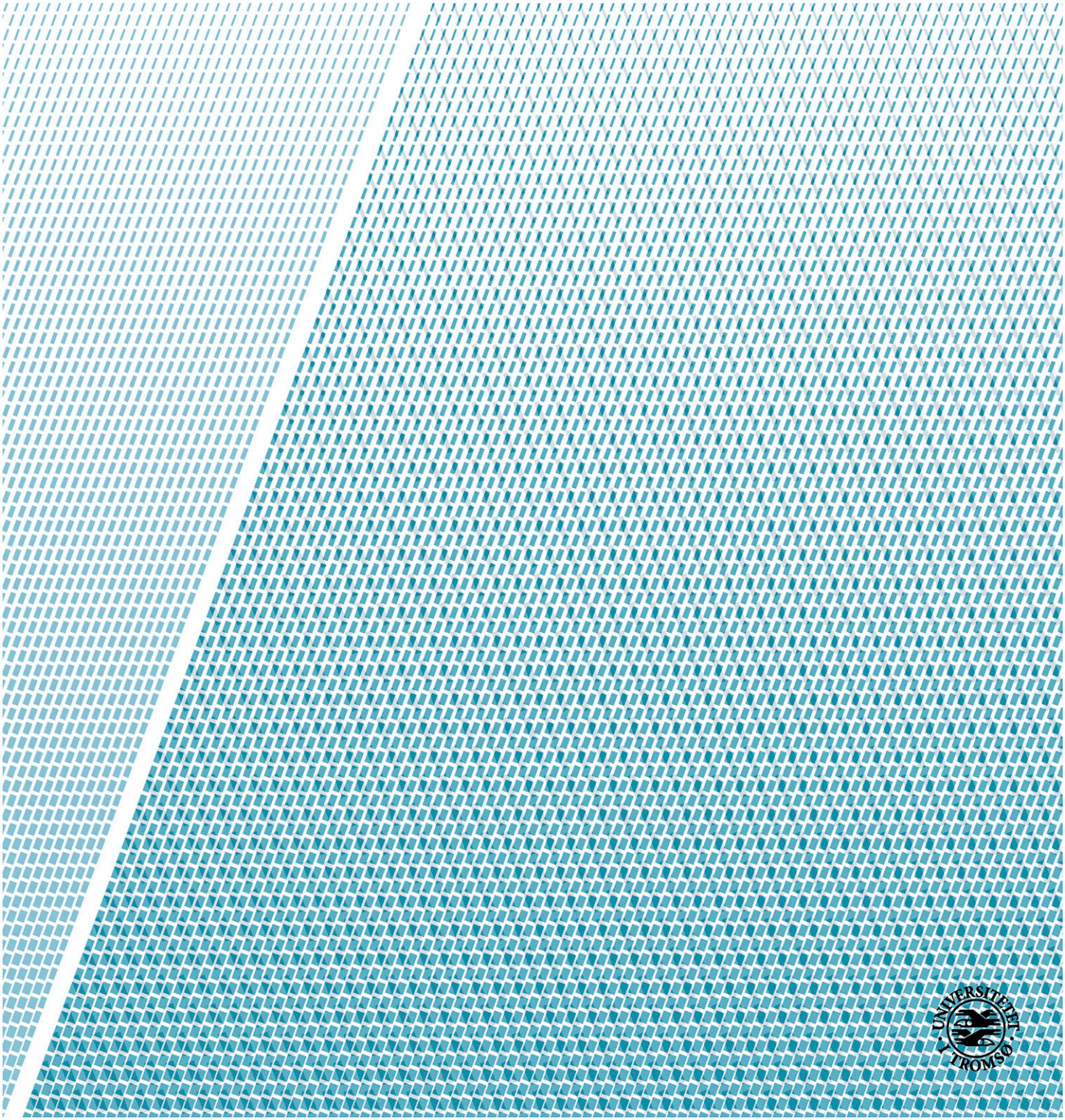

Acknowledgements

This master thesis was performed in the laboratorial facilities of Barents Biocentre, at Norut and the Department of Pharmacy, Arctic University of Norway in Tromsø. Internal supervisor of the project was Associate Professor Terje Vasskog, and Dr. Myagmarsuren Sengee was external supervisor.

I would like to express my gratitude towards Terje Vasskog for all his help and guidance these past ten months. Thank you for introducing me to this thesis. Myagmarsuren Sengee, your tutoring inside and outside of the lab has been of great value to me.

I would also like to express my gratitude towards my family and friends for lifting my spirits when times have been hard. Thank you mum, for listening to all my complaints and supporting me.

At last, I would like to show appreciation to red wine and NOCCO for giving me the strength and energy to write this thesis.

Abstract

Newly discovered compounds through bioprospecting are screened for cytotoxicity, and many of them are found to be highly toxic. Because they are often not specifically toxic only against cancer cells, they are not further studied. These new compounds could be of further interest by temporarily masking a functional group which regulate the anticancer activity of a cytotoxic compound. This means that the compound would be inactive until the effect is restored. A linker is used to chemically modify the functional group which facilitates the cytotoxic effect. In this project the linker connects the drug to a peptide, which would act as a homing beacon to a desired target site. To release the drug, the linker self-eliminates through mediation of glutathione (GSH).

Synthesis of linkers were performed by nucleophilic reaction. The linkers were conjugated with a peptide and two different drugs. The peptide conjugation was achieved by disulphide exchange reaction and the conjugation of drug was accomplished by nucleophilic reaction. The purity of the products were estimated with ultra-high performance liquid chromatography with a photodiode array detector (UPLC-PDA) and the mass was determined by mass spectrometry (MS). Kinetic analyses with GSH were performed on all three of the synthesised drug-linker-peptide conjugates.

The syntheses of self-eliminating linkers with conjugation to hydroxyl- and amine-containing drugs, and a peptide as homing beacon were successful. Kinetic analyses followed with UPLC-PDA and MS showed free drug from only two of the three drug-linker-peptide conjugates. The two drug-linker-peptide conjugates had very different estimation of drug release, where one showed 32% free drug after 20 h, and the other showed 5% free drug after 22.5 h.

Table of contents

1 Introduction

Cancer is a complex disease, where a combination of changes occur within a cell type over a period of time. There are many types of cancer, where these changes differ from type to type. Because of the challenges cancer presents, new compounds are emerging from bioprospecting activities and many of these compounds are screened for cytotoxic activity. Since many of the compounds are highly cytotoxic and not specifically toxic for cancer cells, they are not further studied. It is believed that by regulating the anticancer activity of certain cytotoxic drugs by temporarily masking certain functional groups, these new compounds can be of interest for further research. The inactive prodrug can be distributed within the body and is only active when it reaches its target, thereby restoring the anticancer activity. This means that by using highly toxic compounds or drugs, one may explicitly target the cancer cells. By using a linker to connect the drug to a peptide, one can mask the drug's activity and also release the drug at the target site.

1.1 Cancer therapy

A research project called the GLOBOCAN project aims to anticipate the incidence, mortality and prevalence of 28 cancer types in 184 countries. The GLOBOCAN 2012 estimated 14.1 million new cancer cases, 8.2 million cancer deaths and 32.6 million people living with cancer (within 5 years of diagnosis) in 2012 worldwide (1). In Norway, there were reported 32 827 cancer cases in 2016, which is a 1.2% rise from 2015. Cancer is described as a global burden and is increasing every year. The increase in Norway is largely due to an aging population (2).

Conventional cytotoxic chemotherapy has previously been, and still is to a high degree, fundamental in most treatment regimens for cancer. Conventional cancer therapy includes chemotherapy, radiotherapy and surgery, or a combination of these. Chemotherapy is antineoplastic drugs that kills all fast proliferating cells, which include cancer cells among others. Radiotherapy means using radiation to damage the DNA of all cells in that area. This therapy damages all normal cells and tissue in its path in addition to damaging tumour cells. With surgery, there is a risk in removing healthy tissue in addition to the tumour. Therefore more targeted therapy has and still is being developed. There are currently three main categories of targeted therapy against cancer. They

include small molecules, monoclonal antibodies (mAbs) and antibody-drug conjugates (ADCs) (3).

1.2 Prodrugs

Prodrugs are bioreversible derivatives which are inactive themselves. They undergo transformation *in vivo* to generate the active parent drug (4-6). Approximately 10% of the drugs approved on the market can be classified as prodrugs (5). The main objective of prodrug design is to mask undesirable drug properties, such as low water solubility, low absorption and membrane permeability, low targeted release, and high metabolism and side effects (4-6).

Prodrugs can be classified into carrier-linked prodrugs and bioprecursor prodrugs (4-6). Carrier-linked prodrugs can be described as the active drug being temporarily linked to a carrier group. The linkage is often a covalent bond and is broken *in vivo*. It is ideal if the release of the active drug takes place rapidly, and the carrier is non-toxic and non-immunogenic. The carrier should also be easy to synthesise (4, 5). The active drug molecule must have at least one functional group for which the carrier can attach. Preferred functional groups are hydroxyl or amino groups, which are altered to produce carrier-linked prodrugs with e.g. carbamate as the resulting functional group. The most common group of carrier-linked prodrugs is esters. The activation of the drug can occur by enzymatic or non-enzymatic cleavage of the temporary linkage. Approximately half of all prodrugs in market are activated by enzymatic hydrolysis (5, 6).

Bioprecursor prodrugs do not contain a carrier group, but is a result from molecular modification of the active drug. This generate a new compound which is transformed metabolically or chemically to the active drug *in vivo* (4-6).

1.3 Antibody-drug conjugates

Antibody-drug conjugates (ADC) are a novel class of drugs created by connecting monoclonal antibodies (mAbs) to specific drugs through linkers. Although previously mentioned as novel, the use of ADCs in animal models has been described in literature as early as the 1960s (7, 8). This type of therapy is today mostly used in oncology but has

tremendous potential in all targeted therapy. Specific antibodies are used to guide the payload to the tumour site by targeting tumour-specific antigens. ADCs can reduce potential side effects of highly toxic drugs compared to conventional anticancer therapy (3, 8-10).

The first ADC called gemtuzumab ozogamicin (trade name Mylotarg) was approved by U.S. Food and Drug Administration (FDA) in 2000 but was later withdrawn from market due to fatal cytotoxic side effects (3, 7, 8, 10). Over one hundred ADCs are in different stages of clinical development and trials, and two have acquired FDA approval. In 2011 brentuximab vedotin (trade name Adcetris) was approved by both FDA and European Medicines Agency (EMA), followed by trastuzumab emtansine (trade name Kadcyla) in 2013. Adcetris is currently used to treat relapsed or refractory Hodgkin lymphoma (HL) and systemic anaplastic large cell lymphoma (ALCL). Kadcyla's current medical indication is treatment of human epidermal growth factor receptor 2 (HER2) positive metastatic breast cancer (3, 7-12).

It is ideal if the target antigens are expressed abundantly and homogenously on the surface of the tumour cells but are absent from healthy cells. This is however not likely because an unknown antigen would trigger an immune reaction. Therefore, the optimal antigens would be expressed with a higher degree in tumour cells than in healthy cells. As such an optimal target would be localised on the tumour surface, be recognized by the antibody and has the ability of internalisation upon ADC binding (3, 7, 8, 11, 12). An appropriate mAb would have high binding affinity and specificity to the antigen on tumour cells, receptor-mediated internalisation, low immunogenicity and long systemic circulation time (3, 8, 11, 12). The cytotoxic payload needs to meet certain criteria as well, and currently there are three main types of cytotoxic drugs that are applied for the ADCs. These cytotoxic families are auristatins, maytansinoids and calicheamicins, all of which are too cytotoxic to use without conjugation (7, 8, 11, 12).

1.4 Peptide-drug conjugates

Peptide-drug conjugates (PDCs) are a novel class of prodrugs which is formed by conjugating a drug with a peptide through a linker. PDCs are designed based on the concept of ADCs, but have vastly different properties. ADCs consist of antibodies which,

in addition to have a high specificity for the corresponding antigen, can increase systemic circulation time and induce immunogenicity. Also, the antibody structure is large (often more than 100 kDa) compared to peptides. Peptides used for this purpose generally have a short length and consist only of a few amino acids. This should make them easier to synthesise and purify, they're biodegradable, and have little to no immunogenicity. Furthermore, the amino acid sequence can be customised to control physicochemical properties and to act as a homing beacon to a specific target located on tumour cell surfaces (13, 14).

There are two main types of peptides used for PDCs; cell penetrating peptides (CPPs) and cell targeting peptides (CTPs). CPPs are peptides that are capable to cross a cell membrane, while CTPs have specific binding affinity to a specific target. Because of the binding affinity, they can enrich a specific target site with an active pharmaceutical ingredient, which can reduce the drug distribution to other tissue and in turn reduce side effects (13). One of the differences between solid tumour and healthy tissue is the pH environment. In general, solid tumours have a more acidic extracellular environment. For example, the imidazole side chain of histidine has a pK_a value of 6.5 and is mainly uncharged at pH 7.4. Though in pH conditions lower than 5.5, most of the histidine molecules becomes cationic. Cancer cell membranes carry a more negative charge than normal cells which means that a histidine-rich peptide would have electrostatic attraction with cancer cell membranes, thus ensuring adherence (15).

A linker is necessary to connect the drug to the peptide. Linkers are commonly divided into non cleavable linkers and cleavable linkers. Non cleavable linkers are very stable due to conjugation with a carbon-, amide- or ether chain. This reduces the risk of unwanted drug release in blood circulation, thereby reducing the risk of side effects. Achievement of drug release from a non cleavable linker is dependent on full degradation of the antibody. The linker is still attached to the drug, and therefore this application works best with drugs that exert their effect in spite of being chemically modified by the linker (12).

Cleavable linkers can be divided into pH sensitive linkers, enzyme sensitive linkers and glutathione sensitive linkers. The pH sensitive linkers release the drug by hydrolyses of a bond sensitive to acids. There is an abundance of lactic acid produced by anaerobic glycolysis in tumour cells due to a rapid cell growth and metabolization. Enzyme sensitive linkers are peptides with a specific amino acid sequence which can be cleaved by

proteases. Proteases are normally not active extracellularly due to the presence of protease inhibitors, which makes the linker stable in plasma. Glutathione sensitive linkers are degraded by glutathione (GSH) which resides intracellularly in higher concentrations compared to extracellular environment (3, 7-9, 11-13).

Linkers should be stable in the blood stream to ensure no premature release of the cytotoxic drug, but must also be able to release the drug efficiently upon internalisation to guarantee a high enough concentration to impose cell death (3, 7, 11, 12). Many second generation ADCs have linkers with a maleimide group conjugated with lysine or cysteine, which have shown to be instable in systemic circulation resulting in off-target cytotoxicity (7).

1.5 Glutathione

Glutathione is composed of three amino acids; cysteine, glutamine and glycine. It is found in two forms, reduced and oxidised. Reduced glutathione (GSH) consists of a single glutathione molecule and is the active form. When two reduced glutathione molecules are oxidised and lose electrons, they can form what is known as oxidised glutathione or glutathione disulphide (GSSG). Glutathione reductase transforms oxidised glutathione back to its active form. GSH is also called a scavenger, neutralising reactive oxygen species such as peroxide and superoxide anions which are toxic and damaging to cells (16). The ratio between GSH and GSSG is dependent on cell type and redox stress, and varies from 100:1 to 1000:1, respectively (17). There has been shown a decrease in the ratio in human blood with various diseases, where cancer is amongst the described illnesses (18). In some cancer types such as breast and lung, there is a tendency for increased GSH levels in comparison to healthy tissue. Although, some cancer types show an increase of GSH levels, other types such as brain and liver tumours demonstrate a decrease. In addition to both increased and decreased GSH levels depending on the kind of cancer, other cancer types show no clear trend (19).

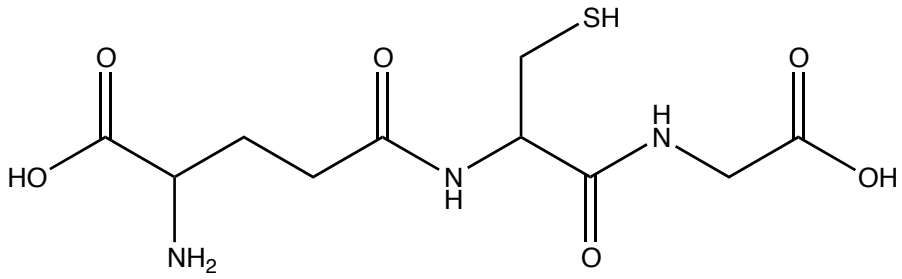

Figure 1.1. Reduced glutathione

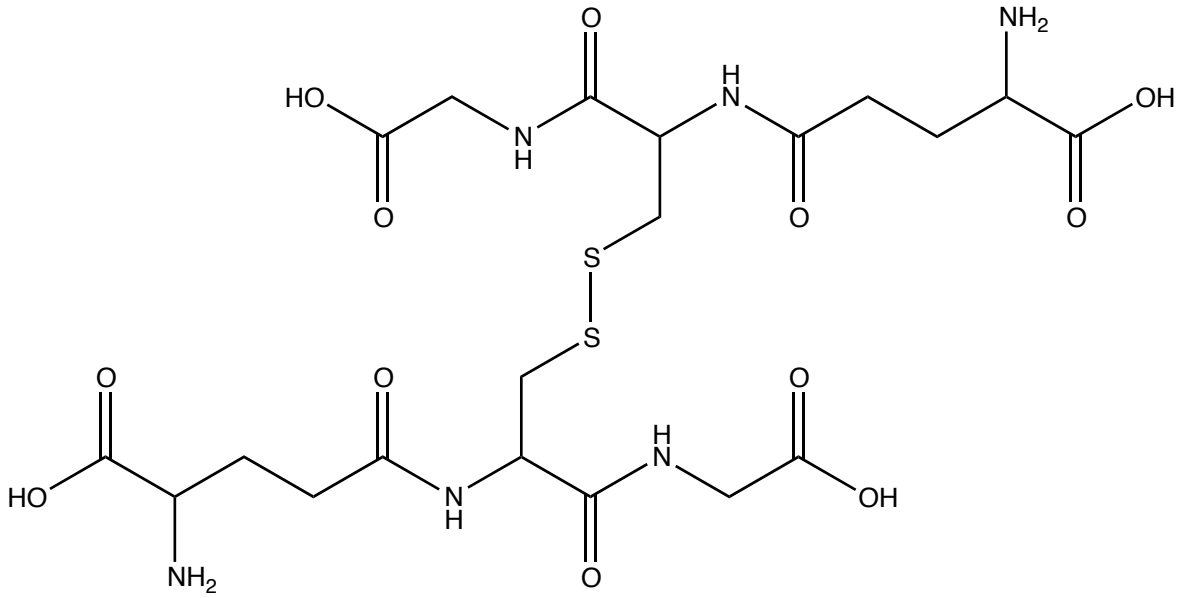

Figure 1.2. Oxidised glutathione

As mentioned earlier, glutathione sensitive linkers are designed to take advantage of the difference in intracellular contra extracellular glutathione concentration (8). Intracellular concentrations are a thousand times higher than extracellular, where concentrations normally range in the millimolar (mM) versus micromolar (μM), respectively (8, 13). This means that the disulphide bond of the linker can be efficiently cleaved inside the cell. Cysteine and albumin in serum contain thiol groups which theoretically can interact with the disulphide bond to the linker, but concentrations are low, and thiols in albumin are inaccessible to disulphide exchange reaction. Therefore, reduction of the bond in systemic circulation is unlikely.

Steric hindrance of the disulphide bond can improve the stability of the linker in plasma. Kellogg et al. showed that introducing methyl groups on the carbon atoms bearing the

disulphide bond would reduce the reduction rate. One methyl group on each side of the disulphide bond showed greater stability than two methyl groups on one side (8).

2 Theoretical background

2.1 HPLC/UPLC

High performance liquid chromatography (HPLC) is a separation technique which is based on how a compound distributes between a solid stationary phase and a liquid mobile phase. Reverse phase chromatography is the most used separation technique, where the stationary phase is hydrophobic, and the mobile phase is more hydrophilic. The HPLC column is packed with uniform silica particles with a size around 3 – 10 µm. With smaller particle size one achieve better separation by increasing the efficiency, thereby increasing the resolution. Throughout the time of the utilisation of HPLC, it has been more common to decrease the particle size. Today, sizes under 2 µm are widely used and is known as ultra-high performance liquid chromatography (UPLC or UHPLC). One disadvantage with applying a smaller particle size is the higher back pressure, which means the HPLC needs to be special made to withstand this extra pressure. In general, the UPLC is a further development of HPLC.

The most common column for reverse phase is the C18 which is a hydrocarbon chain with 18 carbon atoms. The compounds are separated by van der Waals interactions with the stationary phase. The retention of an analyte is also affected by the composition, and sometimes the pH, of the mobile phase (20).

2.2 Photodiode array

In a photo diode array detector (PDA) light is passed through a sample and hits a reflection grating. The light is then directed on a linear array of photodiodes, which can cover wavelengths typically from 190 – 800 nm. Each diode measures radiation in a certain wavelength interval (20).

2.3 Mass spectrometry

Mass spectrometry (MS) is an official method for analysis in Ph. Eur. The sample compounds are lead into the instrument and are ionised. The MS instrument detects atomic or molecular ions where the intensity of the ions is plotted against their mass to

charge ratio (m/z). For small compounds such as drugs, only a single charge is typically present. Therefore the m/z ratio of the corresponding ion is the mass divided by one.

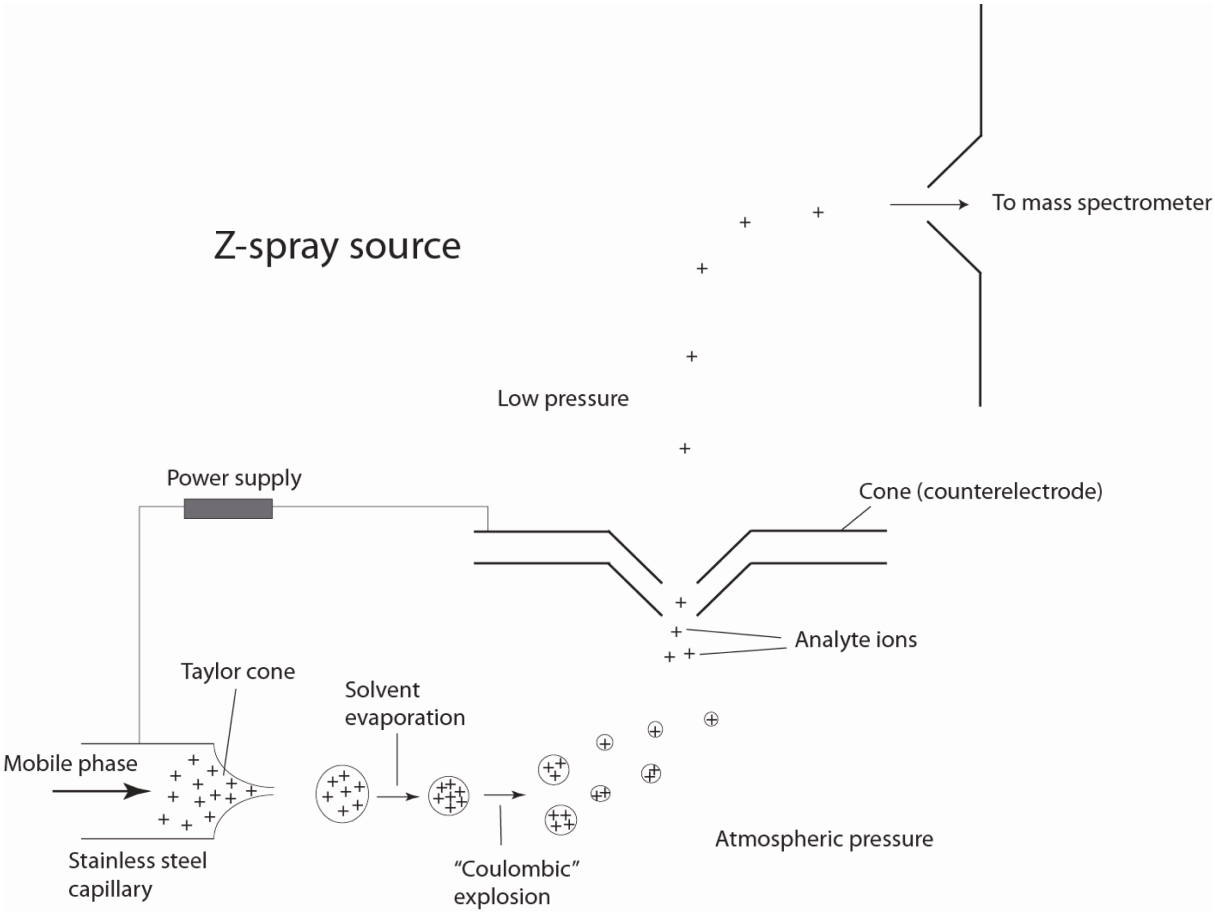

Figure 2.1. Graphic presentation of electrospray ionisation. Used with permission by Terje Vasskog (21).

Electrospray ionisation (ESI) is an important soft ionisation technique in liquid chromatography-mass spectrometry (LC-MS). With this technique, the ionisation happens at atmospheric pressure before the sample reaches the low pressure region of the MS instrument. The mobile phase with the sample from the HPLC column travels through a tight, stainless steel capillary. It reaches the exit of the capillary and the liquid is transformed into an aerosol by a nebulising gas that flows along the slope of the capillary. The aerosol is ionised by the capillary with a high voltage of normally up to 5 kV. If set in positive mode, ionisation is achieved by drawing the electrons from H_2O, which in return furnishes H_3O^+ and acts as a proton donor. The aerosol will eventually vaporise, and a drying gas is used to speed up the drying process. The analyte is transported in and through the MS by electric voltage. The ESI technique is used on

compounds that are able to accept or donate a proton. To acquire a high intensity signal from the MS, it would be beneficial if the analyte is already ionised in the mobile phase, or at least that the ionisation from the pH in the mobile phase and the polarity of the ESI does not counteract each other. The mobile phase must be volatile; therefore, any added buffers or pH-modifying components should also be volatile (e.g. formic acid).

After the analyte is ionised, the ions are lead into the low pressure region of the MS and to a mass filter. A common type of mass filter is the time-of-flight (ToF). In the principle of ToF, the positive ions are accelerated by a set of plates which are negatively charged (and vice versa for negative ions). They drift down a flight path without electromagnetic field and hit the detector. The ions all have the same kinetic energy, which means that heavier ions will drift more slowly than lighter ions. The mass is measured from the time of flight, by knowing the length of the flight path (20). To improve mass accuracy, leucine enkephaline (m/z = 556.2776) or another well-defined compound can be used as a lock mass. The lock mass is a compound with a known mass the instrument uses to correct all other measured masses. The lock mass is measured with set intervals throughout the entire analysis. A high resolution MS such as the ToF, has the ability to separate similar masses and has a high mass accuracy which can be used to indicate the elemental composition of a compound.

2.4 General mechanisms of involved synthesis reactions

The first step of the linker synthesis and conjugation of peptide to the drug-linker conjugate take place through the disulphide exchange mechanism illustrated in Figure 2.2.

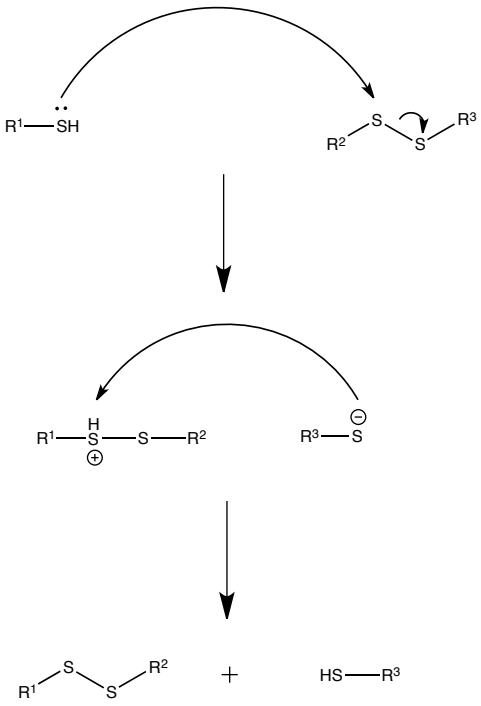

Figure 2.2. Disulphide exchange reaction mechanism

The second step of the linker synthesis and conjugation of drug with the linker proceed through the nucleophilic reaction described in Figure 2.3 and Figure 2.4.

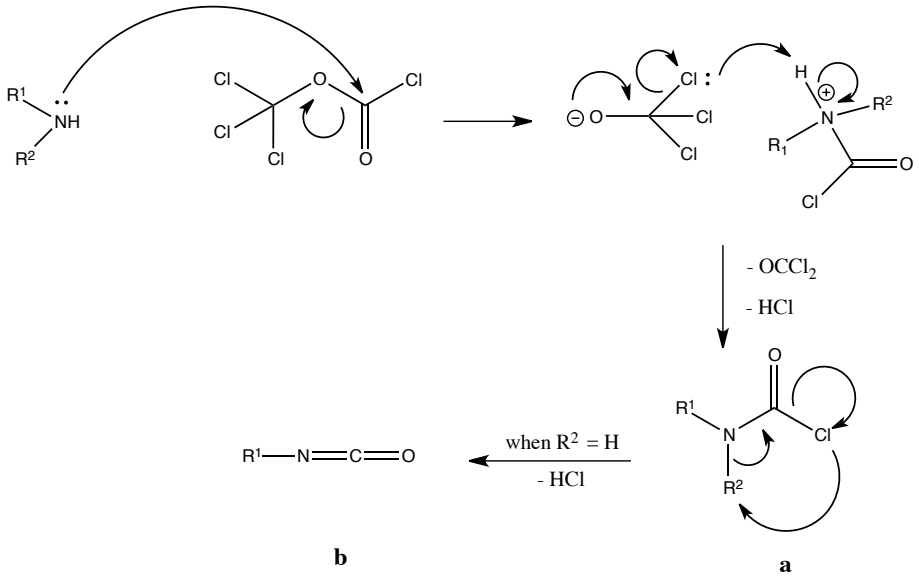

Figure 2.3. Mechanism of the reaction with amines and diphosgene: **a** is formed from secondary amines, **b** is formed from primary amines

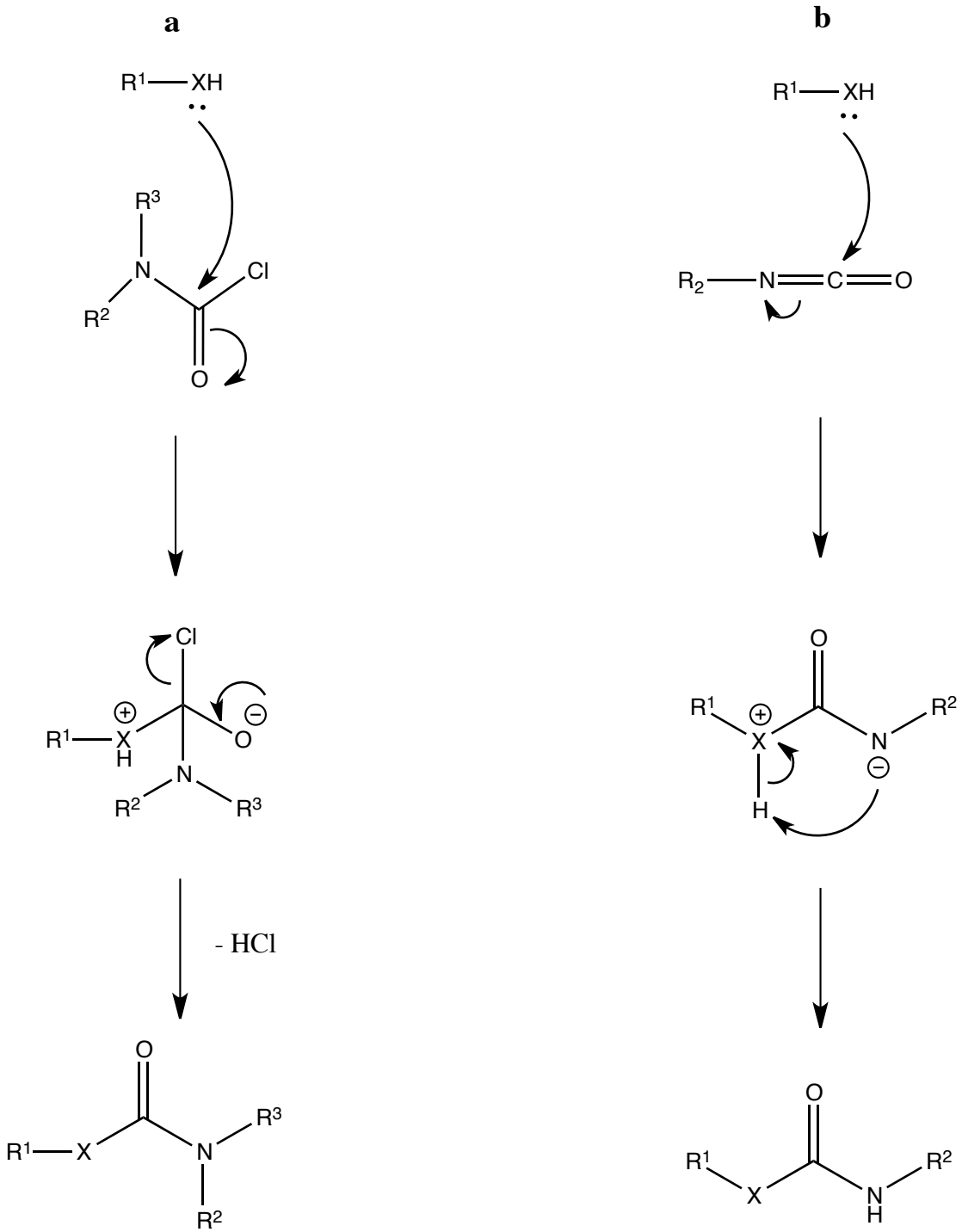

Figure 2.4. Mechanism of drug conjugation with linkers, where X = O or NH. **a** is a carbamoyl chloride linker, **b** is an isocyanate linker

3 Aim of the thesis

The aim of this thesis was to synthesise self-eliminating linkers suitable for hydroxyl- and amine-containing drugs and prepare a full conjugate with model drugs and peptides. The syntheses were planned to be accomplished by disulphide exchange reaction and nucleophilic reaction. The linkers can regulate the anticancer activity of some cytotoxic drugs by temporarily masking certain functional groups and undergo a reaction with glutathione which facilitates the release of the drug at the site of action. The resulting drug-linker-peptide conjugate was therefore subjected to glutathione-rich conditions, and the release kinetics were studied by means of chromatographic and mass spectrometric techniques.

4 Methods and materials

4.1 General

All reactants and reagents were purchased from Sigma-Aldrich, St Louis, Missouri, USA and solvents were purchased from VWR, Philadelphia, Pennsylvania, USA, if otherwise not stated. ACN min. 99.5%, TFA 99%, DCM 99.90%, FA 98%, MeOH 99.80%, EtOAc min. 99.7% from Sigma-Aldrich, diethyl ether 100%, hexane technical, sodium sulfate anhydrous for analysis from Merck, Darmstadt, Germany, trichloromethyl chloroformate min. 97.0%, 1,2-bis(5-nitropyridin-2-yl)disulfane 96%, 2-aminoethanethiol hydrochloride min. 97%, 1,8-bis-(dimethylamino)naphthalene min. 99.0%, 1,2-di(pyridin-2-yl)disulfane 98%, 2-(butylamino)ethanethiol 97%, *N*-(4-aminophenyl)acetamide 99%, L-glutathione oxidized min 98%, L-glutathione reduced min. 98%, paracetamol min. 99.0%, sodium phosphate dibasic dihydrate 98.5 – 101.0%, sodium phosphate monobasic monohydrate min. 99.0%, triethylamine min. 98% from Fluka Analytical, Buchs, Switzerland, 4-(dimethylamino)pyridine min. 99%, acetic acid glacial from VWR, HCl fuming 37% from Merck, NaOH pellets for analysis from Merck, silica gel for flash chromatography from VWR, sea sand extra pure from Merck.

Purified water was obtained from a Rios 100 milliQ purification unit from Merck Millipore, hereby only referred to as water. All amino acids were purchased from Merck with purity of min. 99%. The histidine-rich peptide, HRP1 (AcCGHHPHGHHPH-$CONH_2$) with purity over 95% estimated with UPLC-PDA, was prepared in-house on a Prelude solid phase synthesis instrument by Protein Technologies, Inc. by Northern research institute (Norut) researchers and the same peptide was used for all conjugations.

Nuclear magnetic resonance (NMR) spectra were recorded by Norut researchers on a 400 MHz Avance III spectrometer from Bruker, Billerica, Massachusetts, US, equipped with a 5 mm SmartProbe BB/IH using $CDCl_3$ or DMSO-d_6 as a solvent. Chemical shifts for ^{13}C NMR and ^{1}H NMR were reported as δ, parts per million, relative to the centre line signal of the tetramethylsilane (TMS) at 0.0 ppm, $CDCl_3$ at 77.04 ppm or signal of DMSO-d_6 at 40.45 ppm. The abbreviations s, bs, d, dd, td, t, tt, q, sext, and m stand for the resonance multiplicity singlet, broad singlet, doublet, doublet of doublets, triplet of doublets, triplet, triplet of triplets, quartet, sextet, and multiplet, respectively.

4.2 Syntheses

In this project the aim was to synthesise linkers for conjugation with drugs and peptides. Figure 4.1 gives an overview of which linkers were synthesised, which drugs were used for conjugation, and the peptide sequence.

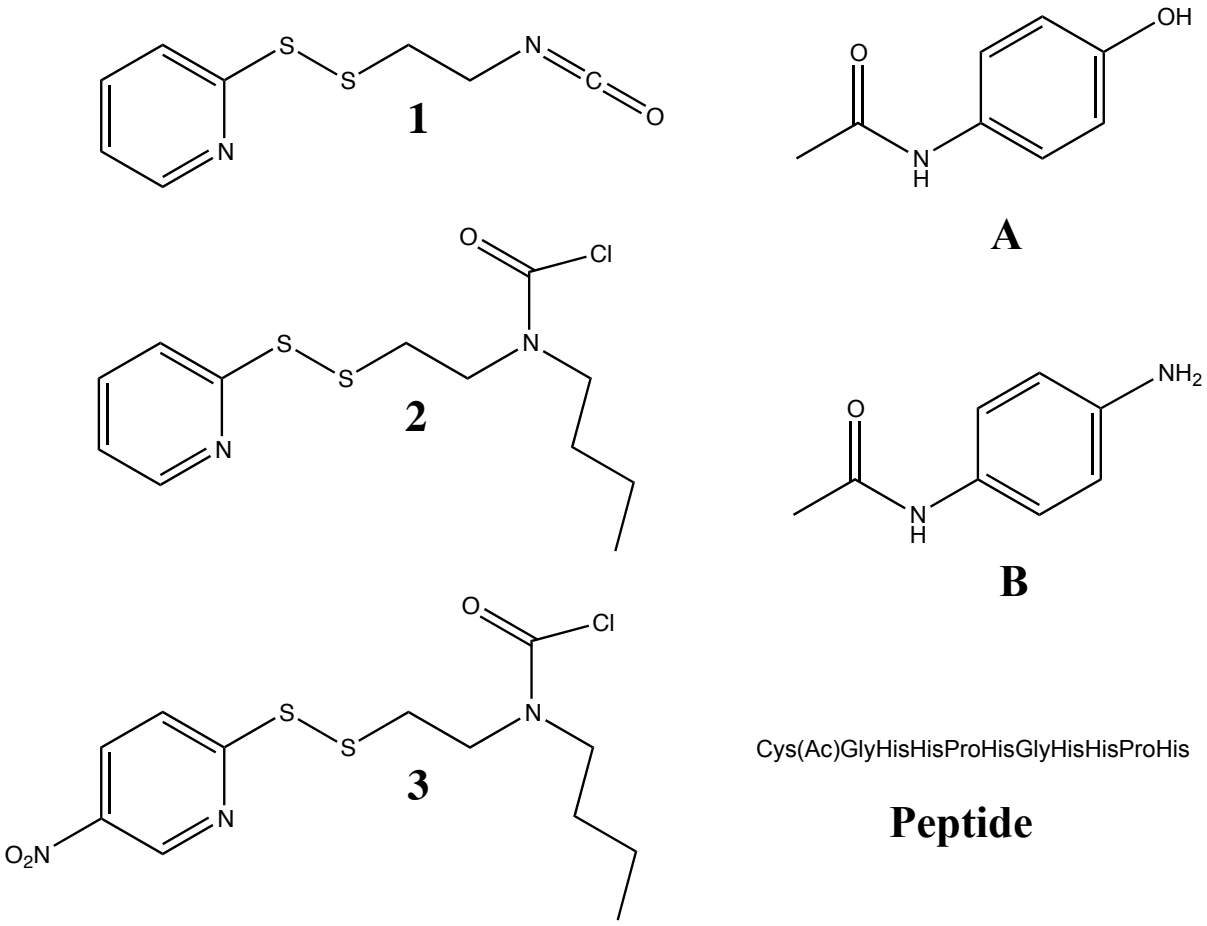

Figure 4.1. An overview over the main components of the drug-linker-peptide conjugates. **1**, **2** and **3** are linkers, **A** and **B** are drugs. The peptide sequence is also shown

Synthesised first step products have been arranged by roman numerals (e.g. I) and synthesised linkers are organised by nominal numbers (e.g. 1). Drugs used for conjugation are classified by letters (e.g. A). When the peptide was conjugated, "Pep-" is introduced into the name of the synthesised product. Paracetamol and 4-aminoacetanilide contain a reactive hydroxyl or amine group and were used as model drugs for simplicity and safety reasons. Synthesis of the first step products in paragraph *4.2.1, 4.2.3* and *4.2.4* are based on the method by Ebright YW., et al. (22). The method for

synthesising the linkers mentioned in paragraph *4.2.2*, *4.2.7* and *4.2.8* are developed by Sigurdsson ST., et al. (23).

4.2.1 2-(Pyridin-2-yldisulfanyl)ethanamine

2-(Pyridin-2-yldisulfanyl)ethanamine (I). 1,2-Di(pyridin-2-yl)disulfane (4.4 g, 20 mmol) was dissolved in a mixture of MeOH (20 ml) and acetic acid (0.8 ml). 2-Aminoethanethiol hydrochloride (1.42 g, 12.5 mmol) was dissolved in MeOH (10 ml), and added dropwise to the solution of 1,2-di(pyridin-2-yl)disulfane over a period of 30 minutes. The reaction mixture was then stirred for further 48 hours before the solvents were evaporated by low pressure with a rotary evaporator, and a yellow oil was left. Preparative HPLC was attempted for purification, though it was somewhat unsuccessful due to low purity of the product. On the second synthesis attempt the product was washed with diethyl ether (50 ml) and dissolved in MeOH (10 ml). The product was precipitated (approximately 30 minutes) by diethyl ether (50 ml) and redissolved in MeOH (10 ml) six times to give **I**.

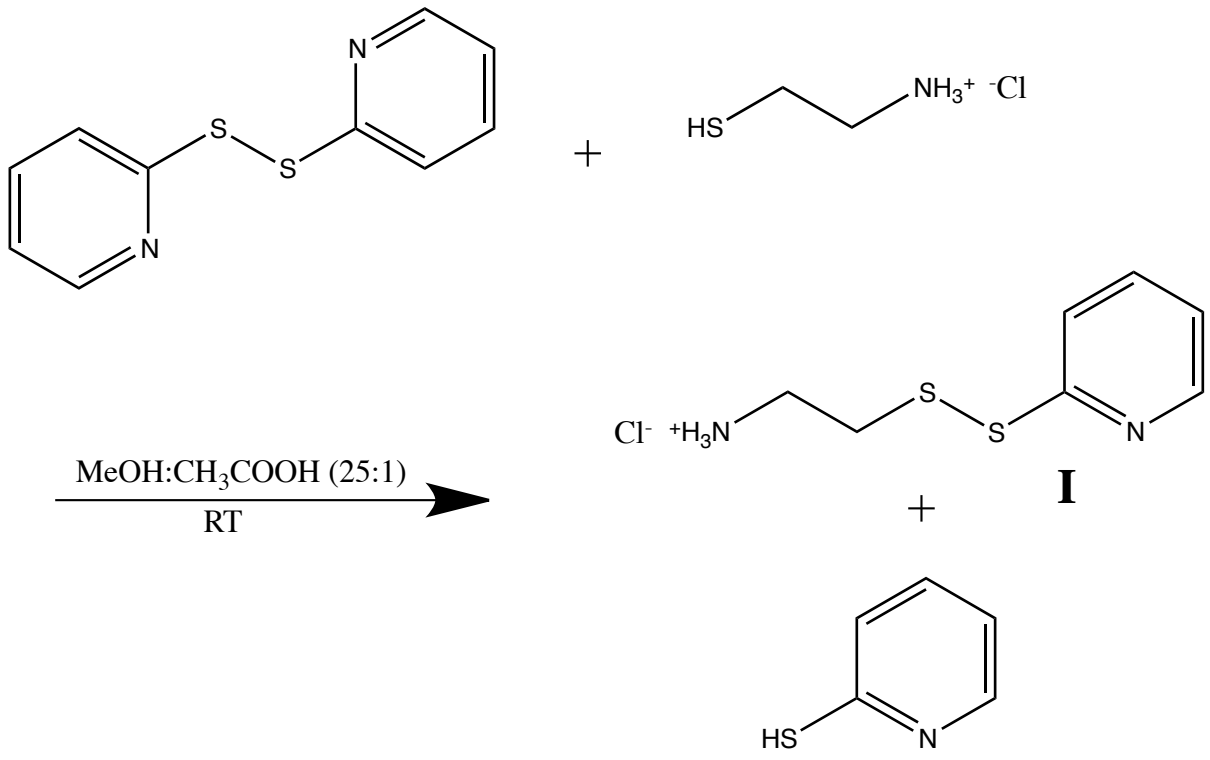

Figure 4.2. Reaction equation where product **I** is formed

4.2.2 Linker 1

2-((2-Isocyanatoethyl)disulfanyl)pyridine (1). 2-(Pyridin-2-yldisulfanyl)ethanamine (0.3483 g, 1.5689 mmol) was partitioned between DCM (12 ml) and 1 N aqueous NaOH (12 ml). The solution was then transferred to a separatory funnel and shaken gently. The organic phase was extracted and approximately 2 tablespoons of anhydrous Na_2SO_4 was added to dry the solvent. The resulting suspension was stirred for 3 minutes and filtered through a sintered glass funnel (size 3). 1,8-Bis-(dimethylamino)naphthalene (0.6522 g, 3.0433 mmol) was dissolved in the anhydrous organic solution and added dropwise to a stirred solution of trichloromethyl chloroformate (0.122 g, 0.6167 mmol) in DCM (2 ml) at 0 ˚C over a period of 1 minute. The solution was stirred for an additional 2 minutes. 1 N aq. HCl (5 ml) and DCM (10 ml) was added, the solution was mixed well and transferred to a separatory funnel. The organic phase was extracted and washed with 1 N aq. HCl (4 x 5 ml) and 1 N aq. NaOH (1 x 5 ml), then dried with Na_2SO_4. The solvent was removed by low pressure with a rotary evaporator to give **1.**

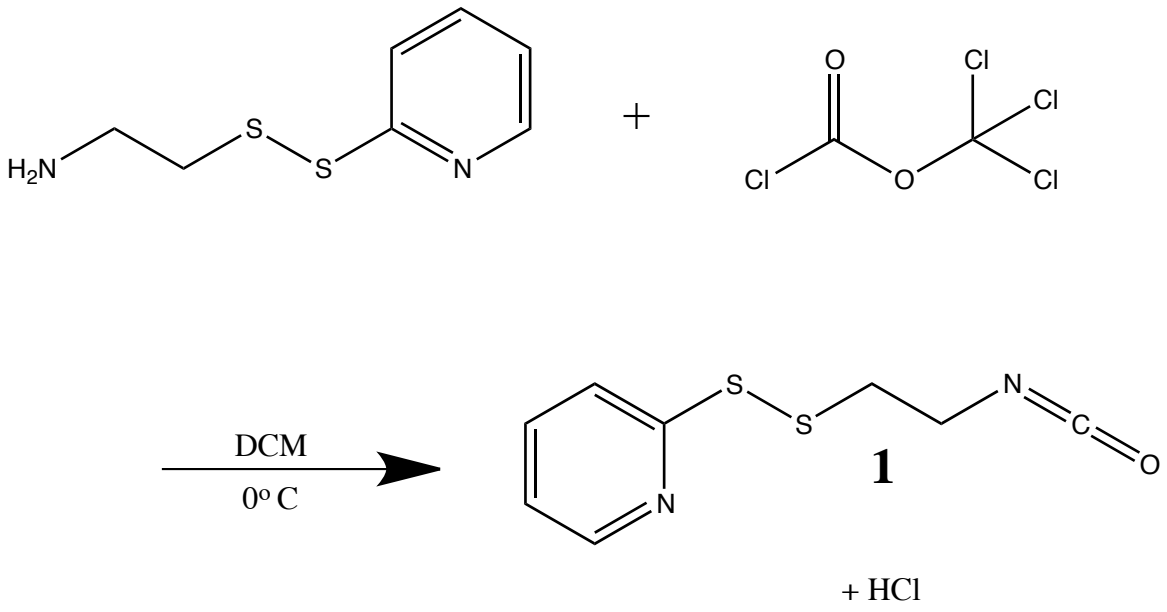

Figure 4.3. Reaction equation where product **1** is formed

4.2.3 2-((5-Nitropyridin-2-yl)disulfanyl)ethanamine

2-((5-Nitropyridin-2-yl)disulfanyl)ethanamine (II). 1,2-Bis(5-nitropyridin-2-yl)disulfane (1.8925 g, 6.0988 mmol) was dissolved in a mixture of DCM (175 ml) and MeOH (9 ml). 2-Aminoethanethiol hydrochloride (0.3612 g, 2.7034 mmol) was dissolved in MeOH (3 ml) and added dropwise to a stirred solution of 1,2-bis(5-nitropyridin-2-yl)disulfane over a period of 30 minutes. The solution was stirred for an additional 24 – 72 hours before the solvents were removed by low pressure with a rotary evaporator to give a yellow-orange solid. MeOH (30 ml) was added and the suspension was filtered through a sintered glass funnel (size 3). The solvent was removed by low pressure with a rotary evaporator and yielded an orange solid. The solid was then dissolved in a 1:1 ratio of ACN and H_2O with 0.1% TFA (4.5 ml) and filtered through a sintered glass funnel (size 3). Preparative HPLC was used to give **II** after lyophilisation.

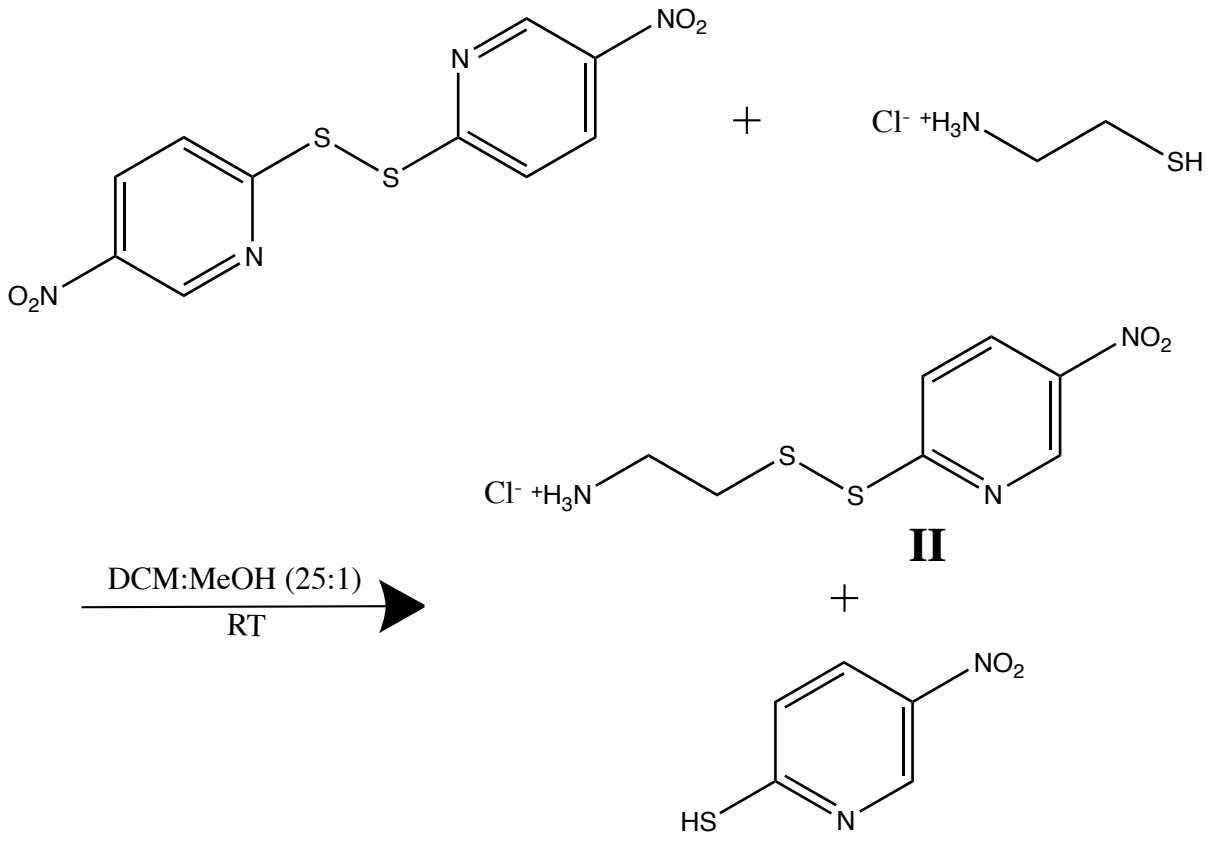

Figure 4.4. Reaction equation where product **II** is formed

4.2.4 *N*-(2-(pyridin-2-yldisulfanyl)ethyl)butan-1-amine

***N*-(2-(pyridin-2-yldisulfanyl)ethyl)butan-1-amine (III).** 1,2-Di(pyridin-2-yl)disulfane (4.4143 g, 20.0368 mmol) was dissolved in MeOH (20 ml) containing acetic acid (0.8 ml). Into this solution, a 2-(butylamino)ethanethiol (0.8145 g, 6.1121 mmol) solution in MeOH (5 ml) was added dropwise over a period of approximately 10 minutes. An instant change of colour was seen from translucent to yellow during the first minute. The mixture was stirred for 60 minutes before the solvents were removed by low pressure with a rotary evaporator. The remaining crude product was further purified by using preparative HPLC to furnish **III** after lyophilisation.

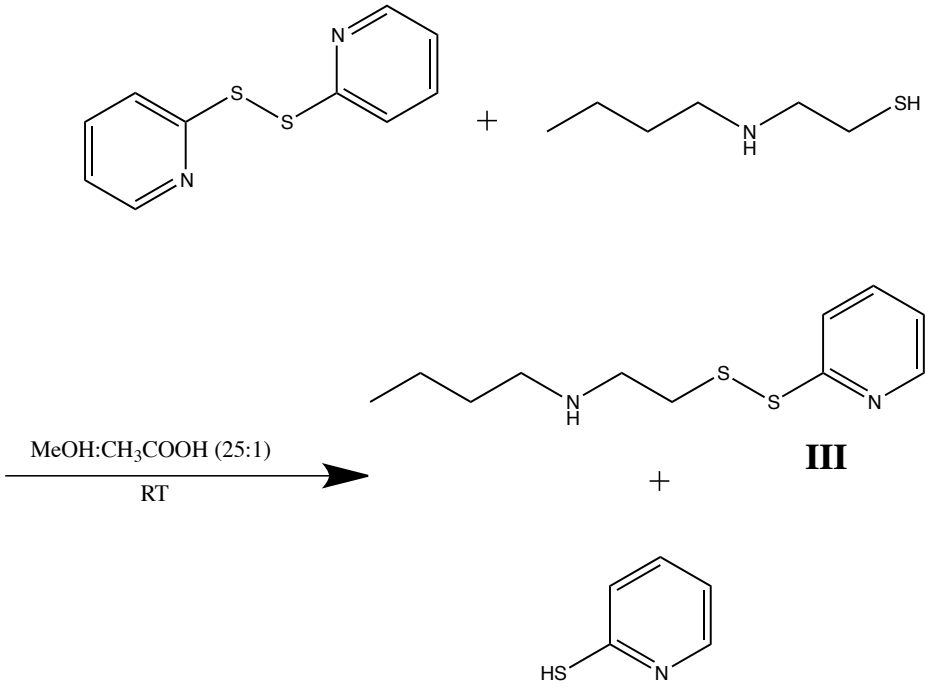

Figure 4.5. Reaction equation where product **III** is formed

4.2.5 Drug-linker conjugate 1A

4-Acetamidophenyl 2-(2-(pyridin-2-yl)disulfanyl)ethylcarbamate (1A). 2-((2-Isocyanatoethyl)disulfanyl)pyridine (0.0221 g, 0.1042 mmol) was mixed with 0.1 M paracetamol solution in ACN (0.95 ml, 0.095 mmol). 0.1 M triethylamine solution in ACN (0.19 ml, 0.019 mmol) was added as a catalyst and the solution was stirred overnight. The solvent was removed by lyophilisation and yielded a white solid. The remaining crude product was purified with preparative HPLC to yield **1A** after lyophilisation.

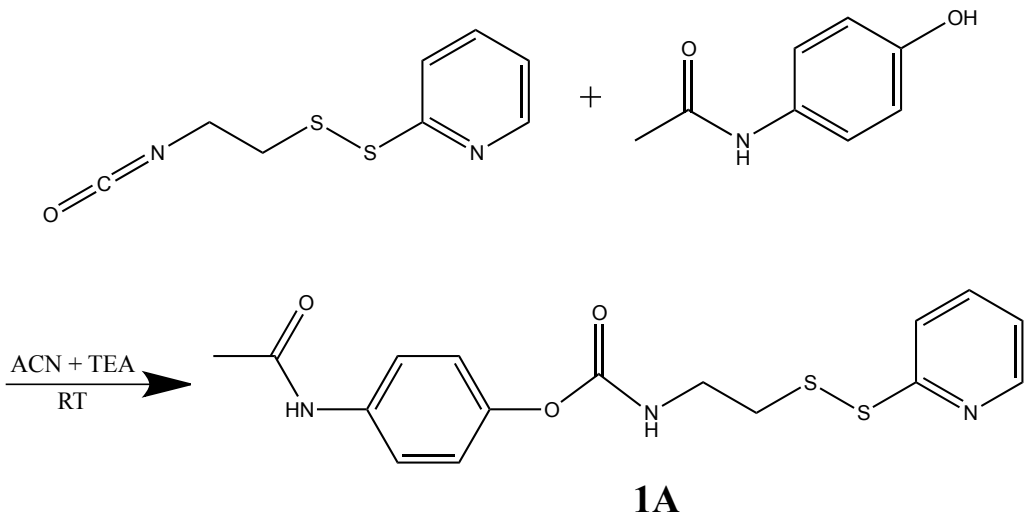

Figure 4.6. Reaction equation where product **1A** is formed

4.2.6 Drug-linker-peptide conjugate of 1A

1A peptide conjugate (Pep-1A). 4-Acetamidophenyl 2-(2-(pyridin-2-yl)disulfanyl)-ethylcarbamate with an excessive amount of HRP1 was dissolved in a 1:1 ratio with H_2O and ACN (2.0 ml). The reaction mixture was stirred overnight. Preparative HPLC was used to purify the crude product and the solvents were removed by lyophilisation to furnish **Pep-1A.**

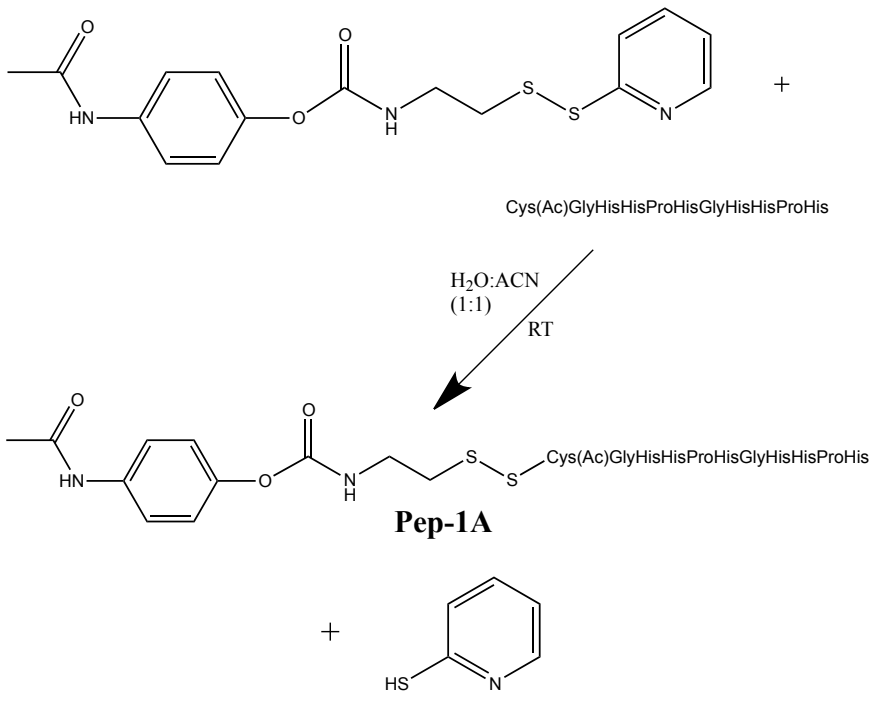

Figure 4.7. Reaction equation where product **Pep-1A** is formed

4.2.7 Linker 2

Butyl(2-(pyridin-2-yldisulfanyl)ethyl)carbamic chloride (2). *N*-(2-(pyridin-2-yldisulfanyl)ethyl)butan-1-amine (0.2250 g, 0.9298 mmol) was partitioned between DCM (12 ml) and 1 N aq. NaOH (12 ml). The solution was then transferred to a separatory funnel and shaken gently. The organic phase was extracted and approximately 2 tablespoons of anhydrous Na_2SO_4 was added to dry the solvent. The resulting suspension was stirred for 3 minutes and filtered through a sintered glass funnel (size 3). 1,8-Bis-(dimethylamino)naphthalene (0.4308 g, 2.0102 mmol) was dissolved in the anhydrous organic solution and added dropwise to a stirred solution of trichloromethyl chloroformate (0.0793 g, 0.4008 mmol) in DCM (2 ml) at 0 ˚C over a period of 1 minute. The solution was stirred for an additional 2 minutes. 1 N aq. HCl (5 ml) and DCM (10 ml) was added, the solution was mixed well and transferred to a separatory funnel. The organic phase was extracted and washed with 1 N aq. HCl (4 x 5 ml) and 1 N aq. NaOH (1 x 5 ml), then dried with Na_2SO_4. The solvent was removed by low pressure with a rotary evaporator to give a yellow oil, and the remaining crude product was purified with flash chromatography. Flash chromatography was carried out using silica gel as the stationary phase and a 9:1 mixture of hexane and ethyl acetate as the mobile phase. Fractions were gathered continuously and checked with UPLC-PDA for eluting compounds. The solvents were removed by low pressure with a rotary evaporator to give **2.**

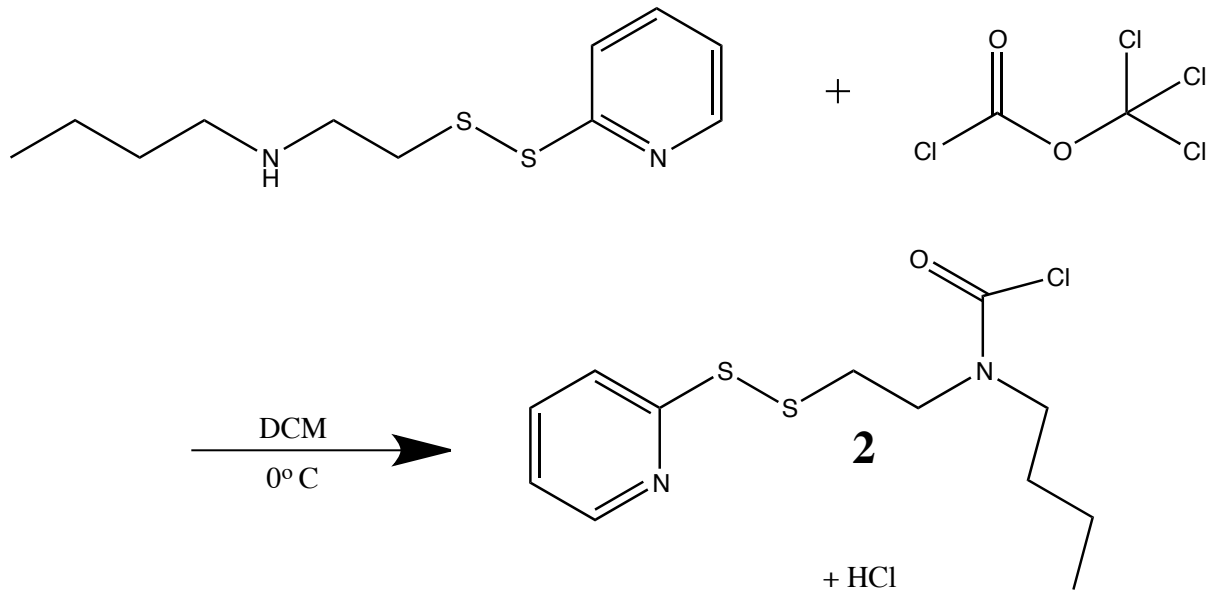

Figure 4.8. Reaction equation where product **2** is formed

4.2.8 Linker 3

Butyl(2-((5-nitropyridin-2-yl)disulfanyl)ethyl)carbamic chloride (3). *N*-(2-((5-nitropyridin-2-yl)disulfanyl)ethyl)butan-1-amine (0.0246 g, 0.0857 mmol) was partitioned between DCM (12 ml) and 1 N aq. NaOH (12 ml). The solution was then transferred to a separatory funnel and shaken gently. The organic phase was extracted and approximately 2 tablespoons of anhydrous Na_2SO_4 was added to dry the solvent. The resulting suspension was stirred for 3 minutes and filtered through a sintered glass funnel (size 3). 1,8-Bis-(dimethylamino)naphthalene (0.0502 g, 0.2342 mmol) was dissolved in the anhydrous organic solution and added dropwise to a stirred solution of trichloromethyl chloroformate (0.0089 g, 0.0450 mmol) in DCM (2 ml) at 0 ˚C over a period of 1 minute. The solution was stirred for an additional 2 minutes. 1 N aq. HCl (5 ml) and DCM (10 ml) was added, the solution was mixed well and transferred to a separatory funnel. The organic phase was extracted and washed with 1 N aq. HCl (4 x 5 ml) and 1 N aq. NaOH (1 x 5 ml), then dried with Na_2SO_4. The solvent was removed by low pressure with a rotary evaporator to give **3.**

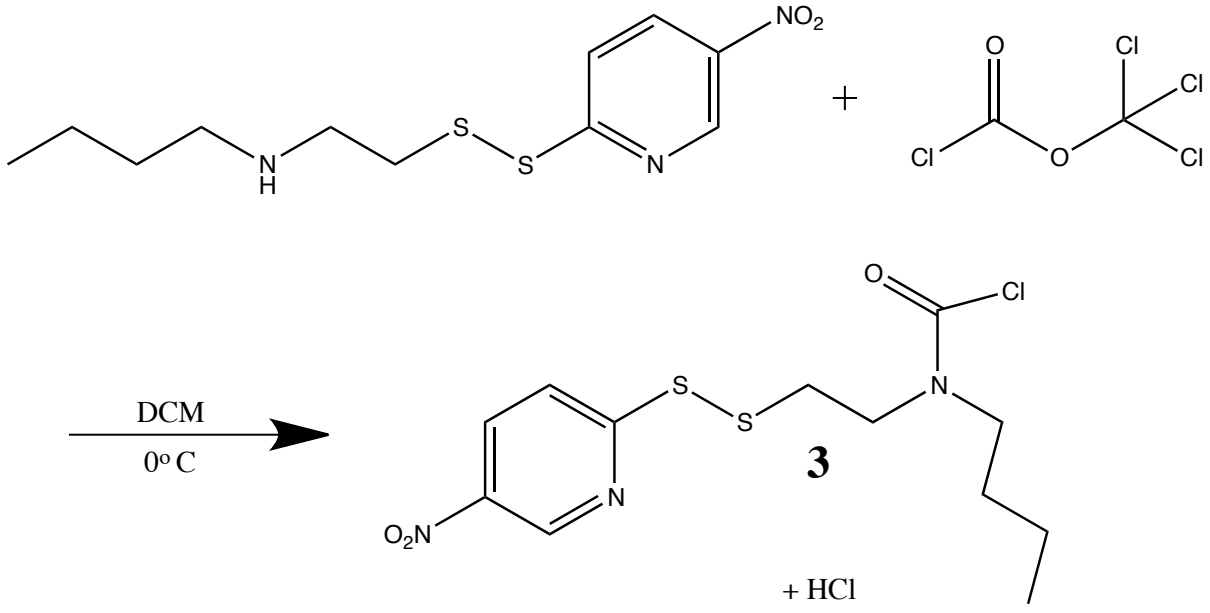

Figure 4.9. Reaction equation where product **3** is formed

4.2.9 Drug-linker conjugate 2A

4-Acetamidophenyl butyl(2-(pyridin-2-yldisulfanyl)ethyl)carbamate (2A). Butyl(2-(pyridin-2-yldisulfanyl)ethyl)carbamic chloride (0.014 g, 0.0461 mmol) was mixed with 0.1 M paracetamol solution in ACN (0.461 ml, 0.0461 mmol). 0.1 M triethylamine solution in ACN (0.922 ml, 0.0922 mmol) and 4-(dimethylamino)pyridine (0.0169 g, 0.1383 mmol) were added to the solution as catalysts and the reaction mixture was stirred overnight. The solvent was removed by low pressure with a rotary evaporator and the remaining crude product was further purified with preparative HPLC to yield **2A** after lyophilisation.

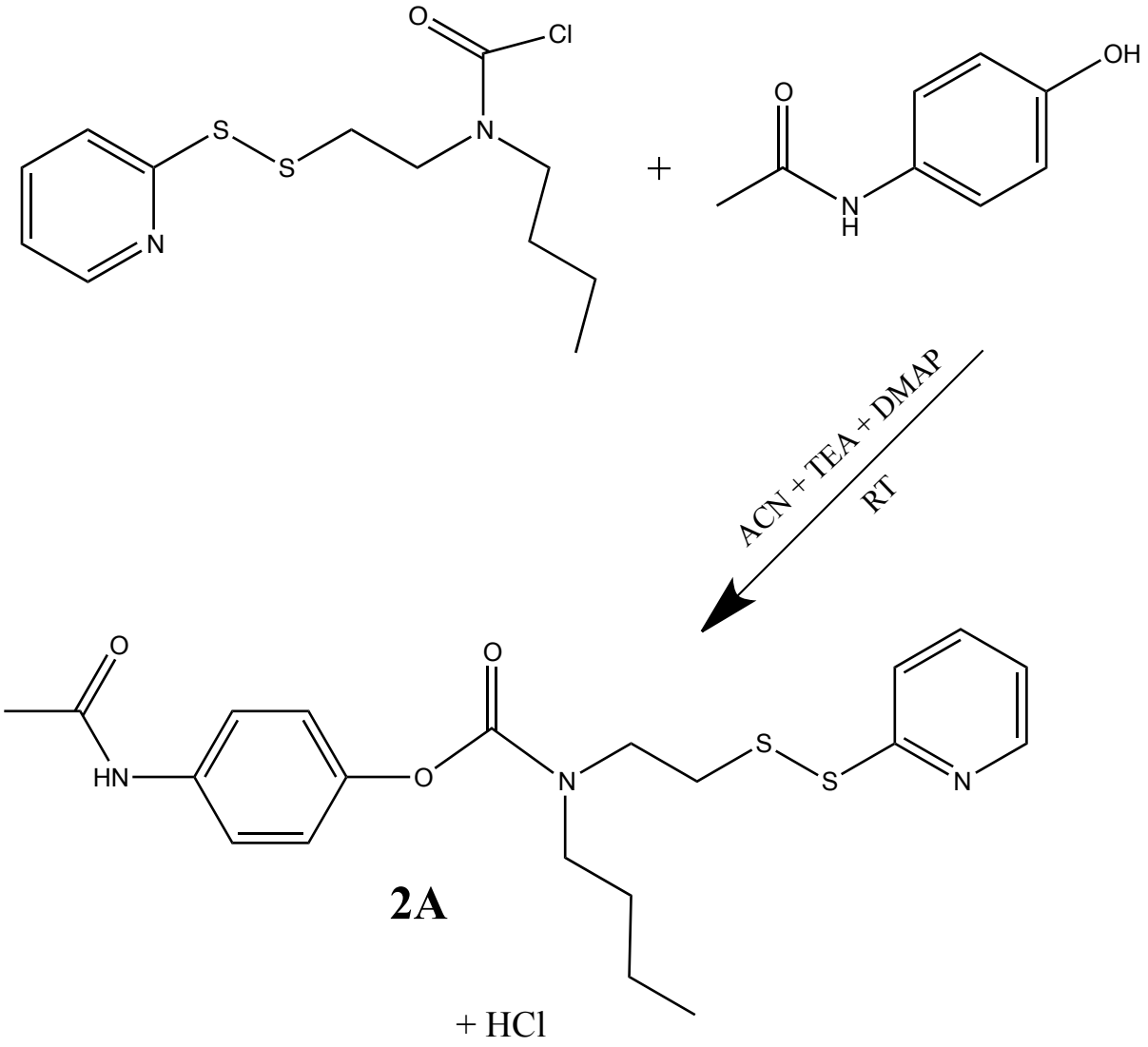

Figure 4.10. Reaction equation where product **2A** is formed

4.2.10 Drug-linker conjugate 3A

4-Acetamidophenyl butyl(2-((5-nitropyridin-2-yl)disulfanyl)ethyl)carbamate (3A). Butyl(2-((5-nitropyridin-2-yl)disulfanyl)ethyl)carbamic chloride (0.0069 g, 0.0198 mmol) was mixed with 0.1 M paracetamol solution in ACN (0.198 ml, 0.0198 mmol). 0.1 M triethylamine solution in ACN (0.396 ml, 0.0396 mmol) and 4-(dimethylamino)pyridine (0.0073 g, 0.0598 mmol) were added to the solution as catalysts and the reaction mixture was stirred for 30 minutes. The solvent was removed by low pressure with a rotary evaporator and the remaining crude product was further purified with preparative HPLC to yield **3A** after lyophilisation.

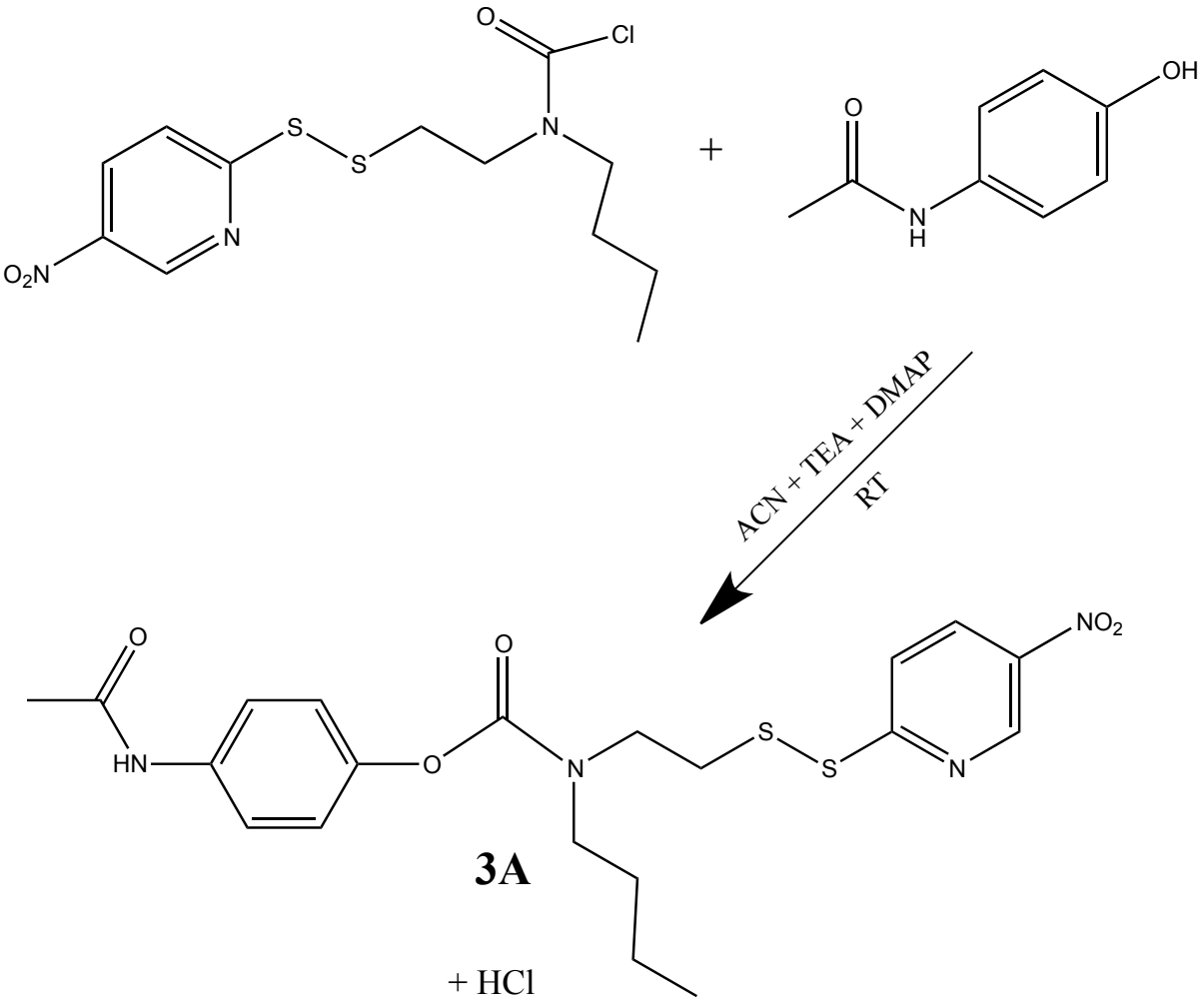

Figure 4.11. Reaction equation where product **3A** is formed

4.2.11 Drug-linker conjugate 1B

***N*-(4-(3-(2-(pyridin-2-yldisulfanyl)ethyl)ureido)phenyl)acetamide (1B).** 2-((2-Isocyanatoethyl)disulfanyl)pyridine (0.0221 g, 0.1042 mmol) was mixed with 0.025 M *N*-(4-aminophenyl)acetamide solution in ACN (5.7 ml, 0.1425 mmol). 0.1 M triethylamine solution in ACN (0.95 ml, 0.095 mmol) was added to the solution as a catalyst and the reaction mixture was stirred overnight. The solvent was removed by lyophilisation to yield **1B**.

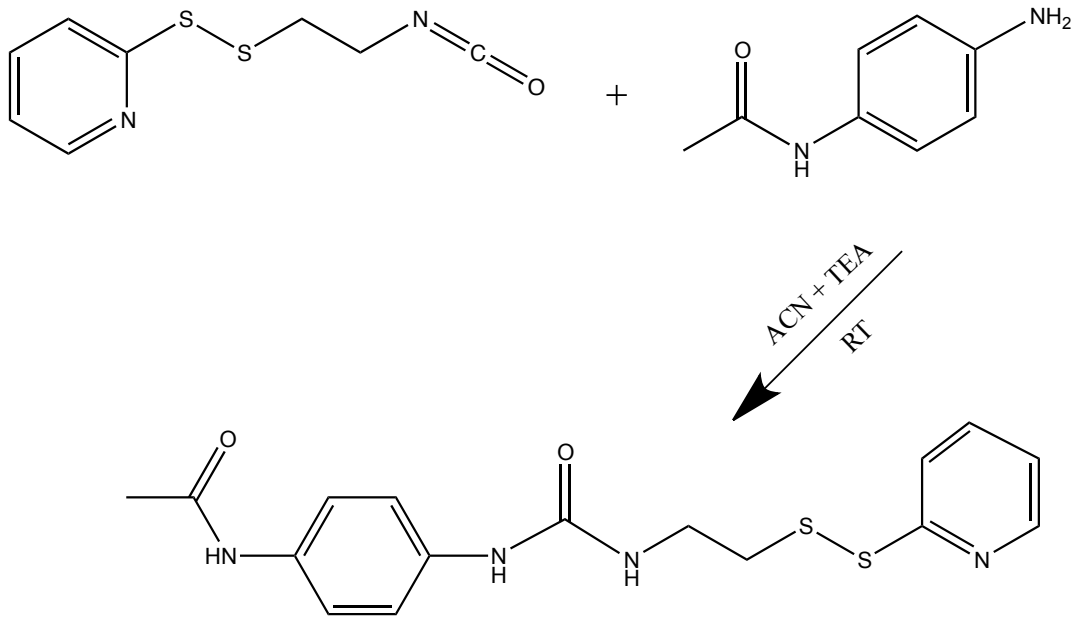

1B

Figure 4.12. Reaction equation where product **1B** is formed

4.2.12 Drug-linker-peptide conjugate of 1B

1B peptide conjugate (Pep-1B). *N*-(4-(3-(2-(Pyridin-2-yldisulfanyl)ethyl)ureido)-phenyl)acetamide (0.0098 g, 0.0271 mmol) was dissolved in a 1:1 ratio of H_2O and ACN (0.5 ml). HRP1 (0.0351 g, 0.0272 mmol) was added to the solution and the reaction mixture was stirred overnight. Preparative HPLC was used to purify the crude product and yielded **Pep-1B** after lyophilisation.

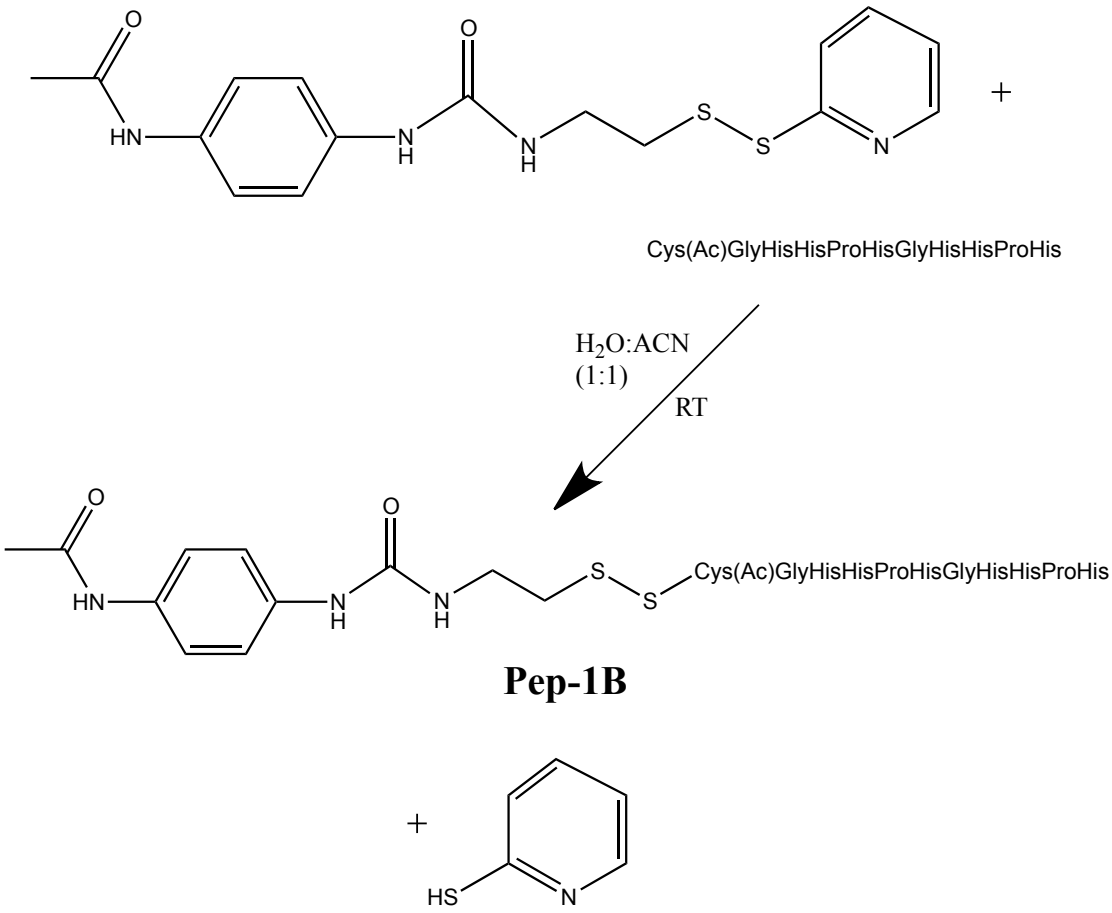

Figure 4.13. Reaction equation where product **Pep-1B** is formed

4.2.13 Drug-linker-peptide conjugate of 2A

2A peptide conjugate (Pep-2A). 4-Acetamidophenyl butyl(2-(pyridin-2-yldisulfanyl)-ethyl)carbamate with an excessive amount of HRP1 was dissolved in in a 1:1 ratio of H_2O and ACN (0.5 ml) and the reaction mixture was stirred overnight. Preparative HPLC was run to purify the crude product and gave **Pep-2A** after lyophilisation.

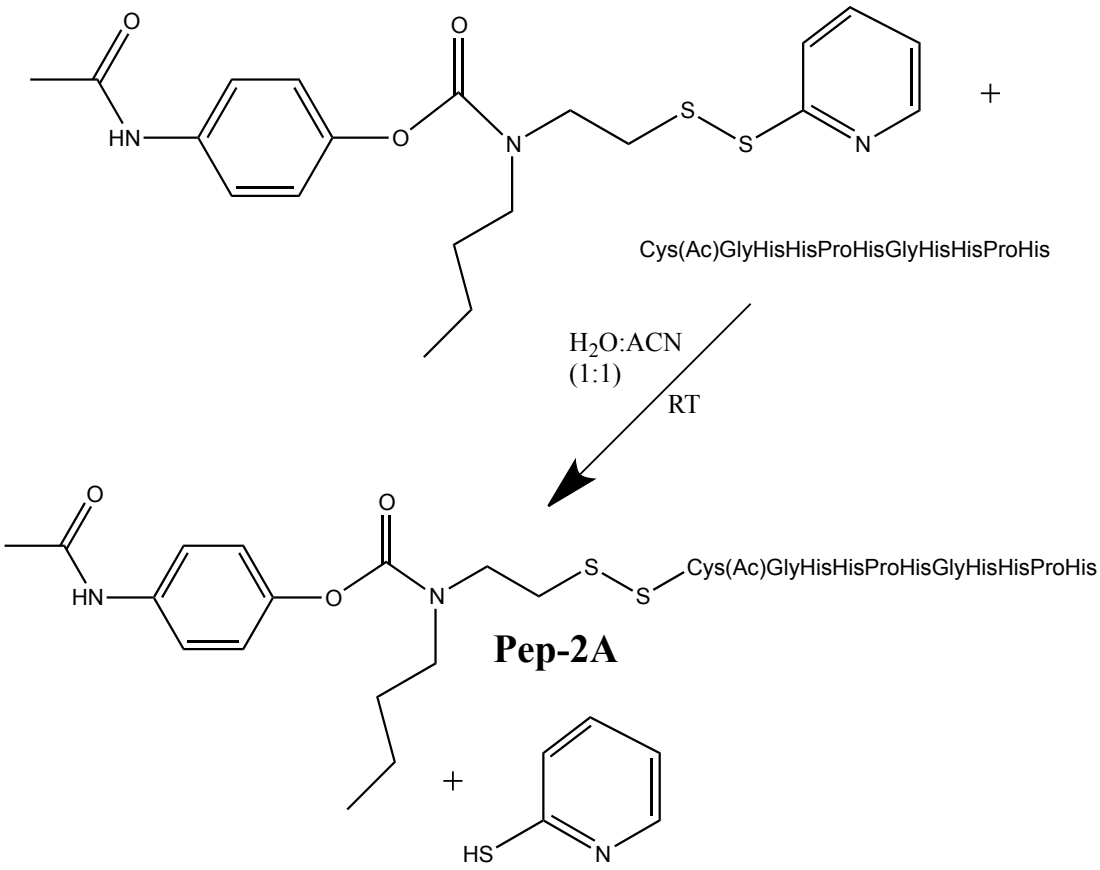

Figure 4.14. Reaction equation where product **Pep-2A** is formed

4.3 Kinetic analyses of synthesised products

Kinetic analyses were performed on the products **Pep-1A**, **Pep-2A** and **Pep-1B** as shown in paragraph *4.2.6, 4.2.12* and *4.2.13.* A solution of 50 mM reduced and 5 mM oxidised glutathione was made from GSH (0.0148 g, 0.05 mmol) and GSSG (0.0031 g, 0.005 mmol) in 0.1 M phosphate buffer with pH 7.4 (1 ml). All drug-linker-peptide conjugates were dissolved in phosphate buffer with pH 7.4 in three separate vials. Next, the drug-linker-peptide conjugate solutions (0.63 ml) were mixed with fresh GSH/GSSG solution (0.07 ml). More fresh GSH/GSSG solution was added to the mixture when none was left or when the drug-linker conjugate concentration was low as shown by UPLC-PDA.

4.4 Preparative high performance liquid chromatography methods for purification of synthesis products

Preparative HPLC was performed on a 2767 sample manager, 2998 photodiode array detector and 2545 pump with MassLynx v4.1 software. All from Waters, Milford, MA, USA. The column and sample temperature was at room temperature (approximately 23 ˚C), and the column used was XBridge Prep C18 5 µm OBD, 19 x 250 mm from Waters. The PDA scanned from wavelength 190 – 500 nm. The mobile phase consisted of water with 0.1% TFA (A) and ACN with 0.1% TFA (B).

A search for the most efficient and optimal injection volume was carried out. Therefore, the injection volume for preparative HPLC varied from 100 – 950 µl with different gradient systems.

Synthesis of all the products, with an exception of products mentioned in paragraph *4.2.1*, *4.2.4*, and *4.2.5*, have been purified with a gradient system as shown in Table 4.1. The injected samples ranged from 100 – 950 µl in volume.

Table 4.1. Gradient system where % B increased from 10 – 100 in 10 minutes, and 100% B was held for 2 minutes

TIME (MIN)	FLOW (ML/MIN)	% A	% B
0.00	20.00	90.0	10.0
10.00	20.00	0.0	100.0
12.00	20.00	0.0	100.0
12.10	20.00	90.0	10.0
15.00	20.00	90.0	10.0

Synthesis of the product mentioned in *4.2.1* has been purified with a gradient system as shown in Table 4.2 where the injected samples ranged from 100 – 950 µl in volume.

Table 4.2. Gradient system where % B increased from 5 – 50 in 10 minutes, then from 50 – 100 in 1 minute, and was held at 100% B for 2 minutes

TIME (MIN)	FLOW (ML/MIN)	% A	% B
0.00	20.00	95.0	5.0
10.00	20.00	50.0	50.0
11.00	20.00	0.0	100.0
13.00	20.00	0.0	100.0
13.10	20.00	95.0	5.0
16.00	20.00	95.0	5.0

Synthesis of the product mentioned in *4.2.5* has been purified with a gradient system as shown in Table 4.3 where the injected samples were 500 µl in volume.

Table 4.3. Gradient system where % B increased from 40 – 75 in 10 minutes, and 75% B was held for 1 minute

TIME (MIN)	FLOW (ML/MIN)	% A	% B
0.00	20.00	60.0	40.0
10.00	20.00	25.0	75.0
11.00	20.00	25.0	75.0
11.10	20.00	60.0	40.0
13.00	20.00	60.0	40.0

Synthesis of the product mentioned in *4.2.4* has been purified with a gradient system as shown in Table 4.4 where the injected samples ranged from 100 – 900 µl in volume.

Table 4.4. Gradient system where % B increased from 30 – 70 in 10 minutes, then from 70 – 100 in 1 minute, and was held at 100% B for 2 minutes

TIME (MIN)	FLOW (ML/MIN)	% A	% B
0.00	20.00	70.0	30.0
10.00	20.00	30.0	70.0
11.00	20.00	0.0	100.0
13.00	20.00	0.0	100.0
14.00	20.00	70.0	30.0
17.00	20.00	70.0	30.0

4.5 Analytical ultra-high performance liquid chromatography methods for purity measurements

UPLC-PDA was performed on a Waters Acquity UPLC H class with MassLynx v4.1 software from Waters. The column used was Acquity UPLC BEH C18 1.7 µm, 2.1 x 50 mm from Waters. The sample temperature was at room temperature (approximately 26 ˚C), and the column temperature was set to 50 ˚C. The PDA scanned from wavelength 200 – 500 nm. The mobile phase consisted of water with 0.1% TFA (A) and ACN with 0.1% TFA (B).

All the samples, with the exception of the samples for the kinetic analyses, were run with a gradient system as shown in Table 4.5 with an injection volume of 5 µl.

There was an unknown problem with the UPLC-PDA causing a shift in retention time for the peaks at unspecified times. When this occurred the UV spectra for each compound was checked and compared with previous UPLC-PDA chromatograms if available.

Table 4.5. Gradient system where % B increased from 5 – 95 in 7 minutes, and 95% B was held for 3 minutes

TIME (MIN)	FLOW (ML/MIN)	% A	% B
0.00	0.600	95.0	5.0
7.00	0.600	5.0	95.0
10.00	0.600	5.0	95.0
10.10	0.600	95.0	5.0
13.00	0.600	95.0	5.0

Kinetic analysis samples were run with a gradient system as shown in Table 4.6 with an injection volume of 5 µl.

Table 4.6. Gradient system where % B increased from 5 – 50 in 10 minutes, then from 50 – 95 in 0.10 minute, and was held at 95% B for 0.9 minute

TIME (MIN)	FLOW (ML/MIN)	% A	% B
0.00	0.600	95.0	5.0
10.00	0.600	50.0	50.0
10.10	0.600	5.0	95.0
11.00	0.600	5.0	95.0
11.10	0.600	95.0	5.0
14.00	0.600	95.0	5.0

4.6 Mass spectrometric analysis of synthesis products

MS analyses were performed on a Waters Acquity UPLC I class with Xevo G2 QTof. The samples were analysed with MassLynx v4.1 software from Waters. The column used was Acquity UPLC BEH C18 1.7 µm, 2.1 x 100 mm from Waters. The sample temperature was 5 ˚C, and the column temperature was set to 65 ˚C. The MS was used in full scan mode m/z 100 – 5000, electrospray positive mode, scan time = 0.3 seconds, capillary voltage 600 V,

cone voltage 30 V, with lock spray leucine enkephalin m/z = 556.2771. The mobile phase consisted of water with 0.1% FA (A) and ACN with 0.1% FA (B).

All samples were run on the same gradient system as shown in Table 4.7 with an injection volume of 5 µl. When samples included phosphate buffer, as with the kinetic analyses, the first minute of mobile phase went to waste before reaching the MS.

Table 4.7. Gradient system where % B increased from 2 – 95 in 9 minutes, and 95% B was held for 1 minute

TIME (MIN)	FLOW (ML/MIN)	% A	% B
0.00	0.600	98.0	2.0
9.00	0.600	5.0	95.0
10.00	0.600	5.0	95.0
10.10	0.600	98.0	2.0
12.50	0.600	98.0	2.0

5 Results and discussion

5.1 Synthesis of 2-(pyridin-2-yldisulfanyl)ethanamine hydrochloride (I)

2-Aminoethanethiol hydrochloride was reacted with 1,2-di(pyridin-2-yl)disulfane as shown in Figure 4.2 to furnish **I** as white solid in 38.5% yield (1.0695 g, 4.8176 mmol). The purity was estimated to 97.9% by UPLC-PDA as shown in Appendix figure 1. The product gave a mass spectrum as shown in Appendix figure 10 giving a protonated molecular ion with m/z 187.0364 corresponding to the elemental composition $C_7H_{10}N_2S_2$, which corresponds to the protonated monoisotopic mass of 187.0359 g/mol of the first step product **I**.

The NMR spectra (see Appendix figure 27 and Appendix figure 28) gave the following results: ^{1}H NMR (400 MHz, DMSO-d_6) δ 8.50 (dd, *J* = 5.0, 1.5 Hz, 1H), 8.42 (bs, 3H), 7.83 (td, *J* = 7.7, 1.8 Hz, 1H), 7.75 (d, *J* = 8.1 Hz, 1H), 7.28 (dd, *J* = 7.3, 4.9 Hz, 1H), 3.15 – 3.03 (m, 4H). ^{13}C NMR (100 MHz, DMSO) δ 158.1, 149.8, 137.9, 121.6, 120.0, 37.7, 34.8.

This synthesis was initially tested by using 2-aminoethanethiol as reactant. However, a vigorous reaction took place and the resulting reaction mixture appeared to be so complex that isolation of the product would become problematic. For this reason hydrochloric salt of 2-aminoethanethiol was used as a reactant, which in turn gave a relatively simple reaction mixture for further purification. The reaction mixture was analysed on UPLC-PDA and when formation of biproducts appeared the reaction was stopped.

When the crude product was purified by preparative HPLC by using water and acetonitrile as the mobile phase and the collected fraction containing the product was lyophilised, the resulting hygroscopic substance appeared to be a mixture of free amine and hydrochloric salt and adsorbed water. However, recrystallisation of the crude product and subsequent drying gave a homogenous product consisting only of the hydrochloric salt. The UPLC-PDA confirms this difference in the product obtained by the two different purifying methods. UPLC-PDA results showed peak splitting in the product from preparative HPLC, whilst there was no peak splitting in the product from recrystallisation. Also, the product obtained by preparative HPLC was not completely dry after over 72 h of lyophilisation.

The yield was substantially lower than the published article by Ebright YW., et al. (22), in which the product was obtained in 75.5% yield. The MS and NMR data combined show that the expected compound was successfully synthesised.

5.2 Synthesis of linker 1

2-(Pyridin-2-yldisulfanyl)ethanamine was reacted with trichloromethyl chloroformate as shown in Figure 4.3 to furnish **1** as a yellow oil in 33.7% yield (0.0441 g, 0.2080 mmol). The product gave a mass spectrum as shown in Appendix figure 11 giving a protonated molecular ion with m/z 213.0162 corresponding to the elemental composition of $C_8H_8N_2OS_2$, which corresponds to the protonated monoisotopic mass of 213.0157 g/mol of linker **1**.

The NMR spectra (see Appendix figure 29 and Appendix figure 30) gave the following results: ^{1}H NMR (400 MHz, Chloroform-d) δ 8.50 (d, *J* = 4.8 Hz, 1H), 7.66 (d, *J* = 4.0 Hz, 2H), 7.13 (q, *J* = 4.4 Hz, 1H), 3.61 (t, *J* = 6.1 Hz, 2H), 2.99 (t, *J* = 6.2 Hz, 2H). ^{13}C NMR (100 MHz, $CDCl_3$) δ 159.2, 150.0, 137.2, 123.8, 121.2, 120.4, 41.7, 40.8.

Synthesis of **1** was initially attempted by using a phosgene solution which appeared to give a complex reaction mixture. The use of diphosgene by adopting the protocol by Sigurdsson ST., et al. (23) gave the desired isocyanate in acceptable yield, although NMR analysis of the product showed that the synthesised isocyanate had not been essentially pure. The isocyanate **1** was found to be very unstable in the presence of water. A solution of **1** in a mixture of water and acetonitrile was analysed over time by UPLC-PDA and MS. The analysis showed that some of **1** was converted back to starting material **I** and an unknown compound **Y** (see Figure 5.1) within 10 minutes (see Figure 5.2). The analysis of a neat sample put at room temperature overnight showed a full conversion to **Y** (not shown). Suggested reaction to form compound **Y** is a nucleophilic substitution of starting material **I** with isocyanate **1**. The structure of **Y** was not confirmed by NMR due to the sample's low amount, but was indicated by the m/z value of MS.

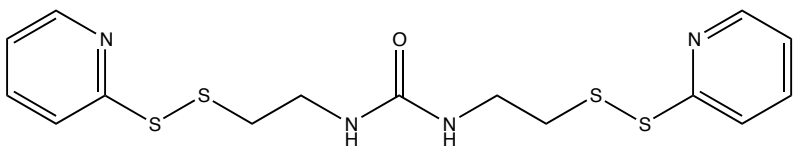

Figure 5.1. Suggested structure of compound **Y**

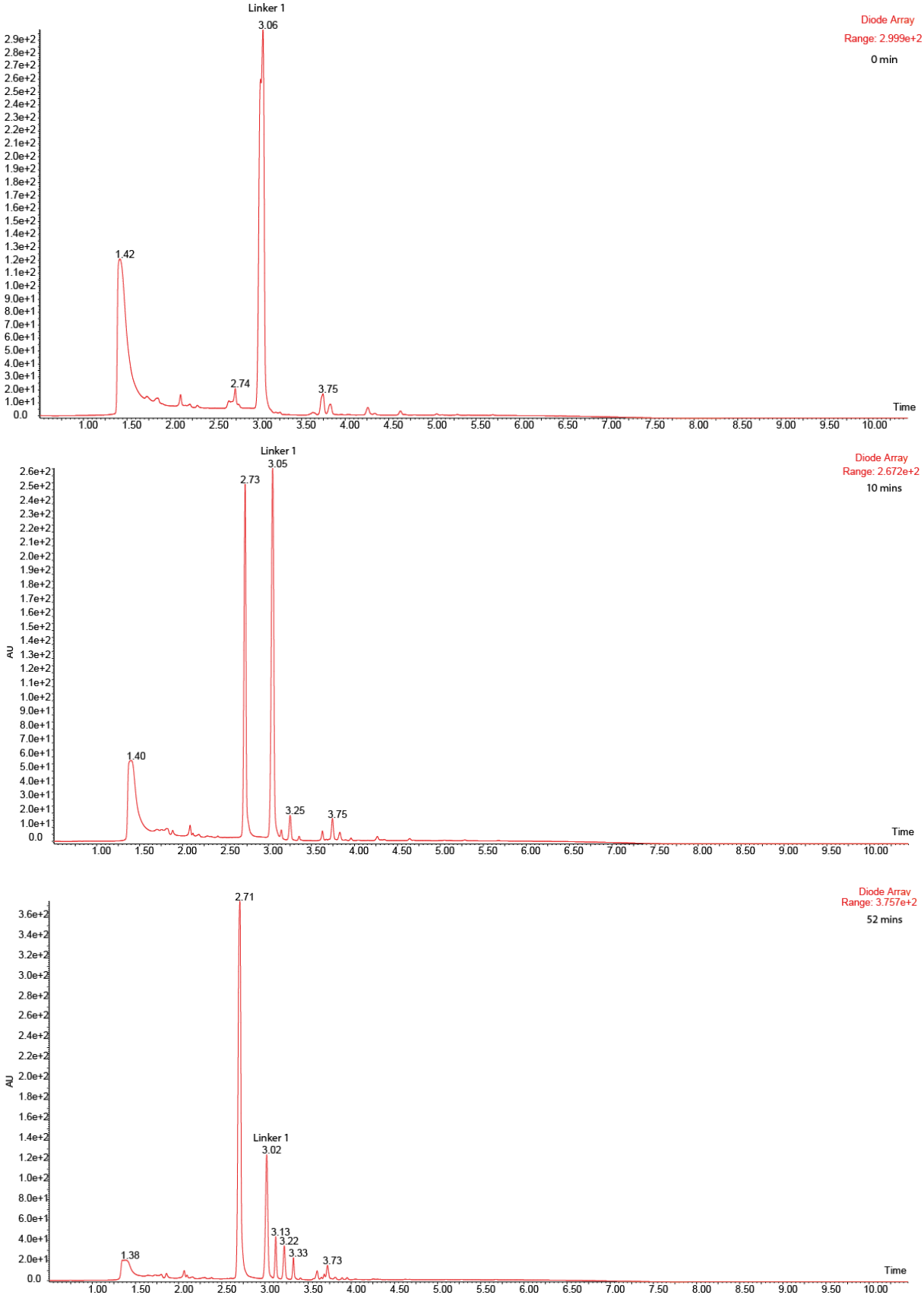

Figure 5.2. UPLC-PDA chromatograms of compound **1** mixed with water after 0, 10, and 52 minutes. Peak with $t_r \approx 3.06$ is compound **1**, $t_r \approx 2.73$ is compound **Y**, and $t_r \approx 1.40$ is starting material **I.** For the chromatogram taken at 52 mins there was a shift in retention time of approximately 0.03 compared to the chromatograms taken at 0 and 10 mins

Another challenge of the synthesis was also related to the product's stability. When the final product solution was concentrated on a rotary evaporator, the temperature of the water bath turned out to have strong influence on the stability. The warmer the bath was, the higher degree of degradation of **1** was observed. Therefore, this product was recovered from DCM solution at 30 ˚C, where as normal water bath temperature for removing DCM is typically at 60 ˚C.

Since product **1** is unstable in contact with water, work-up with aqueous solution is not a suitable condition if it is long-lasting. Hence, washing steps with acid and base had to be done within a short amount of time.

5.3 Synthesis of 2-((5-nitropyridin-2-yl)disulfanyl)ethanamine (II)

1,2-Bis(5-nitropyridin-2-yl)disulfane was reacted with 2-aminoethanethiol hydrochloride as shown in Figure 4.4 to furnish **II** as a white solid in 9.4% yield (0.0587 g, 0.254 mmol). The purity was estimated to 100% by UPLC-PDA as shown in Appendix figure 2. The product gave a mass spectrum as shown in Appendix figure 12 giving a protonated molecular ion with m/z 232.0213 corresponding to the elemental composition $C_7H_9N_3O_2S_2$, which corresponds to the protonated monoisotopic mass of 232.0211 g/mol of first step product **II**.

The NMR spectra (see Appendix figure 31 and Appendix figure 32) gave the following results: ^{1}H NMR (400 MHz, DMSO-d_6) δ 9.31 (d, *J* = 2.6 Hz, 1H), 8.58 (dd, *J* = 8.9, 2.6 Hz, 1H), 8.09 (bs, 3H), 8.05 (d, *J* = 8.9 Hz, 1H), 3.13 (bs, 4H). ^{13}C NMR (100 MHz, DMSO) δ 166.1, 145.1, 142.5, 132.7, 120.2, 37.8, 34.9.

This reaction was analogous to the reaction described in paragraph *5.1* and the only difference was that the pyridine ring of the starting material contained a nitro group. This additional nitro group had an influence on the solubility of the reaction product. Unlike **I**, **II** was found to be insoluble in the recrystallisation solvents used in **I**. Therefore, purification by preparative HPLC was carried out instead of recrystallisation. The final product was obtained as a mixture of free base and hydrochloric acid salt. Peak splitting of the PDA chromatogram is most likely due to the exchange of chloride salt with the corresponding base of TFA.

This compound was used for the synthesis of the corresponding linker which unfortunately gave a very complex mixture, which in turn made the synthesis of the linker unsuccessful. The formation of a complex mixture during the reaction between **II** and diphosgene was believed to be caused by the presence of nitro groups. It is unknown how these nitro groups reacted, however, it is know that aliphatic nitro compounds react with isocyanate (24).

5.4 Synthesis of *N*-(2-(pyridin-2-yldisulfanyl)ethyl)butan-1-amine (III)

1,2-Di(pyridin-2-yl)disulfane was reacted with 2-(butylamino)ethanethiol as shown in Figure 4.5 to furnish **III** as a yellow oil in 4.4% yield (0.0655 g, 0.2707 mmol). The purity was estimated to 98.8% by UPLC-PDA as shown in Appendix figure 3. The product gave a mass spectrum as shown in Appendix figure 13 giving a protonated molecular ion with m/z 243.0994 corresponding to the elemental composition $C_{11}H_{18}N_2S_2$, which corresponds to the protonated monoisotopic mass of 243.0990 g/mol of first step product **III**.

The NMR spectra (see Appendix figure 33 and Appendix figure 34) gave the following results: ^{1}H NMR (400 MHz, Chloroform-d) δ 10.31 (bs, 1H), 8.50 (d, *J* = 5.1 Hz, 1H), 7.66 (td, *J* = 7.8, 1.8 Hz, 1H), 7.44 (d, *J* = 8.0 Hz, 1H), 7.34 – 7.17 (m, 1H), 5.95 (bs, 1H), 3.40 – 3.35 (m, 2H), 3.20 (t, *J* = 5.9 Hz, 2H), 3.06 – 2.99 (m, 2H), 1.81 (q, *J* = 7.5 Hz, 2H), 1.45 (sext, *J* = 7.5 Hz, 2H), 0.97 (t, *J* = 7.4 Hz, 3H). ^{13}C NMR (100 MHz, $CDCl_3$) δ 158.3, 149.7, 137.8, 123.1, 122.6, 46.7, 44.6, 34.4, 28.4, 20.1, 13.6.

A free amine was used for this synthesis and therefore a quick reaction was expected, however, the reaction time was 60 mins. This clearly reflects the reactivity difference between primary and secondary amines. The reaction was monitored by UPLC-PDA and the analysis showed higher conversion rate although the actual isolated yield was found much lower. The most likely reason was loss during chromatographic separation which was caused by a somewhat unsuccessful separation of the product and some contaminants. Because this synthesis was only carried out twice, the optimisation of a purification method has not been done at the time of this report.

5.5 Synthesis of drug-linker conjugate 1A

2-((2-Isocyanatoethyl)disulfanyl)pyridine was reacted with 0.1 M paracetamol solution in ACN as shown in Figure 4.6 to furnish **1A** as a white powder in 61.8% yield (0.0213 g, 0.0587 mmol). The purity was estimated to 82.8% by UPLC-PDA as shown in Appendix figure 4. The product gave a mass spectrum as shown in Appendix figure 14 giving a protonated molecular ion with m/z 364.0799 corresponding to the elemental composition $C_{16}H_{17}N_3O_3S_2$, which corresponds to the protonated monoisotopic mass of 364.0790 g/mol of drug-linker conjugate **1A**.

The NMR spectra (see Appendix figure 35 and Appendix figure 36) gave the following results: ^{1}H NMR (400 MHz, DMSO-d_6) δ 9.96 (s, 1H), 8.53 – 8.39 (m, 1H), 8.02 – 7.70 (m, 3H), 7.54 (d, *J* = 8.8 Hz, 2H), 7.30 – 7.18 (m, 1H), 7.01 (dd, *J* = 9.0, 3.0 Hz, 2H), 3.82 (s, 7H), 3.36 (q, *J* = 6.5 Hz, 2H), 3.08 (tt, *J* = 7.5, 3.8 Hz, 1H), 2.97 (t, *J* = 6.8 Hz, 2H), 2.03 (s, 3H), 1.17 (t, *J* = 7.3 Hz, 1H). ^{13}C NMR (101 MHz, DMSO) δ 168.2, 159.0, 154.6, 149.6, 149.6, 146.2, 137.9, 136.3, 121.9, 121.3, 119.7, 119.3, 45.7, 37.5, 23.9.

Isocyanate is known to be highly reactive toward nucleophiles, which proved to be true when it came to the stability of **1** under contact with water. For this reason, a spontaneous reaction was expected between paracetamol and linker **1**. However, reaction screening by UPLC-PDA analysis revealed that the reaction had not underwent as planned after being left overnight unsupervised. The addition of TEA as catalyst was necessary to make the reaction take place.

5.6 Synthesis of drug-linker-peptide conjugate of 1A (Pep-1A)

4-Acetamidophenyl 2-(2-(pyridin-2-yl)disulfanyl)ethylcarbamate was reacted with HRP1 as shown in Figure 4.7 to furnish **Pep-1A** as a white powder. The purity was estimated to 77.9% by UPLC-PDA as shown in Figure 5.3. The product gave a mass spectrum as shown in Figure 5.4 giving a molecular protonated ion with m/z 1545.6100 corresponding to the elemental composition of $C_{66}H_{83}N_{26}O_{15}S_2$, which corresponds to the protonated monoisotopic mass of 1545.6050 g/mol of drug-linker-peptide conjugate **Pep-1A**.

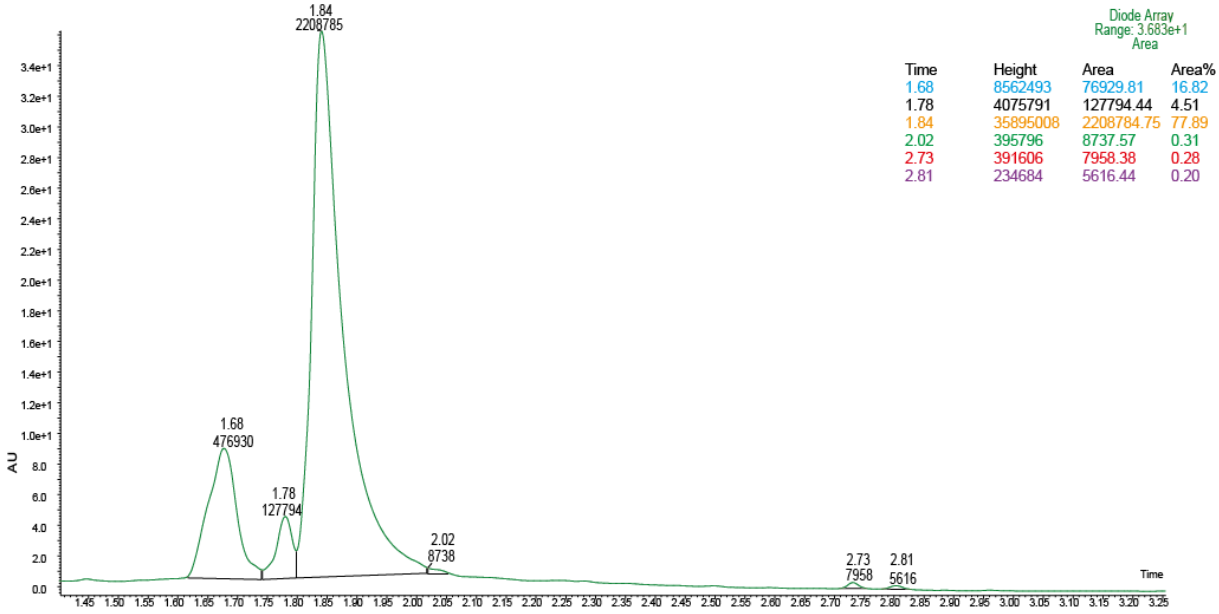

Figure 5.3. UPLC-PDA chromatogram of compound **Pep-1A**

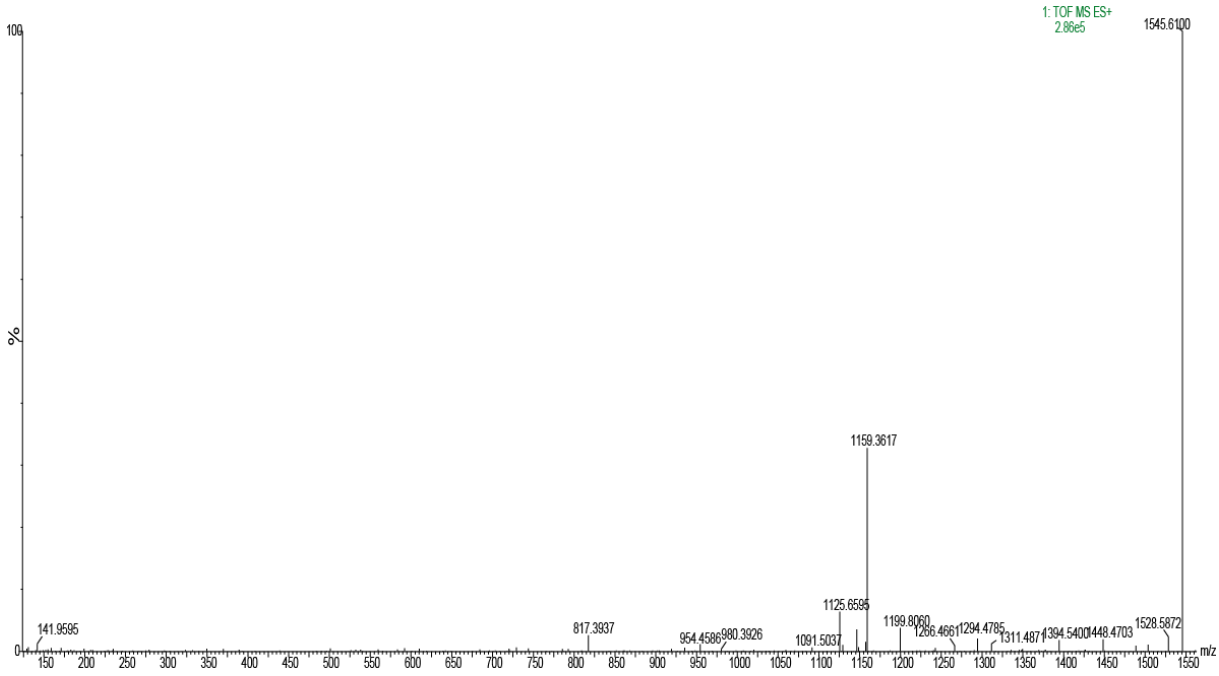

Figure 5.4. ESI-QToF spectrum of compound **Pep-1A**

A relatively slow reaction of approximately 16 h took place for the final conjugation of peptide to the drug-linker conjugate **1A**. The drug-linker conjugate is more soluble in acetonitrile whereas the peptide is soluble in water. Therefore, finding a suitable ratio between water and acetonitrile appeared to be important to get all components into solution. The reaction mixture developed a yellow colour as the concentration of thiopyridine increased. The thiol group of the peptide can attack both sulphur atoms of

the disulphide bond. If the attack took place at the sulphur atom on the drug side, it would result in formation of drug-linker-peptide and thiopyridine. If the attack took place at the sulphur atom on the pyridine side, it would result in formation of peptide thiopyridyl disulphide and drug-linker-thiol (see Figure 5.5). The latter would then undergo self-release and free drug would be formed. The formation of free drug was not observed and this suggests that disulphide-thiol exchange reaction took place in a selective manner, mainly through pathway **a**. This drug-linker-peptide conjugate was further used for kinetic analysis.

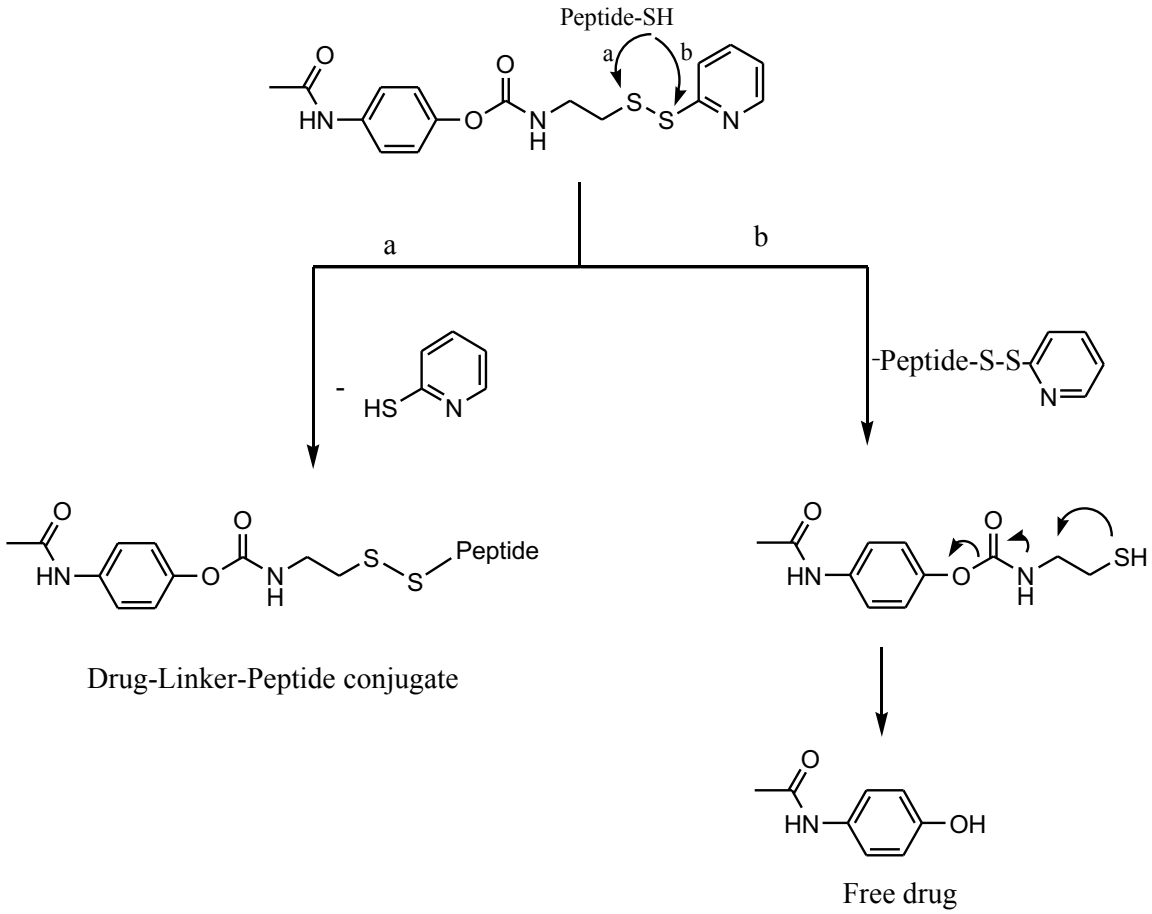

Figure 5.5. Graphic representation showing the outcome from pathway **a** and **b** of peptide conjugation

5.7 Synthesis of linker 2

N-(2-(pyridin-2-yldisulfanyl)ethyl)butan-1-amine was reacted with trichloromethyl chloroformate as shown in Figure 4.8 to furnish **2** as a clear oil in 11.5% yield (0.014 g, 0.0461 mmol). The purity was estimated to 78.5% by UPLC-PDA as shown in Appendix figure 5. The product gave a mass spectrum as shown in Appendix figure 15 giving a protonated ion with m/z 305.0538 corresponding to the elemental composition $C_{12}H_{17}N_2OS_2Cl$, which corresponds to the protonated monoisotopic mass of 305.0550 g/mol of linker **2**.

The NMR spectra (see Appendix figure 37 and Appendix figure 38) gave the following results: ^{1}H NMR (400 MHz, Chloroform-d) δ 8.50 (t, *J* = 5.2 Hz, 1H), 7.77 – 7.56 (m, 2H), 7.21 – 7.04 (m, 1H), 3.77 – 3.67 (m, 2H), 3.46 (t, *J* = 7.7 Hz, 1H), 3.36 (t, *J* = 7.6 Hz, 1H), 3.13 – 2.90 (m, 2H), 1.61 – 1.53 (m, 2H), 1.32 – 1,28 (m, 2H), 0.95 – 0.88 (m, 3H). ^{13}C NMR (100 MHz, $CDCl_3$) Rotamer 1: δ 159.3, 149.9, 149.6, 137.3, 121.2, 120.3, 52.4, 49.1, 35.4, 30.7, 19.9, 13.8. Rotamer 2: δ 159.1, 150.0, 149.0, 137.3, 121.3, 120.4, 50.5, 50.3, 36.2, 29.8, 20.0, 13.8.

Although the starting material was in the form of a free amine, an exploratory synthesis was carried out according to the protocol adopted from literature. Due to the assumption of a very short reaction time, the reaction was not followed by UPLC-PDA analysis. By performing another synthesis of **2** one could try a prolonged reaction time beyond what was described to see if the yield improves. The same pre-work up condition was applied, although it might not have been necessary to wash with aqueous base prior to the reaction. The analysis of the crude product indicated that the expected product had been generated. Optimization of this reaction is today under way and was beyond the scope of this thesis. The product obtained was used for further transformation.

5.8 Synthesis of linker 3

N-(2-((5-nitropyridin-2-yl)disulfanyl)ethyl)butan-1-amine was reacted with trichloro-methyl chloroformate as shown in Figure 4.9 to furnish **3** as a yellow oil in 61.1% yield (0.0096 g, 0.0275 mmol). The purity was estimated to 82.7% by UPLC-PDA as shown in Appendix figure 6. The product gave a mass spectrum as shown in Appendix figure 16 giving a protonated molecular ion with m/z 350.0399 corresponding to the elemental

composition $C_{12}H_{16}N_3O_3S_2Cl$, which corresponds to the protonated monoisotopic mass of 350.0401 g/mol of linker **3**.

The NMR spectra (see Appendix figure 39 and Appendix figure 40) gave the following results: ^{1}H NMR (400 MHz, $CDCl_3$) δ 9.32 (dd, *J* = 5.4, 2.6 Hz, 1H), 8.43 (dd, *J* = 8.8, 2.4 Hz, 1H), 7.84 (dd, *J* = 8.9, 5.8 Hz, 1H), 3.78 – 3.66 (m, 2H), 3.49 – 3.36 (m, 2H), 3.11 – 3.06 (m, 2H), 1.65 – 1.54 (m, 2H), 1.37 – 1.26 (m, 2H), 0.97 – 0.91 (m, 3H). ^{13}C NMR (100 MHz, $CDCl_3$) δ 167.6, 149.8, 145.5, 142.4, 131.9, 119.8, 52.4 (rotamer 1) and 50.6 (rotamer 2), 50.3 (rotamer 2) and 49.1 (rotamer 1), 36.3 (rotamer 2) and 35.5 (rotamer 1), 30.8 (rotamer 2) and 29.8 (rotamer 1), 20.0, 13.8.

There was no essential difference between the synthesis of **3** and **2**.

5.9 Synthesis of drug-linker conjugate 2A

Butyl(2-(pyridin-2-yldisulfanyl)ethyl)carbamic chloride was reacted with 0.1 M paracetamol solution in ACN as shown in Figure 4.10 to furnish **2A** as a light, yellow oil. The purity was estimated to 100% by UPLC-PDA as shown in Appendix figure 7. The product gave a mass spectrum as shown in Appendix figure 17 giving a protonated molecular ion with m/z 420.1433 corresponding to the elemental composition $C_{20}H_{25}N_3O_3S_2$, which corresponds to the protonated monoisotopic mass of 420.1416 g/mol of drug-linker conjugate **2A**. The amount of the sample used for NMR was unfortunately too low to obtain a signal with sufficient resolution. The elemental composition of the synthesis product combined with the correct mass obtained by MS indicate that the compound was synthesised successfully.

When linker **2** was mixed with drug in the presence of TEA, no reaction took place even after 20 h. Addition of DMAP into the reaction mixture made the reaction occur. Analyses showed that in addition to the desired drug-linker conjugate, an unknown product was formed. MS analysis suggested that this compound could be an adduct consisting of **2** and DMAP, however, structure of this compound could not be elucidated.

5.10 Synthesis of drug-linker conjugate 3A

Butyl(2-((5-nitropyridin-2-yl)disulfanyl)ethyl)carbamic chloride was reacted with 0.1 M paracetamol solution in ACN as shown in Figure 4.11 to furnish **3A** as a white powder in 100% yield (0.0092 g, 0.0198 mmol). The purity was estimated to 99.2% by UPLC-PDA as shown in Appendix figure 8. The product gave a mass spectrum as shown in Appendix figure 18 giving a protonated molecular ion with m/z 465.1260 corresponding to the elemental composition $C_{20}H_{24}N_4O_5S_2$, which corresponds to the protonated monoisotopic mass of 465.1267 g/mol of drug-linker conjugate **3A**. The amount of the sample used for NMR was unfortunately too low to obtain a signal with sufficient resolution. Suggested elemental composition combined with the correct mass obtained by MS indicate that the compound was synthesised successfully.

The synthesis of **3A** was essentially the same as **2A** with the structural difference of a nitro group in para position on the pyridine ring. Two fractions were collected from preparative HPLC, where one of the fractions showed a mass that corresponds with an adduct consisting of linker **3** and DMAP. The yield was unnaturally high due to some impurities shown in the UPLC-PDA chromatogram. Though the compound was impure, the correct mass was identified but the biproduct could not be revealed. The decision to not go any further with compound **3A** was made because it would give the same product as **2A** would furnish.

5.11 Synthesis of drug-linker conjugate 1B

2-((2-Isocyanatoethyl)disulfanyl)pyridine was reacted with 0.25 M *N*-(4-aminophenyl)-acetamide solution in ACN as shown in Figure 4.12 to furnish **1B** as an off-white powder in 44.2% yield (0.0167 g, 0.0461 mmol). The purity was estimated to 80.9% by UPLC-PDA as shown in Appendix figure 9. The product gave a mass spectrum as shown in Appendix figure 19 giving a protonated molecular ion with m/z 363.0958 corresponding to the elemental composition $C_{16}H_{18}N_4O_2S_2$, which corresponds to the protonated monoisotopic mass of 363.0950 g/mol of drug-linker conjugate **1B**.

The NMR spectra (see Appendix figure 41 and Appendix figure 42) gave the following results: ^{1}H NMR (400 MHz, DMSO-d_6) δ 9.75 (s, 1H), 8.63 – 8.35 (m, 2H), 7.92 – 7.69 (m, 2H), 7.53 – 7.07 (m, 4H), 6.34 (t, *J* = 5.9 Hz, 1H), 3.39 – 3.34 (m, 2H), 2.94 (t, *J* = 6.6 Hz, 2H),

1.99 (s, 3H). ^{13}C NMR (100 MHz, DMSO) δ 167.7, 159.0, 155.1, 149.6, 149.6, 137.8, 135.7, 133.2, 121.2, 121.1, 119.6, 119.5, 119.3, 119.2, 118.1, 45.7, 38.5, 38.4, 38.2, 23.8.

The MS and NMR data combined shows that the expected compound was successfully synthesised.

5.12 Synthesis of drug-linker-peptide conjugate of 1B (Pep-1B)

N-(4-(3-(2-(pyridin-2-yldisulfanyl)ethyl)ureido)phenyl)acetamide was reacted with HRP1 as shown in Figure 4.13 to furnish **Pep-1B** as a light, yellow powder in 56.8% yield (0.0237 g, 0.0154 mmol). The purity was estimated to 99.6% by UPLC-PDA as shown in Figure 5.6. The product gave a mass spectrum as shown in Figure 5.7 giving a protonated molecular ion with m/z 1544.6171 corresponding to the elemental composition $C_{66}H_{84}N_{27}O_{14}S_2$, which corresponds to the protonated monoisotopic mass of 1544.6177 g/mol of drug-linker-peptide conjugate **Pep-1B**.

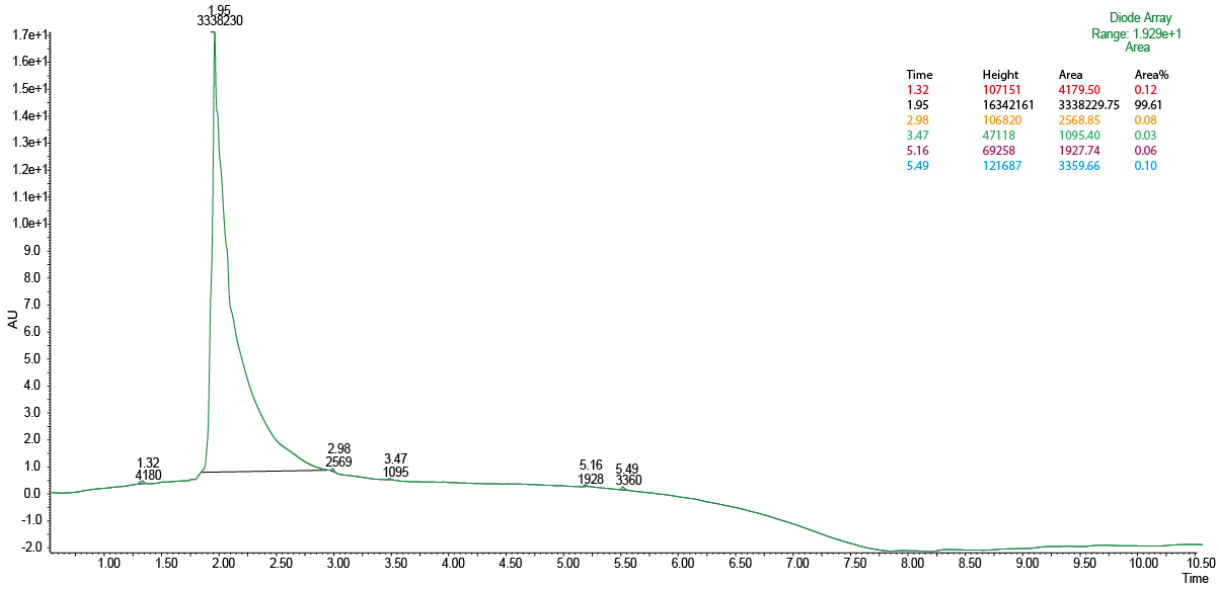

Figure 5.6. UPLC-PDA chromatogram of compound **Pep-1B**

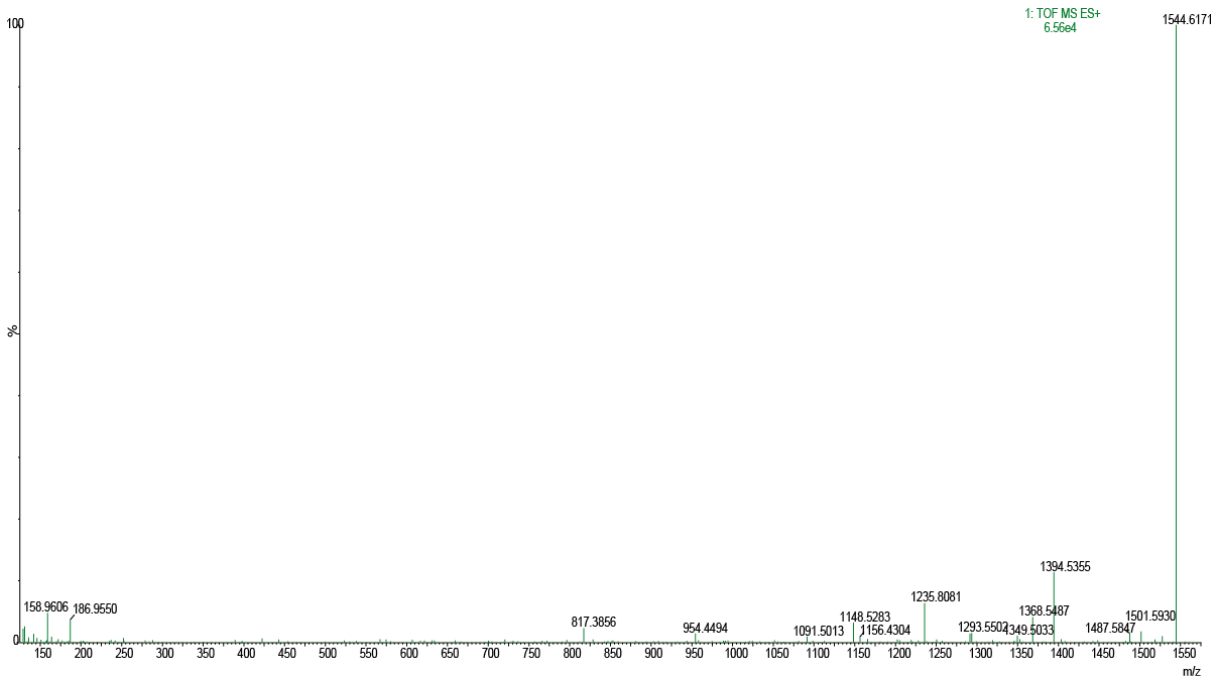

Figure 5.7. ESI-QToF spectrum of compound **Pep-1B**

The peptide used consisted of both HRP1 and a deletion sequence that contained one histidine less than the original sequence. This was of no consequence as the compound **Pep-1B** was successfully synthesised according to the MS data. The reaction was followed on UPLC-PDA and MS, and the results showed that some of the starting material did not react with the peptide. This drug-linker-peptide conjugate was further used for kinetic analysis.

5.13 Synthesis of drug-linker-peptide conjugate of 2A (Pep-2A)

4-Acetamidophenyl butyl(2-(pyridin-2-yldisulfanyl)ethyl)carbamate was reacted with HRP1 as shown in Figure 4.14 to furnish **Pep-2A** as a white powder. The purity was estimated to 90.8% by UPLC-PDA as shown in Figure 5.8. The product gave a mass spectrum as shown in Figure 5.9 giving a protonated molecular ion with m/z 1601.6715 corresponding to the elemental composition $C_{70}H_{91}N_{26}O_{15}S_2$, which corresponds to the protonated monoisotopic mass of 1601.6755 g/mol of drug-linker-peptide conjugate **Pep-2A**.

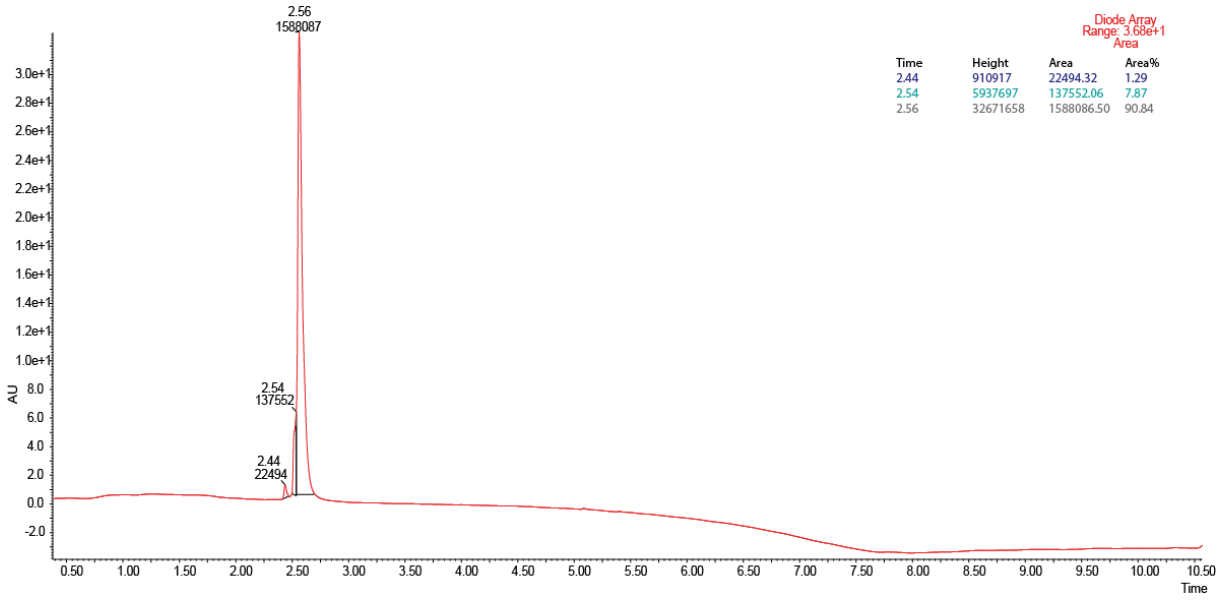

Figure 5.8. UPLC-PDA chromatogram of compound **Pep-2A**

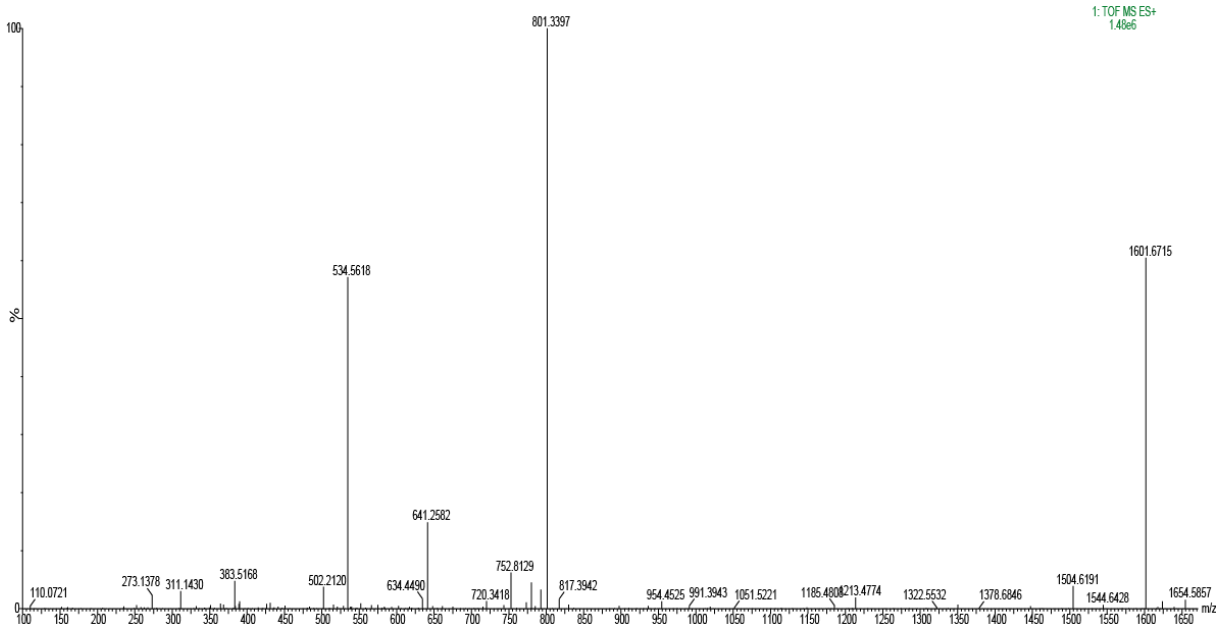

Figure 5.9. ESI-QToF spectrum of compound **Pep-2A**

The same peptide was used for **Pep-2A** as with **Pep-1B**. The chromatography from the PDA showed a peak shoulder which could be the deletion peptide. The reaction was followed on UPLC-PDA and MS and showed no starting material present in the reaction after approximately 20 h. The weight of the synthesised product was too low to present a yield. This drug-linker-peptide conjugate was further used for kinetic analysis.

5.14 Kinetic analyses of synthesised products

The release profile with two different glutathione concentrations over a 24 h period has been studied by Cheetam AG., et al. (25). They examined the release of camptothecin (CPT) from self-assembling drug amphiphiles induced by intracellular reduction. It showed that different GSH concentrations influence the stability and the drug release from the disulphide dimer. In another study by Xu Z., et al., the release of CPT from a glutathione sensitive disulphide linker was examined (26). In vitro cumulative release of CPT with 10 mM GSH solution was compared with 0 mM GSH solution, where there was a greater release of CPT with 10 mM GSH. These studies show that the concentration of reduced glutathione is of importance when performing kinetic analyses, and should therefore not be neglected.

To measure the drug release, glutathione was added to the drug-linker-peptide conjugates. To imitate intracellular glutathione concentrations, a solution of 50 mM reduced and 5 mM oxidised glutathione was added. The ratio of GSH/GSSG used for kinetic analyses was 10:1, respectively, and could be considered low compared to the intracellular ratio which varies from 100:1 to 1000:1. It is problematic to predict the drug release from the drug-linker-peptides with a larger GSH ratio, but it may induce a greater release of free drug compared to what was seen in this project.

In general, when measuring the drug release from the kinetic analyses, the measurements were more frequent in the beginning. After approximately one hour, the frequency of the measurements were adapted to the changes in concentration seen on UPLC-PDA.

The following figure is chromatograms taken at different times showing the drug release from **Pep-1A**.

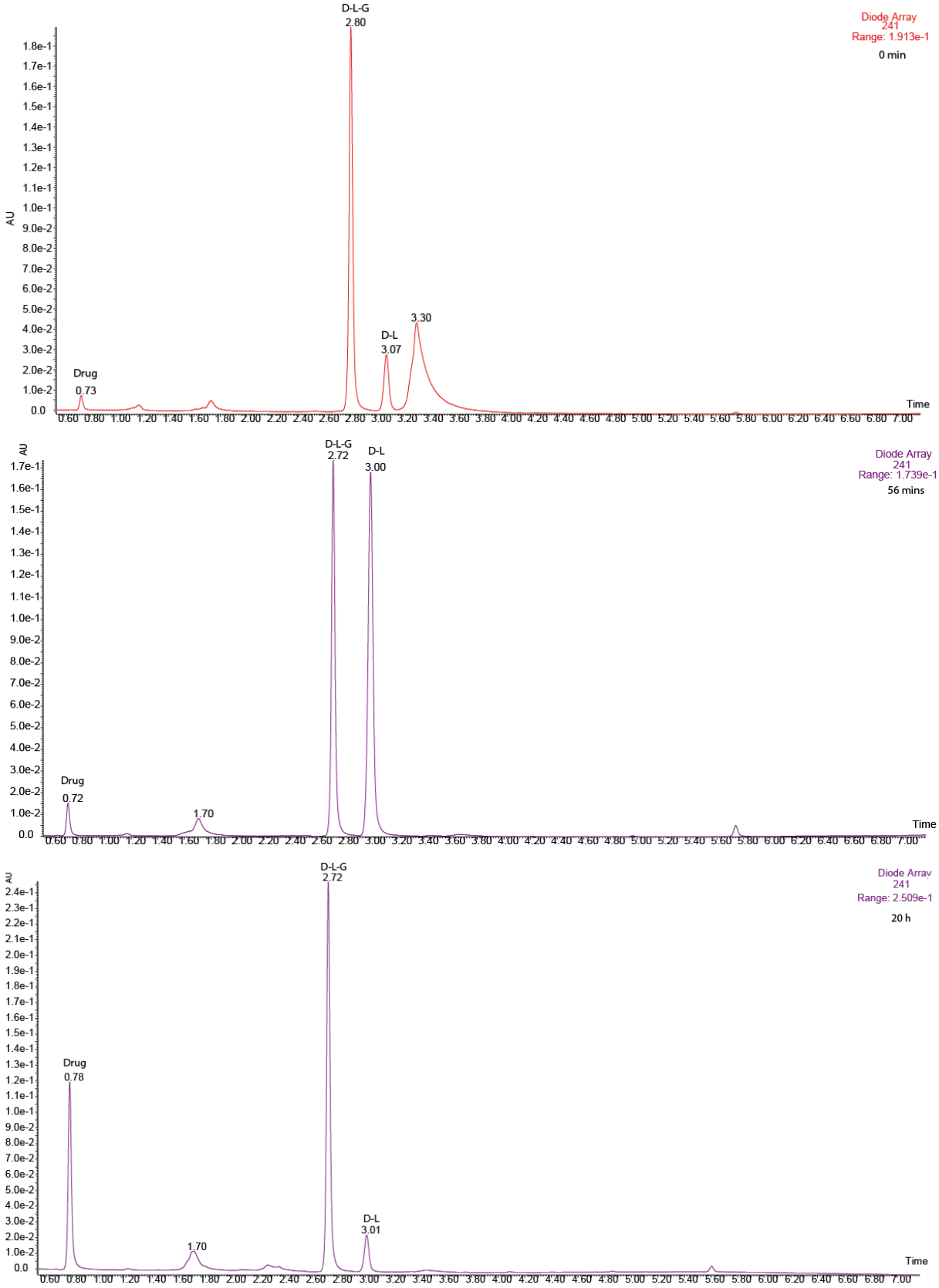

Figure 5.10. UPLC-PDA chromatograms with selected wavelength of 241 nm, taken at 0 min, 56 mins, and 20 h of **Pep-1A** with GSH/GSSG solution in phosphate buffer with pH 7.4. For the chromatograms taken at 56 mins and 20 h there was a shift in retention time of approximately 0.07 compared to the chromatogram taken at 0 min

When comparing the chromatograms shown in Figure 5.10 you can see the increase of free drug which has a retention time (t_R) ≈ 0.7. The selected wavelength of 241 nm is paracetamol's absorption maximum. Drug-linker-glutathione has a t_R ≈ 2.72, and t_R for drug-linker is ≈ 3.00. Furthermore, the figure shows an increase of drug-linker at 56 min, and then a decrease at 20 h. MS spectra for the mentioned degradation products are shown in Appendix figure 20, Appendix figure 21, and Appendix figure 22.

Figure 5.11 shows the release of paracetamol (drug) from the drug-linker (D-L) conjugate **1A**. In the beginning of the analysis, the formation of drug-linker-glutathione (D-L-G) from the drug-linker-peptide conjugate happened almost instantly. During the first three hours, there was a considerable escalation of formation of drug-linker from drug-linker-glutathione. In the beginning of the kinetic analysis, the drug release was exponentially higher compared to approximately 18 h when the release slows down and forms what is known as a plateau. At 34 h, 35% of the drug was released. The drug-linker concentration got lower as the drug was released. What you also see from this plot is that the drug-linker-glutathione concentration increased accordingly as the drug-linker concentration decreased.

There was a second addition of GSH/GSSG solution at 44 h when the drug-linker concentration was very low. This showed an increase in drug-linker concentration and a decrease of drug-linker-glutathione, but not an increase of free drug. Because of the same trend as previously discussed, it was not deemed necessary to include in the plot.

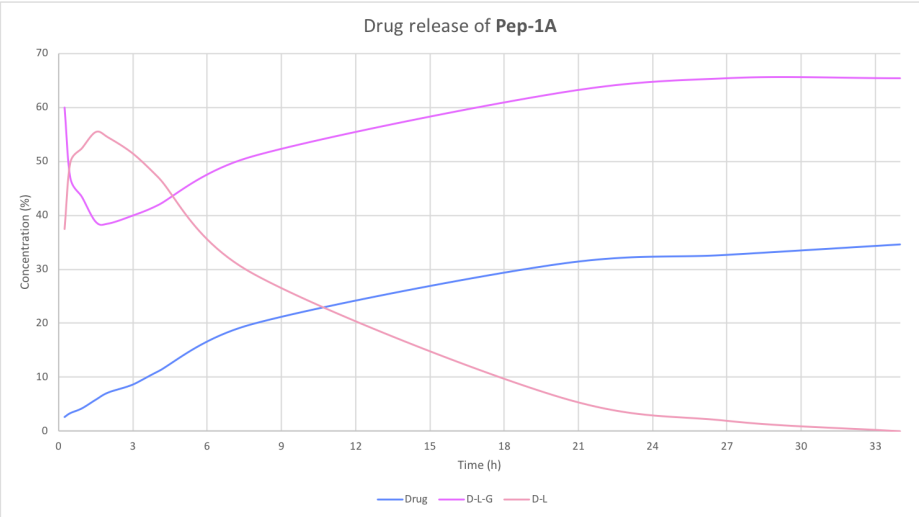

Figure 5.11. Scatter plot showing changes in concentration over time for the three degradation products from **Pep-1A**

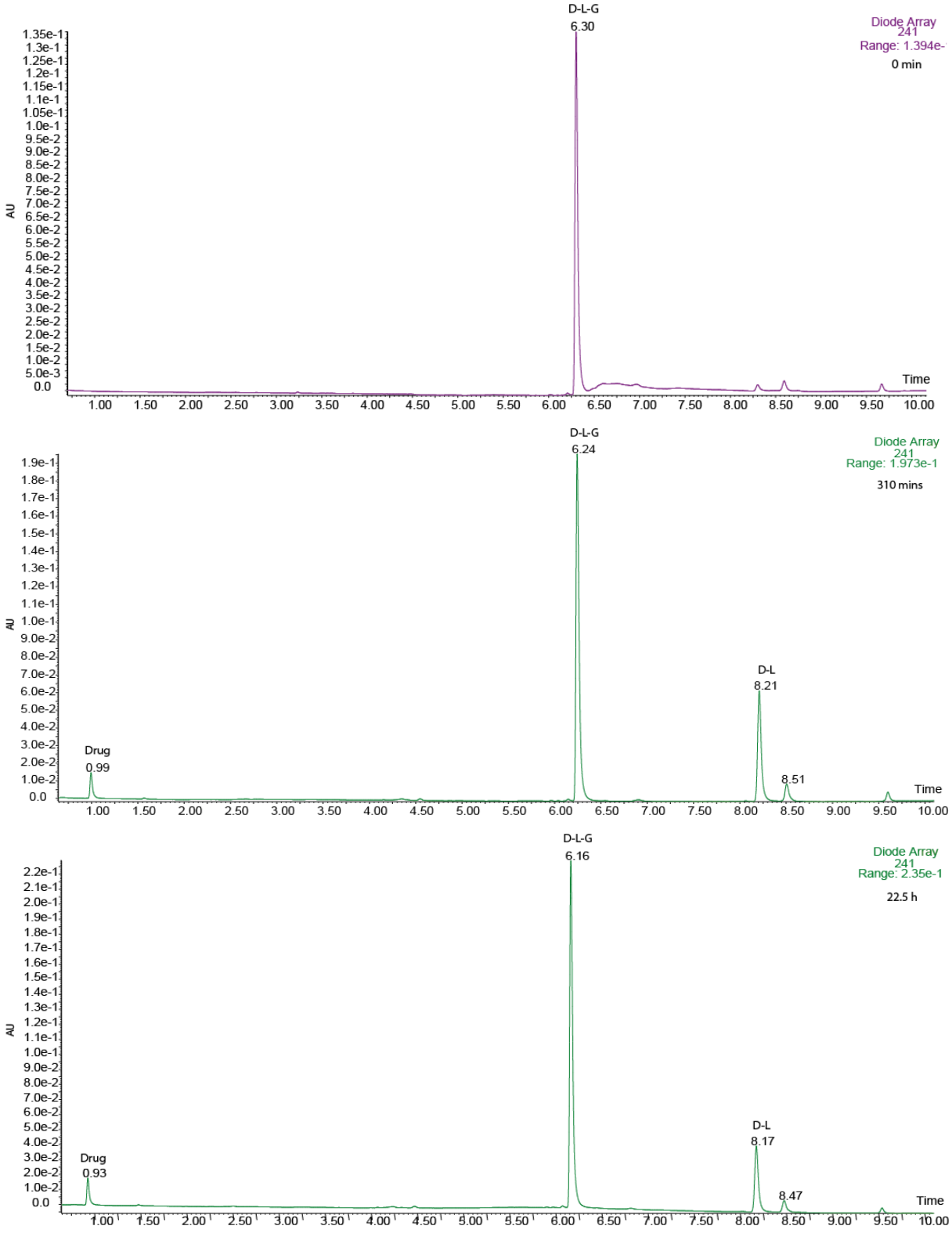

Figure 5.12. UPLC-PDA chromatograms with selected wavelength of 241 nm, taken at 0 min, 310 mins, and 22.5 h of **Pep-2A** with GSH/GSSG solution in phosphate buffer with pH 7.4. For all the chromatograms there was a shift in retention time of approximately 0.07

In Figure 5.12 the chromatograms show high peaks of drug-linker-glutathione (D-L-G) at $t_r \approx 6.16$. Drug-linker (D-L) is represented at $t_r \approx 8.17$, and released drug at $t_r \approx 0.9$. There was a clear increase in drug-linker concentration and drug release between 0 min and 310 mins. MS spectra for the mentioned degradation products are shown in Appendix figure 23, Appendix figure 24, and Appendix figure 25.

Figure 5.13 shows the release of paracetamol (drug) from **Pep-2A**. There is a similar trend for drug-linker-glutathione and drug-linker concentration in this analysis as with the analysis shown in Figure 5.11. There is a big difference in drug release between these two plots. Only 5% of the drug in Figure 5.13 was released in 22.5 h, whereas in Figure 5.11, 32% of the drug was released in 20 h. As with the other kinetic analysis there was a second addition of GSH/GSSG solution to see if the drug release improved. Though it did increase, it only reached 12% after 141 h altogether. Because of the slow release of drug, there was a slow decrease of drug-linker concentration. Over time the drug-linker fragment became oxidized giving rise to a drug-linker-dimer confirmed by MS as shown in Appendix figure 26. Concentrations shown in Figure 5.11 and Figure 5.13 are calculated from relative PDA peak areas and must only be seen as semi-quantitative, but they will still give a fair estimation of relative drug release from different conjugates.

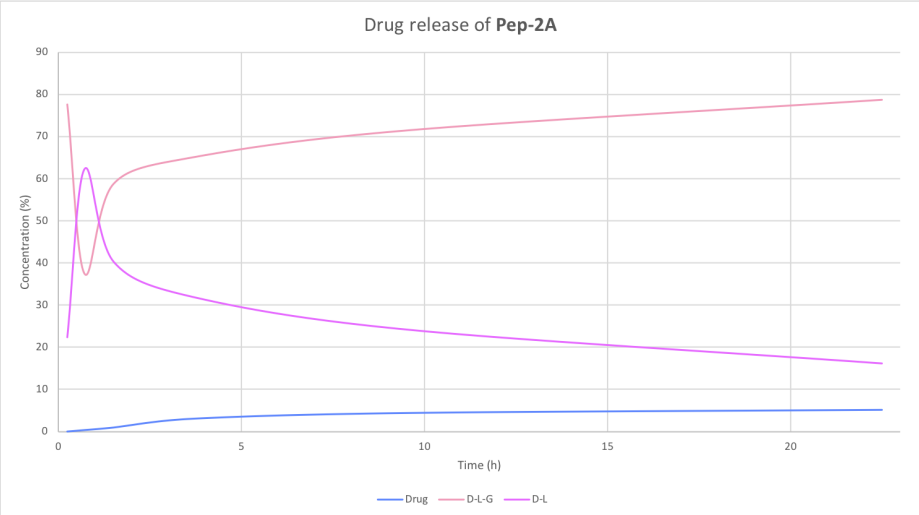

Figure 5.13. Scatter plot showing changes in concentration over time for the three degradation products from **Pep-2A**

Figure 5.14 shows the glutathione reaction with the end product of drug release from the drug-linker, and drug-linker-glutathione reacting with GSH to form the drug-linker conjugate. This reaction is consistent with the findings in both kinetic analyses.

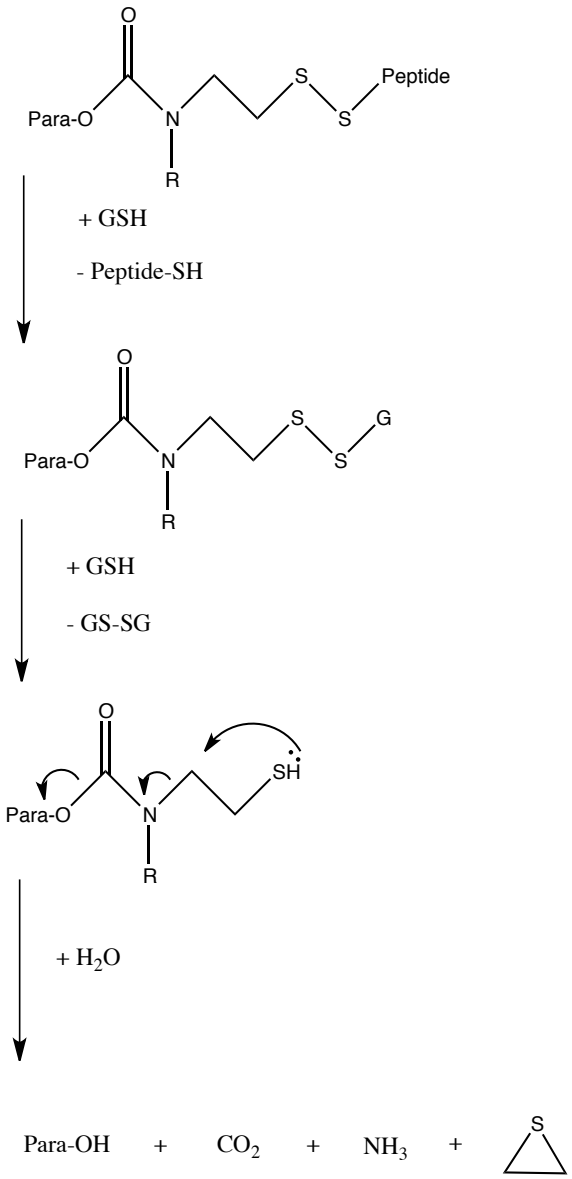

Figure 5.14. Glutathione reaction with drug-linker-peptide conjugate. R = H or butyl

The drug-linker-peptide **Pep-2B** was also tested for drug release by reaction with glutathione, though there was no release of 4-aminoacetanilide after 24 h as confirmed by MS. Compared to carbamoyl, the urea composition (see Figure 5.15) of compound **Pep-2B** might be too stable for self-elimination to take place, thus impairing drug release.

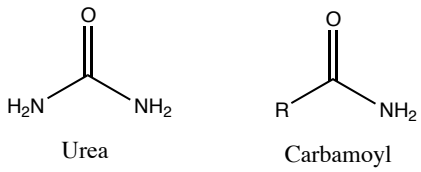

Figure 5.15. Structure of urea and carbamoyl

6 Conclusion

Synthesis of self-eliminating linkers with conjugation to hydroxyl- and amine-containing drugs, and peptide was successful. Overall, synthesis of three first step products, three linkers, four drug-linker conjugates and three drug-linker-peptide conjugates were accomplished.

As previously mentioned, optimisation of the synthesis procedure was not the aim of this thesis, therefore the synthesis yield was not attempted improved. The purity of the synthesis products was 78% or more estimated by UPLC-PDA and was deemed acceptable for further use.

Kinetic analysis of drug release with glutathione was performed on all three drug-linker-peptide conjugates. The urea composition of **Pep-1B** was considered too stable for linker self-elimination, and therefore the observation of free drug was absent. Drug release was observed with drug-linker-peptides **Pep-1A** and **Pep-2A**. Only 5% of the drug from **Pep-2A** was released in 22.5 h, whereas from **Pep-1A**, 32% of the drug was released in 20 h. **Pep-1A** shows a higher release of drug than **Pep-2A**, and could possibly be a better candidate for a potential cytotoxic drug.

7 Future perspectives

The aim of this thesis was to synthesise self-eliminating linkers. Although this was achieved successfully by synthesis of three linkers, they only proved to be suitable for conjugation with hydroxyl-containing drugs due to an extremely stable urea composition with an amine-containing drug. The resulting conjugates showed sufficient stability at physiological pH in the absence of thiol-containing substances. This indicates that both isocyanate and carbamoyl chloride type of linkers are worthy to be studied for further development.

Essentially, the synthesis of isocyanate found to be challenging due to the presence of the highly reactive group and its stability appeared to be low. Alternative synthesis methods for linker **1** should be explored. The presence of substituents on the carbon atom bearing a sulphur atom tends to expedite the release of the drug. Therefore, synthesis of analogous linkers from 1-alkyl-2-aminoethanethiols and a study of their release kinetics are naturally the next thing to explore (27).

Linker **2** and **3** have a bulky substituent on the amine, in which linker **2** showed a substantially reduced drug release compared to linker **1**. This was most likely due to the butyl group on the amine. Linkers with greater and quicker drug release than linker **2** is of obvious interest, and the butyl substituent on the nitrogen can be replaced by a less bulky substituent. Although the linker synthesis during this work was limited to the commercially available starting materials, synthesis of variously substituted 2-aminoethanethiols are worthy to be studied.

When the drug release was tested by kinetic analysis with glutathione on the drug-linker-peptides, only one GSH/GSSG ratio was tested. There is an interest to further investigate a linker's responsiveness with several ratios. The analysis should also be carried out with cytotoxic drugs and find the accurate concentration of the released drug using a standard curve of the drug. To calculate the release in e.g. mg/h, thus achieving a release rate, is of importance for further research.

References

1. Ferlay J, Soerjomataram I, Ervik M, Dikshit R, Eser S, Mathers C, et al. GLOBOCAN 2012 v1.0, Cancer Incidence and Mortality Worldwide: IARC CancerBase No. 11 [Internet]. Lyon, France: International Agency for Research on Cancer; 2013 [Available from: http://globocan.iarc.fr, accessed on 21.11.17].
2. Cancer in Norway 2016 - Cancer incidence, mortality, survival and prevalence in Norway. Oslo: Cancer Registry of Norway; 2017.
3. Chen H, Lin Z, Arnst KE, Miller DD, Li W. Tubulin Inhibitor-Based Antibody-Drug Conjugates for Cancer Therapy. Molecules (Basel, Switzerland). 2017;22(8).
4. Abet V, Filace F, Recio J, Alvarez-Builla J, Burgos C. Prodrug approach: An overview of recent cases. European Journal of Medicinal Chemistry. 2017;127:810-27.
5. Zawilska JB, Wojcieszak J, Olejniczak AB. Prodrugs: a challenge for the drug development. Pharmacological reports : PR. 2013;65(1):1-14.
6. Rautio J, Kumpulainen H, Heimbach T, Oliyai R, Oh D, Jarvinen T, et al. Prodrugs: design and clinical applications. Nature reviews Drug discovery. 2008;7(3):255-70.
7. Beck A, Goetsch L, Dumontet C, Corvaia N. Strategies and challenges for the next generation of antibody-drug conjugates. Nature reviews Drug discovery. 2017;16(5):315-37.
8. Wang J, Shen W, Zaro JL. Antibody-Drug Conjugates: The 21st Century Magic Bullets for Cancer: Springer International Publishing; 2015.
9. Kalim M, Chen J, Wang S, Lin C, Ullah S, Liang K, et al. Intracellular trafficking of new anticancer therapeutics: antibody-drug conjugates. Drug design, development and therapy. 2017;11:2265-76.
10. Firer MA, Gellerman G. Targeted drug delivery for cancer therapy: the other side of antibodies. Journal of hematology & oncology. 2012;5:70.
11. Peters C, Brown S. Antibody-drug conjugates as novel anti-cancer chemotherapeutics. Bioscience reports. 2015;35(4).
12. Perez HL, Cardarelli PM, Deshpande S, Gangwar S, Schroeder GM, Vite GD, et al. Antibody-drug conjugates: current status and future directions. Drug discovery today. 2014;19(7):869-81.
13. Ma L, Wang C, He Z, Cheng B, Zheng L, Huang K. Peptide-Drug Conjugate: A Novel Drug Design Approach. Current medicinal chemistry. 2017;24(31):3373-96.
14. Wang Y, Cheetham AG, Angacian G, Su H, Xie L, Cui H. Peptide-drug conjugates as effective prodrug strategies for targeted delivery. Advanced drug delivery reviews. 2017;110-111:112-26.
15. Zhang W, Song J, Zhang B, Liu L, Wang K, Wang R. Design of acid-activated cell penetrating peptide for delivery of active molecules into cancer cells. Bioconjugate chemistry. 2011;22(7):1410-5.
16. Townsend DM, Tew KD, Tapiero H. The importance of glutathione in human disease. Biomedicine & Pharmacotherapy. 2003;57(3):145-55.
17. Hermann G, Heffeter P, Kryeziu K, Berger W, Hann S, Koellensperger G. The study of reduced versus oxidized glutathione in cancer cell models employing isotopically labelled standards. Analytical Methods. 2014;6(9):3086-94.
18. Yeh CC, Hou MF, Wu SH, Tsai SM, Lin SK, Hou LA, et al. A study of glutathione status in the blood and tissues of patients with breast cancer. Cell Biochemistry and Function. 2006;24(6):555-9.
19. Gamcsik MP, Kasibhatla MS, Teeter SD, Colvin OM. Glutathione levels in human tumors. Biomarkers. 2012;17(8):671-91.

20. Pedersen-Bjergaard S, Rasmussen KE. Legemiddelanalyse. 2 ed. Bergen: Fagbokforlaget; 2010.
21. Vasskog T. HPLC-MS/MS FAR-3002. 2017.
22. Ebright Y, Chen Y, Pendergrast P, Ebright R. Incorporation of an EDTA-Metal complex at a rationally selected site within a protein: Application to EDTA-Iron DNA affinity cleaving with catabolite gene activator protein (CAP) and Cro. 1992;31:10664-70.
23. Sigurdsson ST, Seeger B, Kutzke U, Eckstein F. A Mild and Simple Method for the Preparation of Isocyanates from Aliphatic Amines Using Trichloromethyl Chloroformate. Synthesis of an Isocyanate Containing an Activated Disulfide. The Journal of organic chemistry. 1996;61(11):3883-4.
24. Mukaiyama T, Hoshino T. The Reactions of Primary Nitroparaffins with Isocyanates. Journal of the American Chemical Society. 1960;82(20):5339-42.
25. Cheetham AG, Ou Y-C, Zhang P, Cui H. Linker-Determined Drug Release Mechanism of Free Camptothecin from Self-Assembling Drug Amphiphiles. Chemical communications. 2014;50(45):6039-42.
26. Xu Z, Wang D, Xu S, Liu X, Zhang X, Zhang H. Preparation of a Camptothecin Prodrug with Glutathione-Responsive Disulfide Linker for Anticancer Drug Delivery. Chemistry – An Asian Journal. 2014;9(1):199-205.
27. Sengee M. Personal communication. 2018.

Appendix

PDA chromatograms

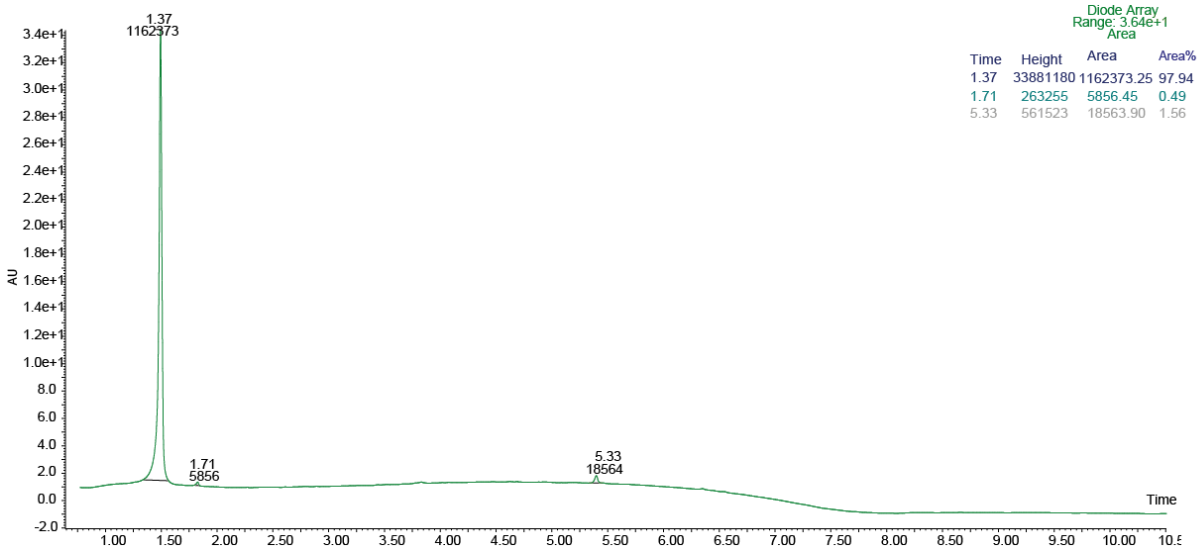

Appendix figure 1. UPLC-PDA chromatogram of compound **I**

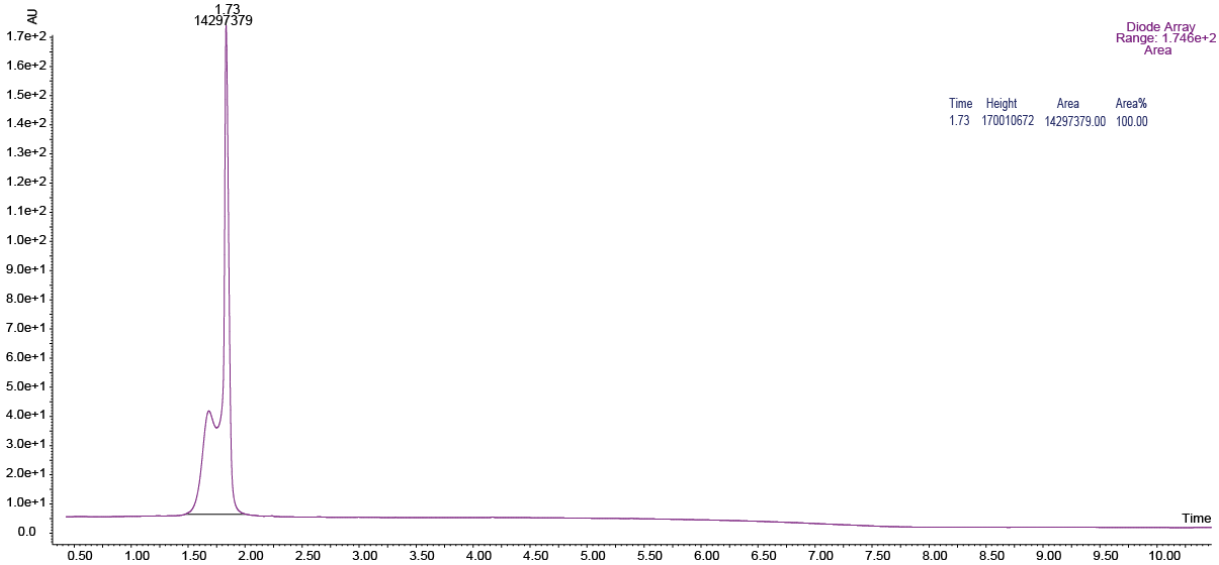

Appendix figure 2. UPLC-PDA chromatogram of compound **II**

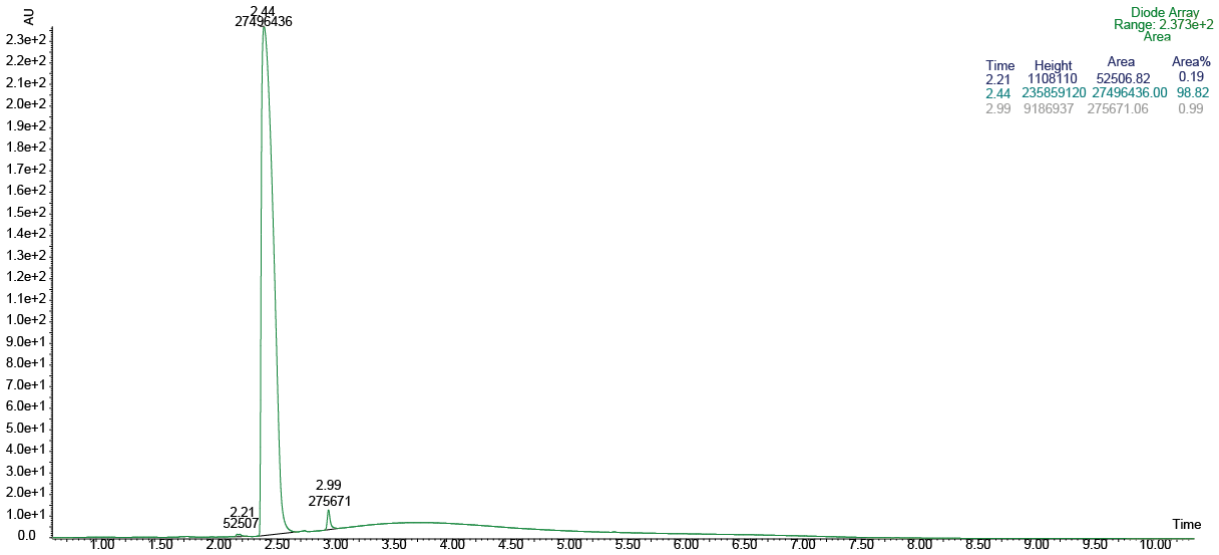

Appendix figure 3. UPLC-PDA chromatogram of compound **III**

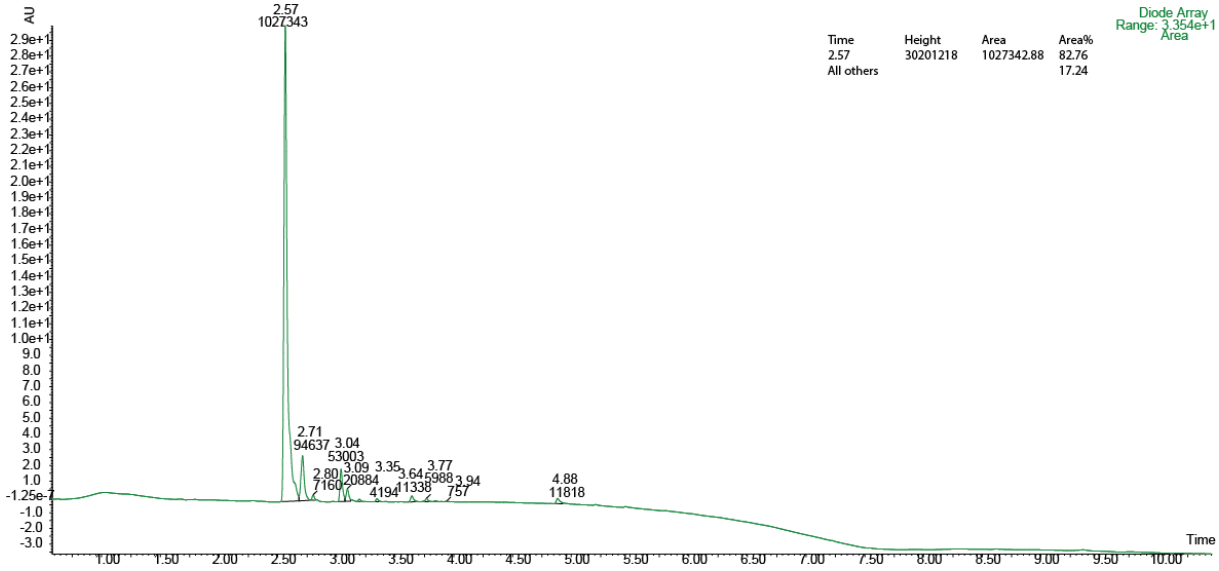

Appendix figure 4. UPLC-PDA chromatogram of compound **1A**

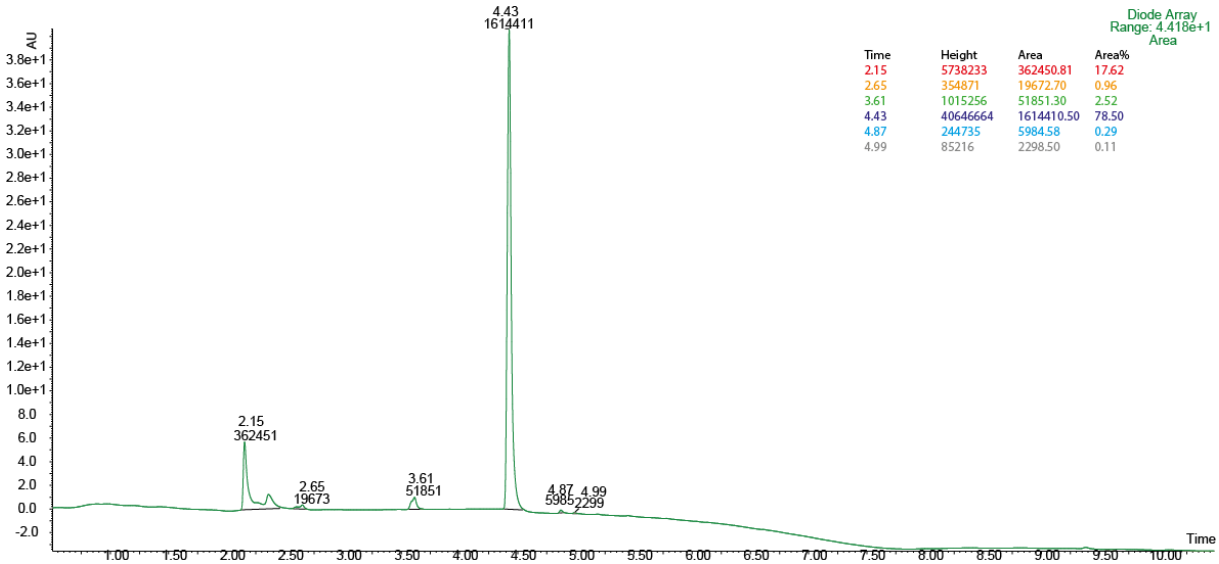

Appendix figure 5. UPLC-PDA chromatogram of compound **2**

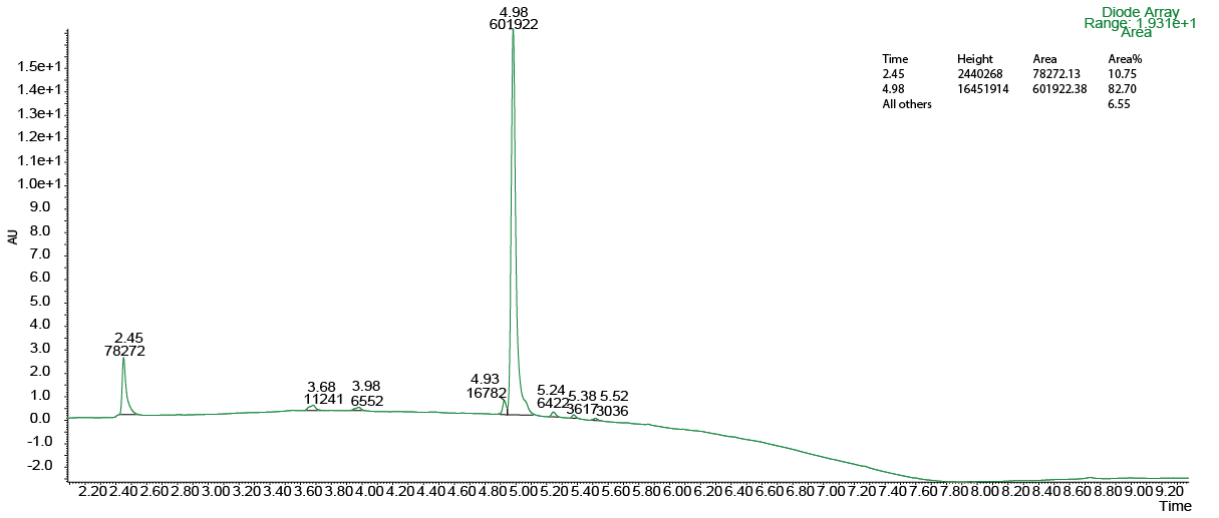

Appendix figure 6. UPLC-PDA chromatogram of compound **3**

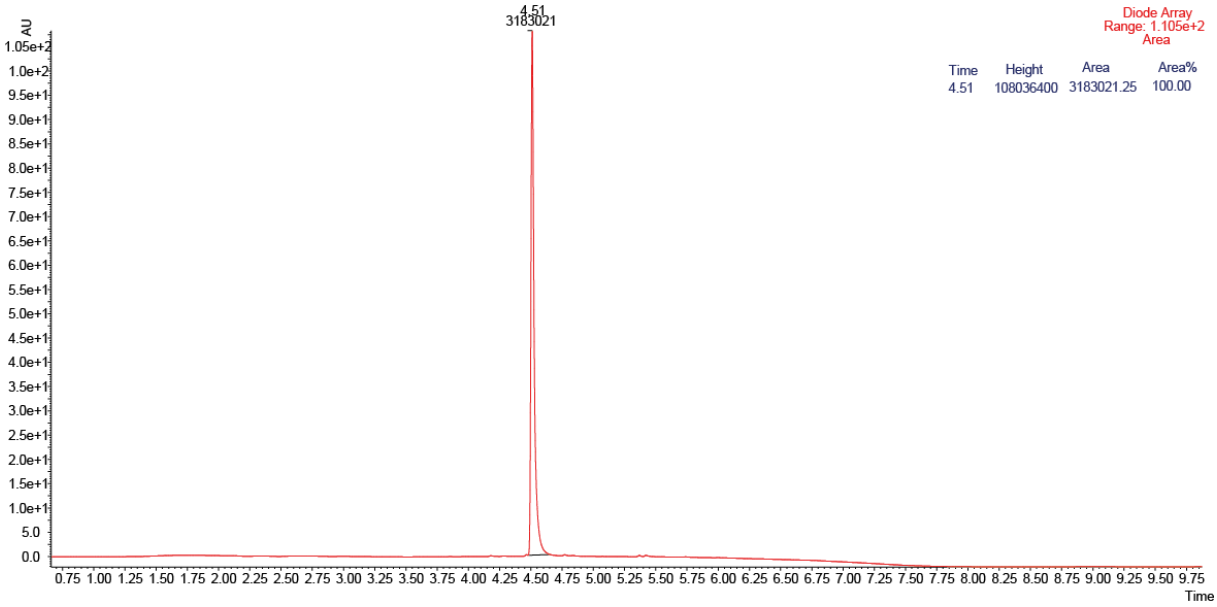

Appendix figure 7. UPLC-PDA chromatogram of compound **2A**

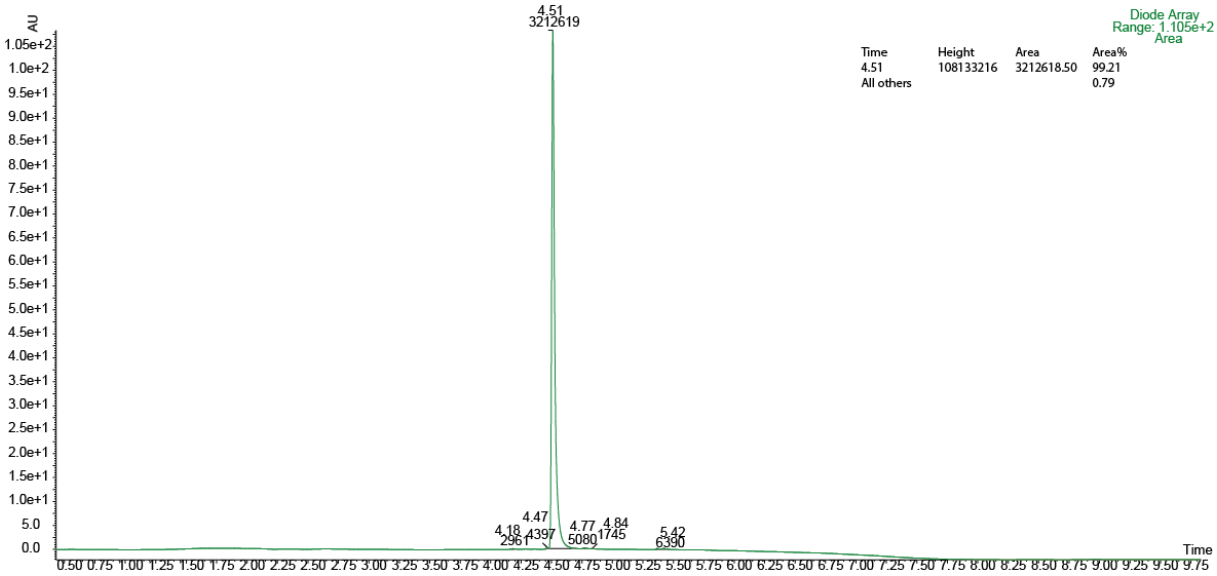

Appendix figure 8. UPLC-PDA chromatogram of compound **3A**

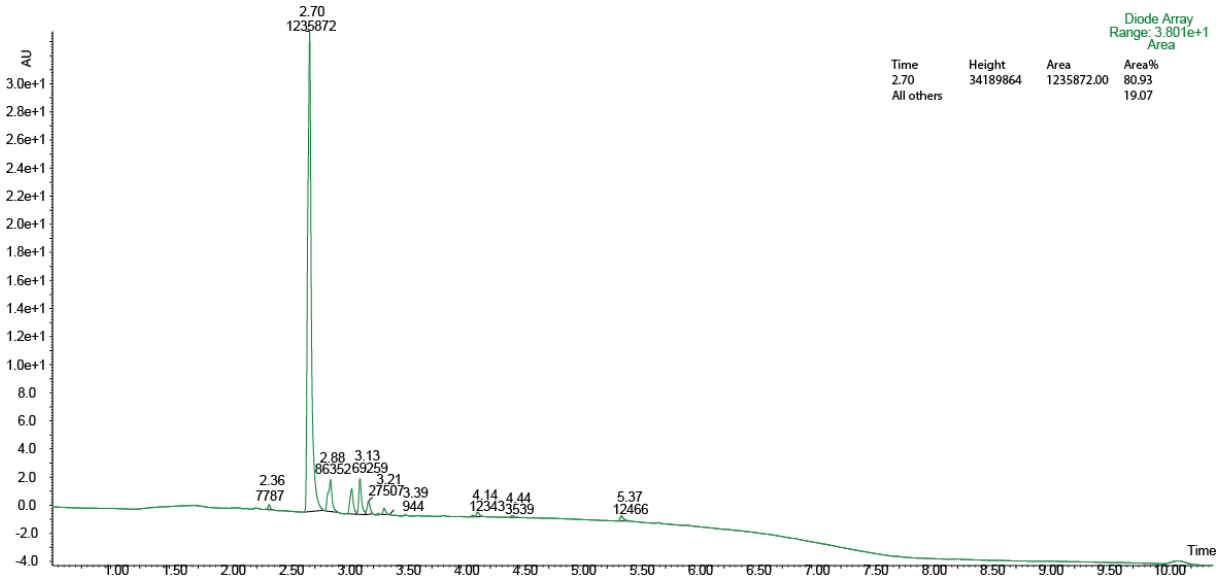

Appendix figure 9. UPLC-PDA chromatogram of compound **1B**

MS spectra

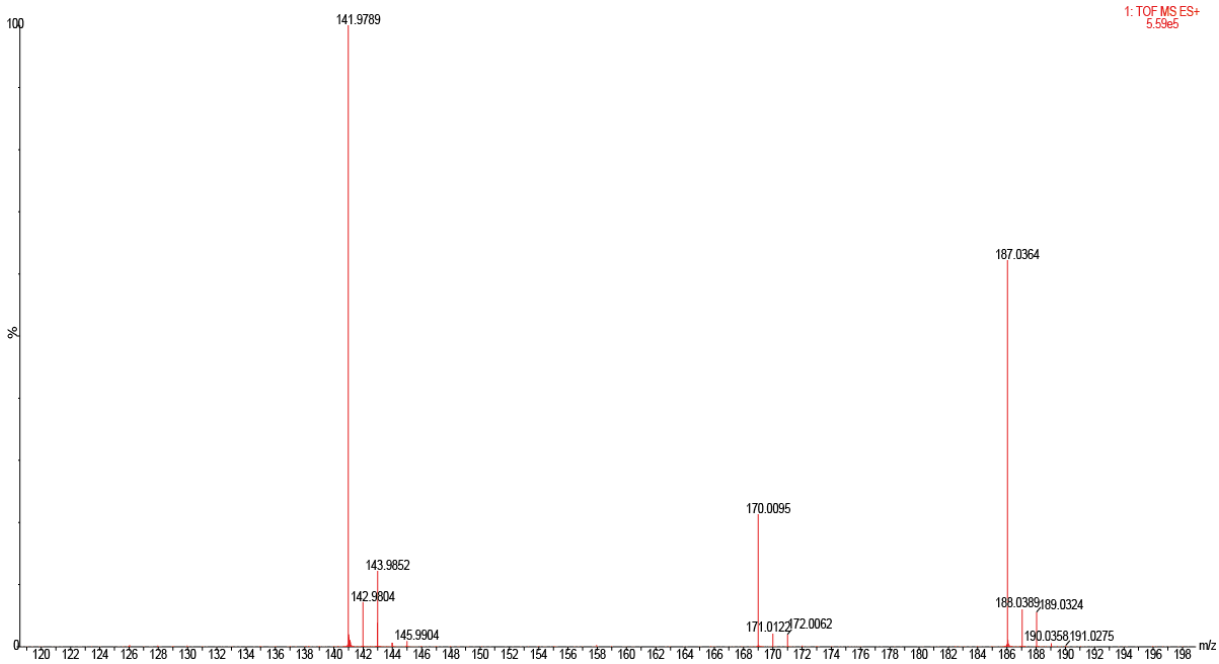

Appendix figure 10. ESI-QToF spectrum of compound **I**

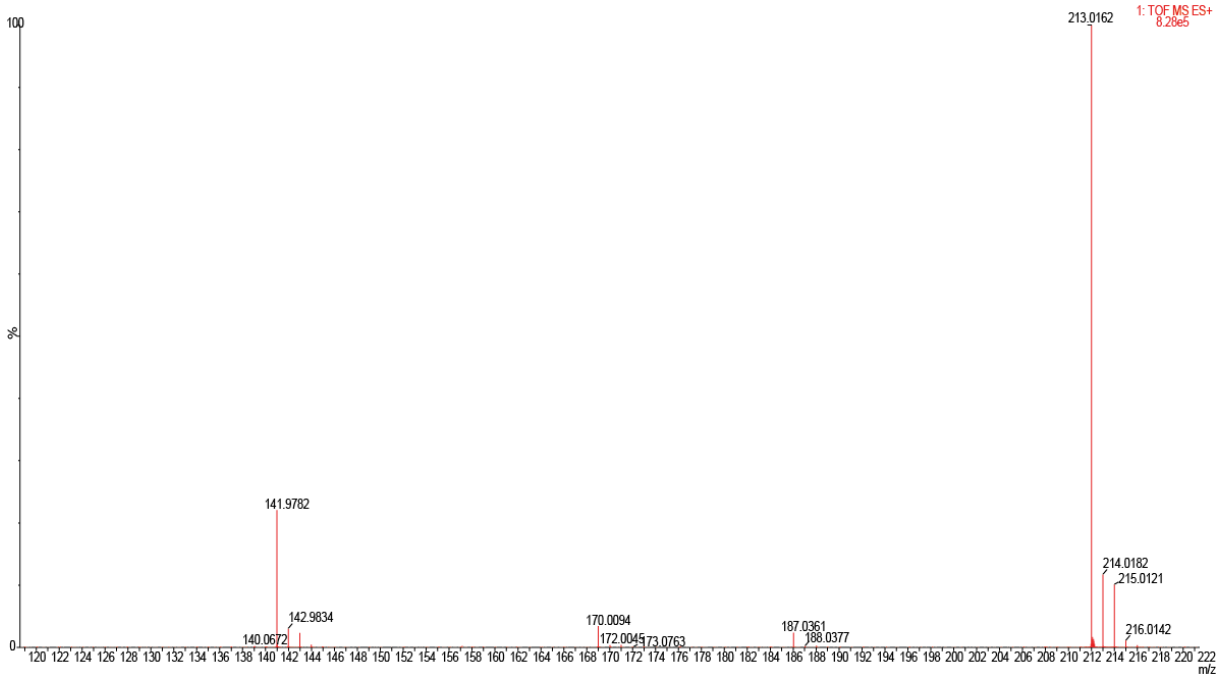

Appendix figure 11. ESI-QToF spectrum of compound **1**

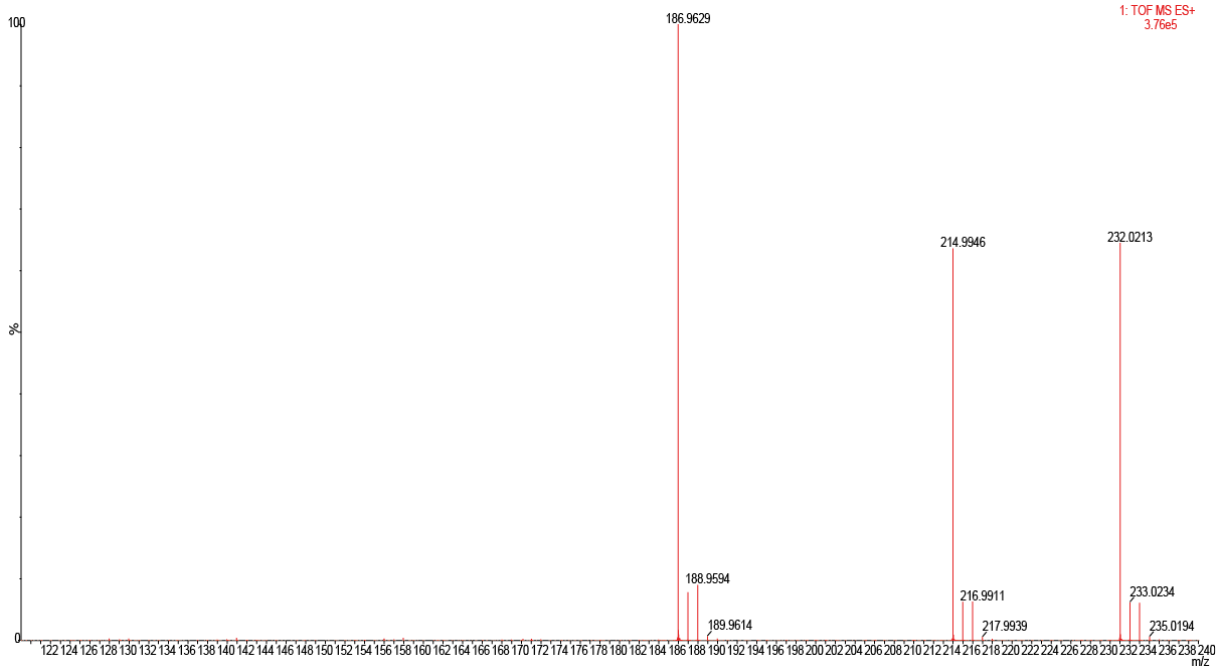

Appendix figure 12. ESI-QToF spectrum of compound **II**

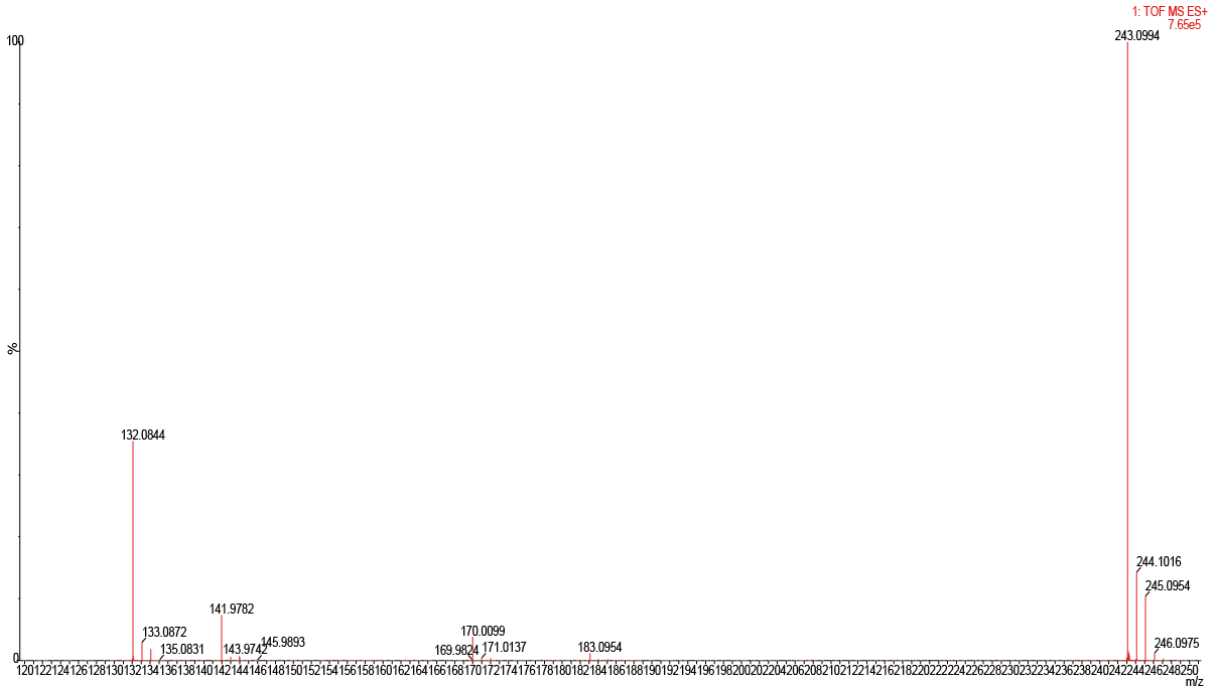

Appendix figure 13. ESI-QToF spectrum of compound **III**

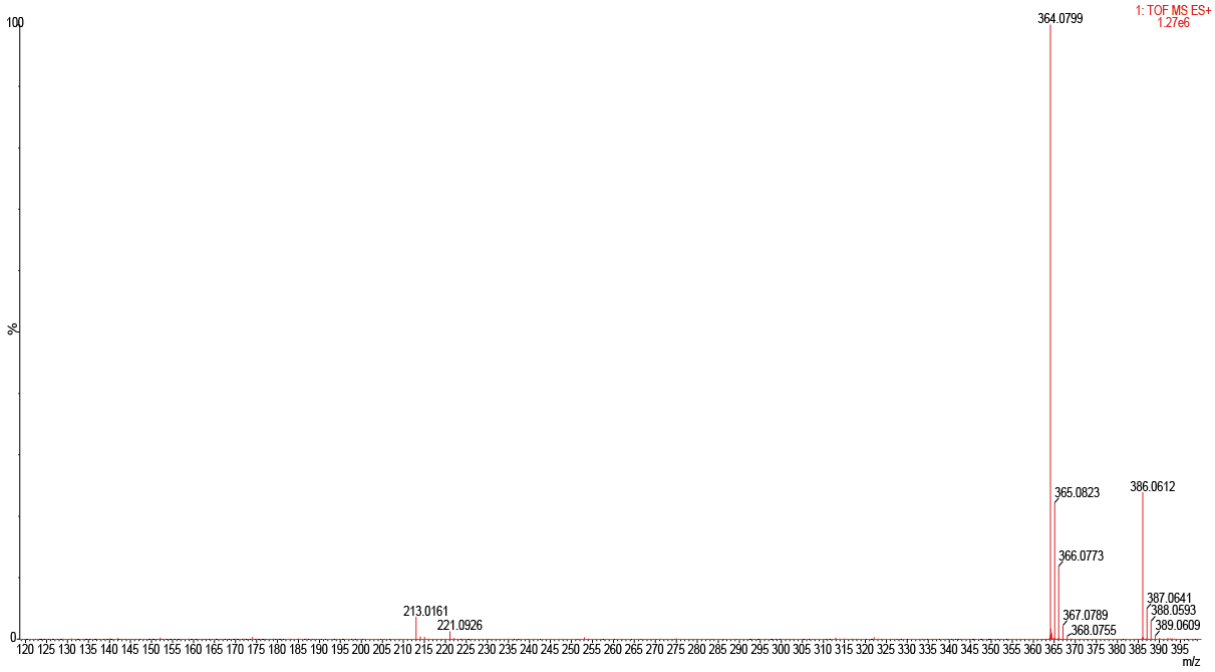

Appendix figure 14. ESI-QToF spectrum of compound **1A**

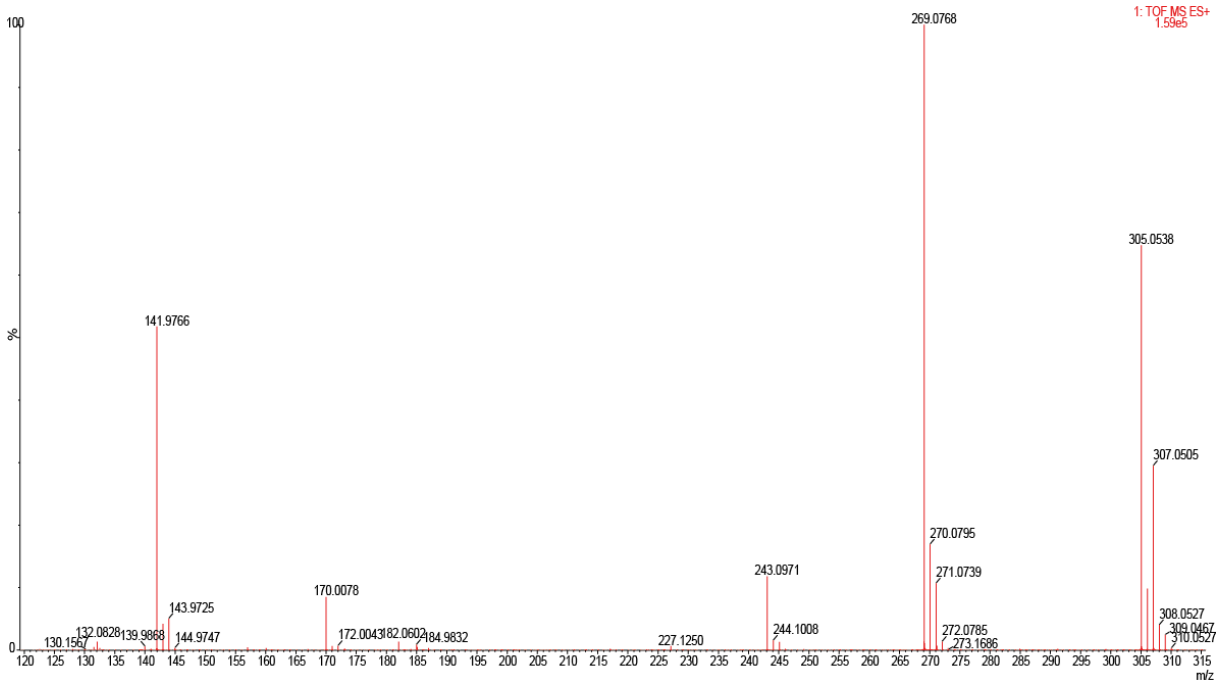

Appendix figure 15. ESI-QToF spectrum of compound **2**

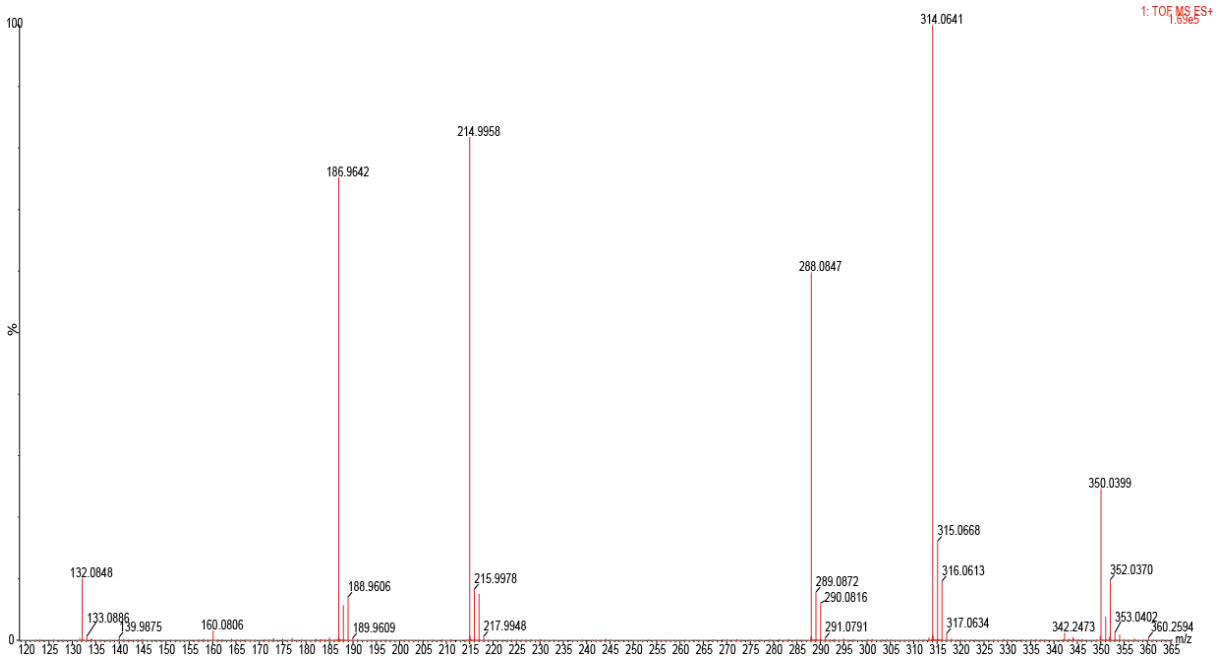

Appendix figure 16. ESI-QToF spectrum of compound **3**

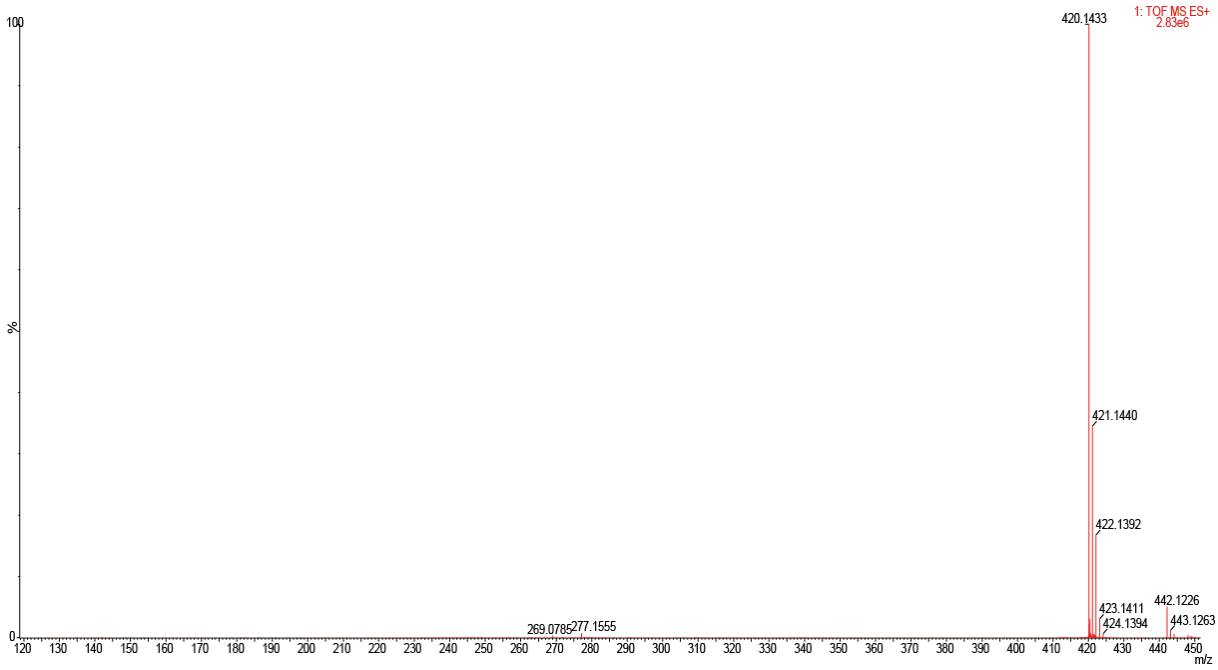

Appendix figure 17. ESI-QToF spectrum of compound **2A**

Appendix figure 18. ESI-QToF spectrum of compound **3A**

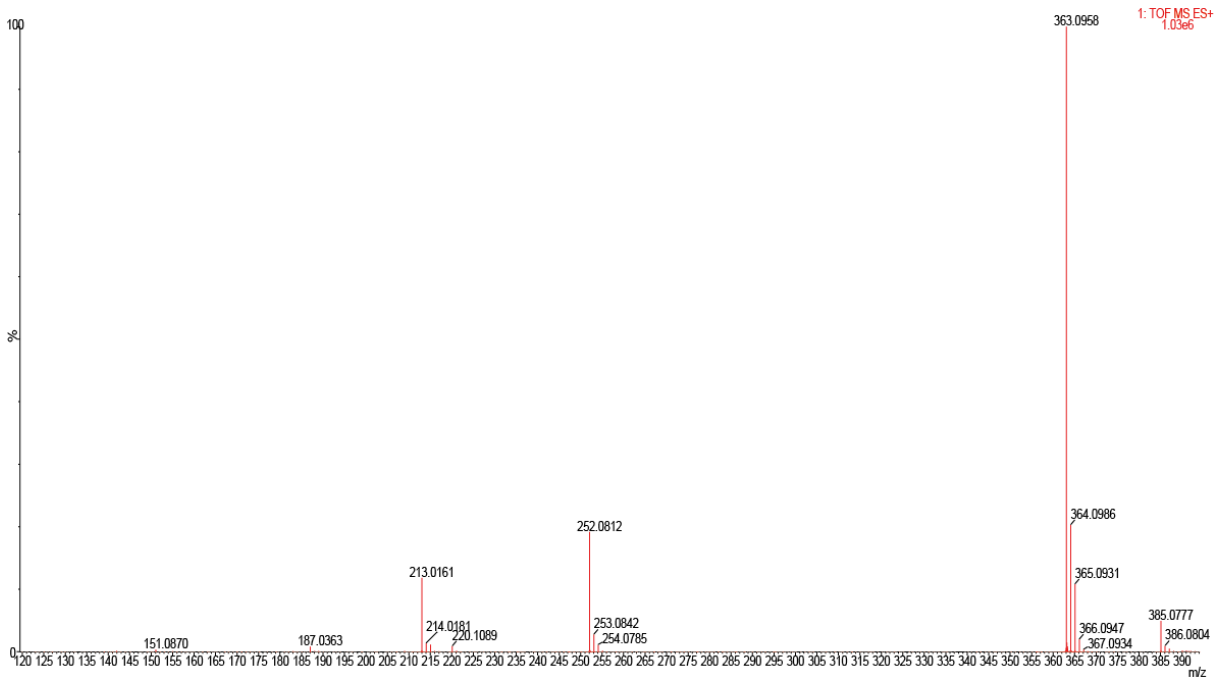

Appendix figure 19. ESI-QToF spectrum of compound **1B**

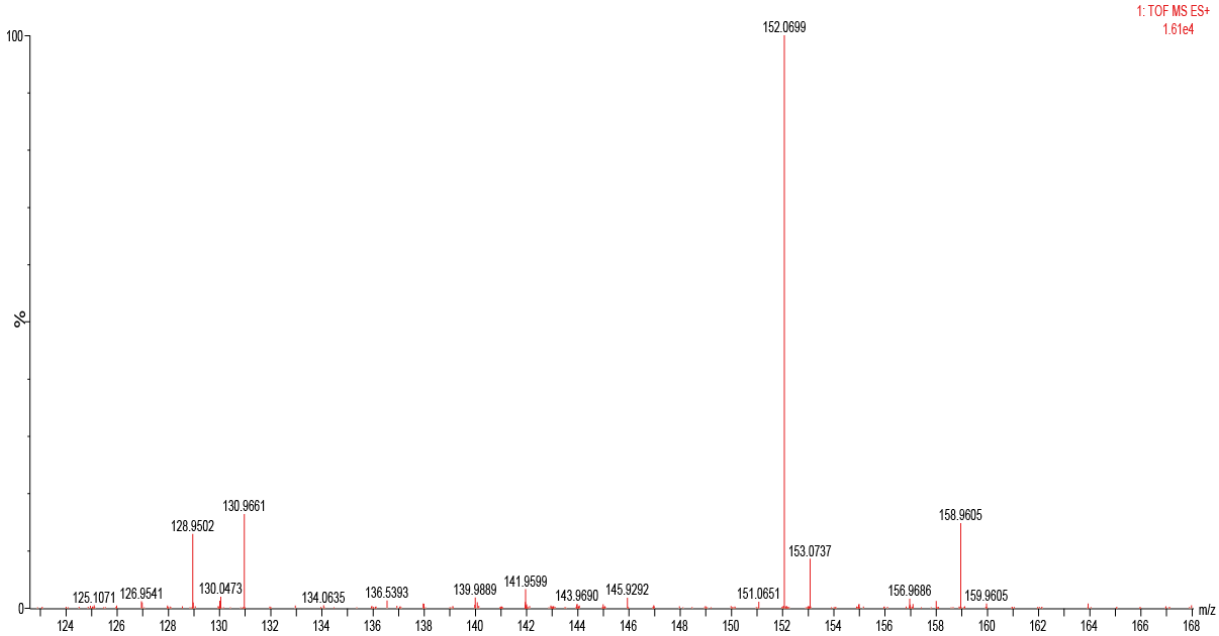

Appendix figure 20. ESI-QToF spectrum taken during kinetic analysis of **Pep-1A** showing drug release

Appendix figure 21. ESI-QToF spectrum taken during kinetic analysis of **Pep-1A** showing drug-linker compound

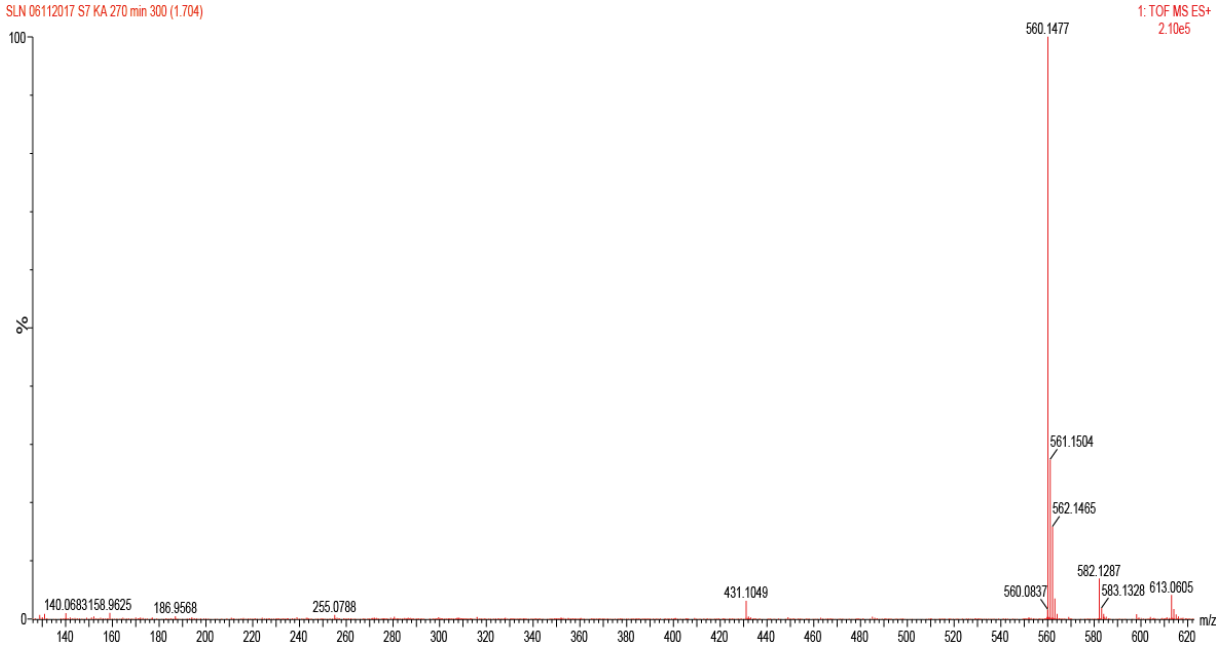

Appendix figure 22. ESI-QToF spectrum taken during kinetic analysis of **Pep-1A** showing drug-linker-glutathione compound

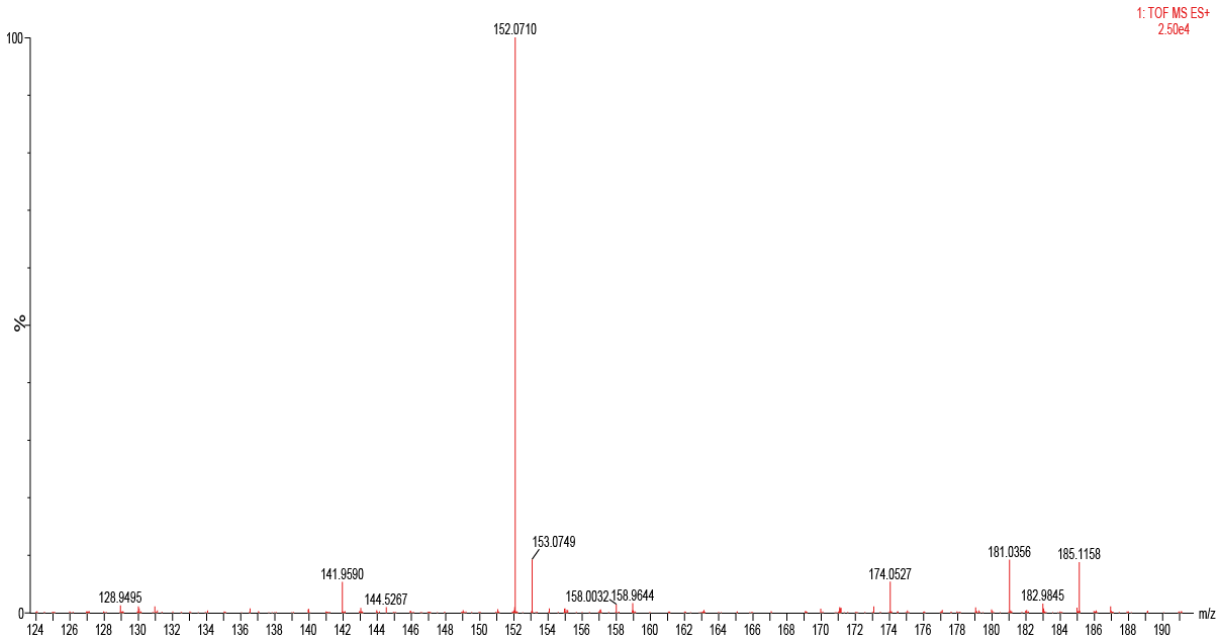

Appendix figure 23. ESI-QToF spectrum taken during kinetic analysis of **Pep-2A** showing drug release

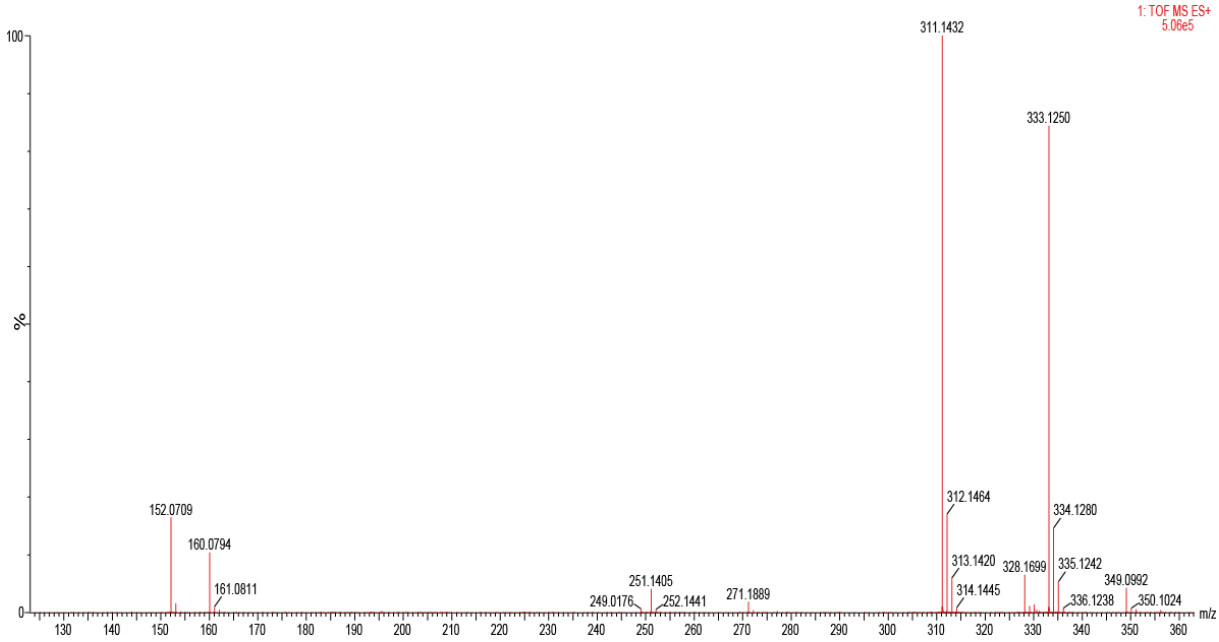

Appendix figure 24. ESI-QToF spectrum taken during kinetic analysis of **Pep-2A** showing drug-linker compound

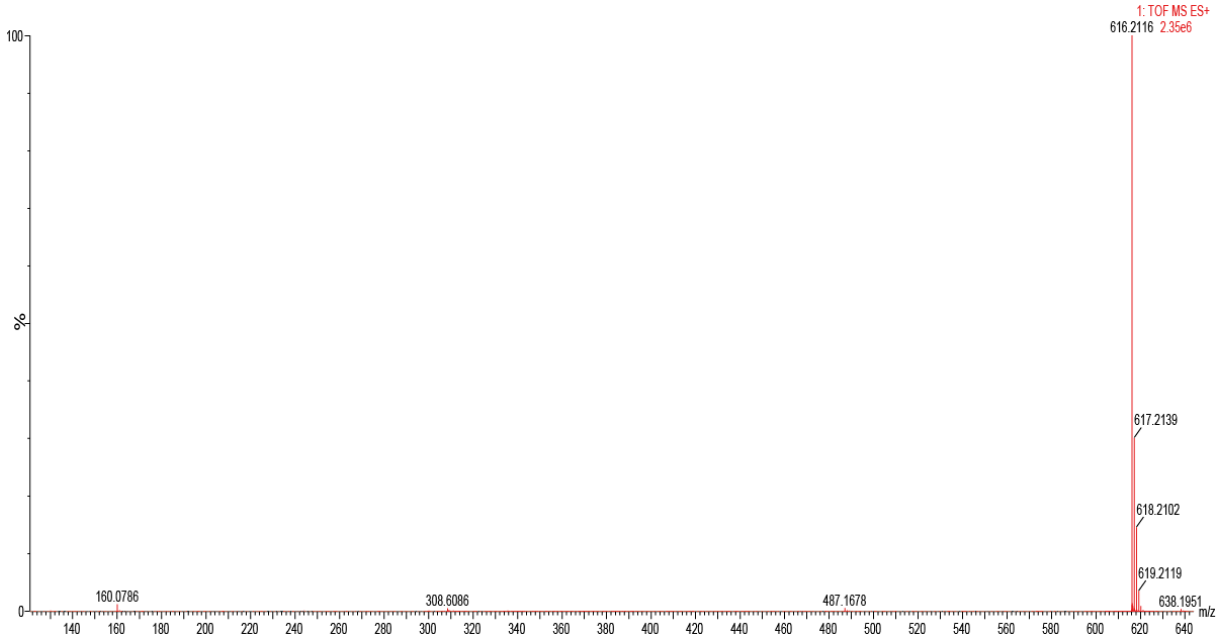

Appendix figure 25. ESI-QToF spectrum taken during kinetic analysis of **Pep-2A** showing drug-linker-glutathione compound

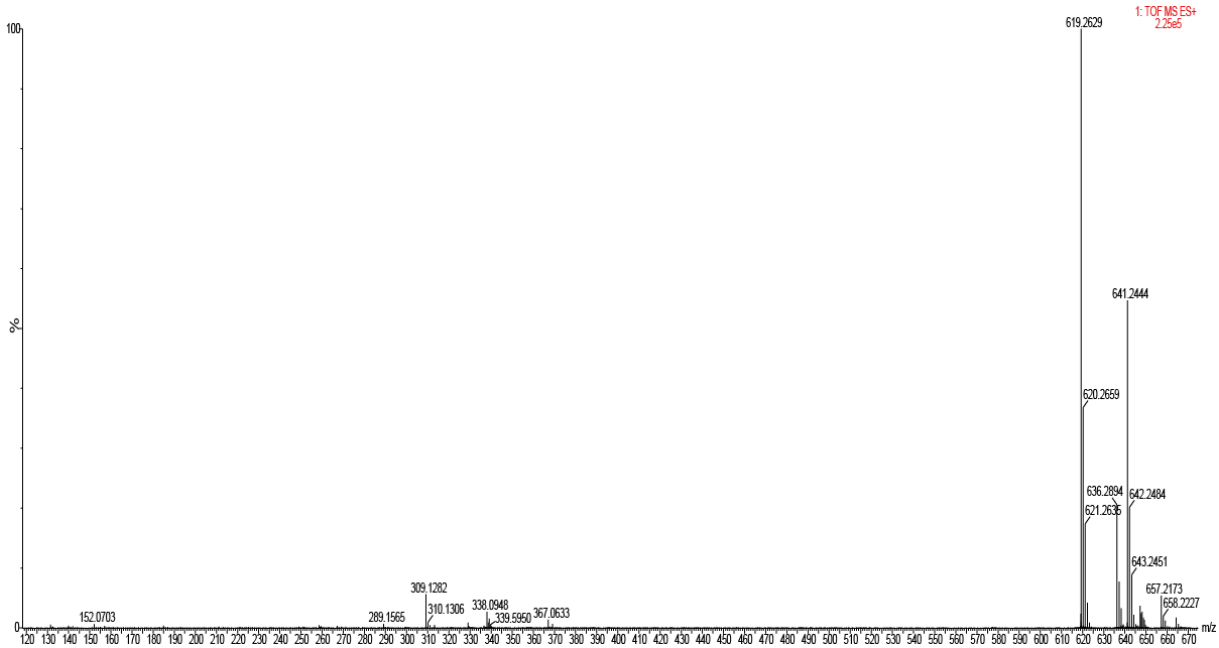

Appendix figure 26. ESI-QToF spectrum taken during kinetic analysis of **Pep-2A** showing drug-linker-linker-drug dimer

NMR spectra

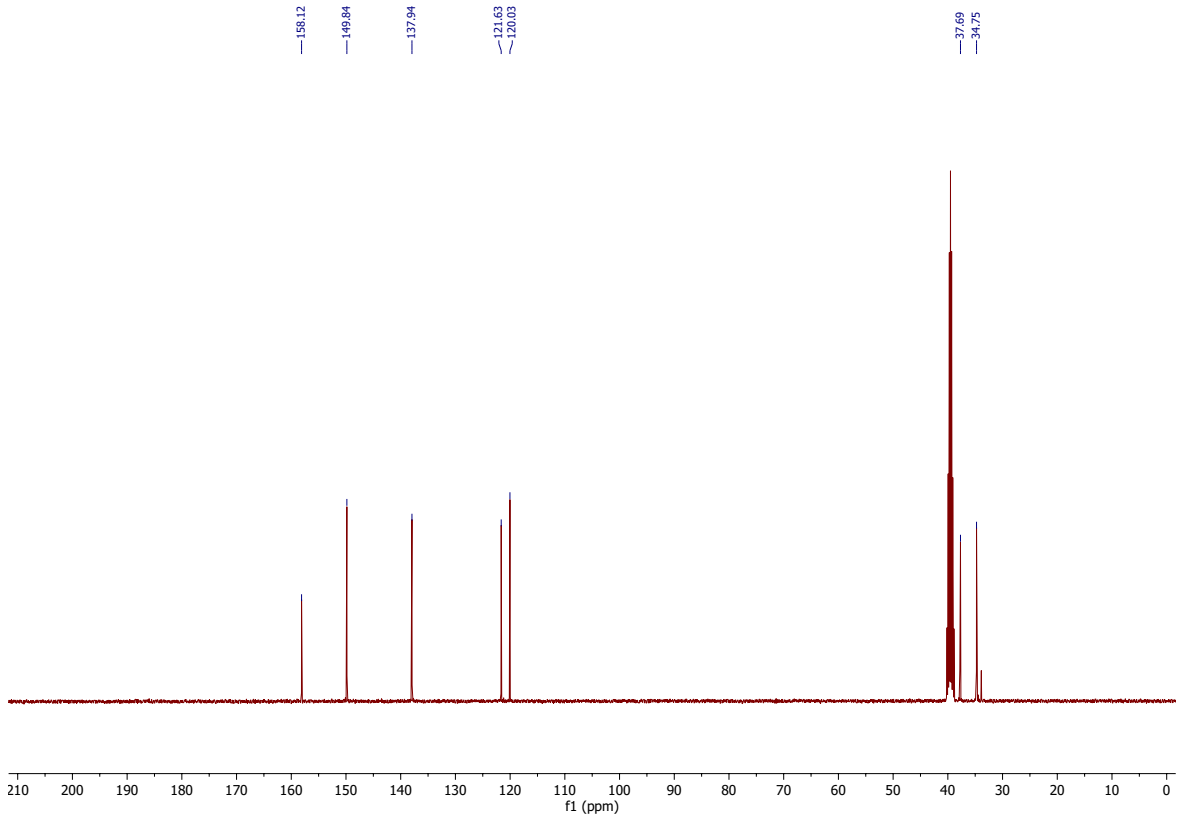

Appendix figure 27. ^{13}C NMR spectrum of compound **I**

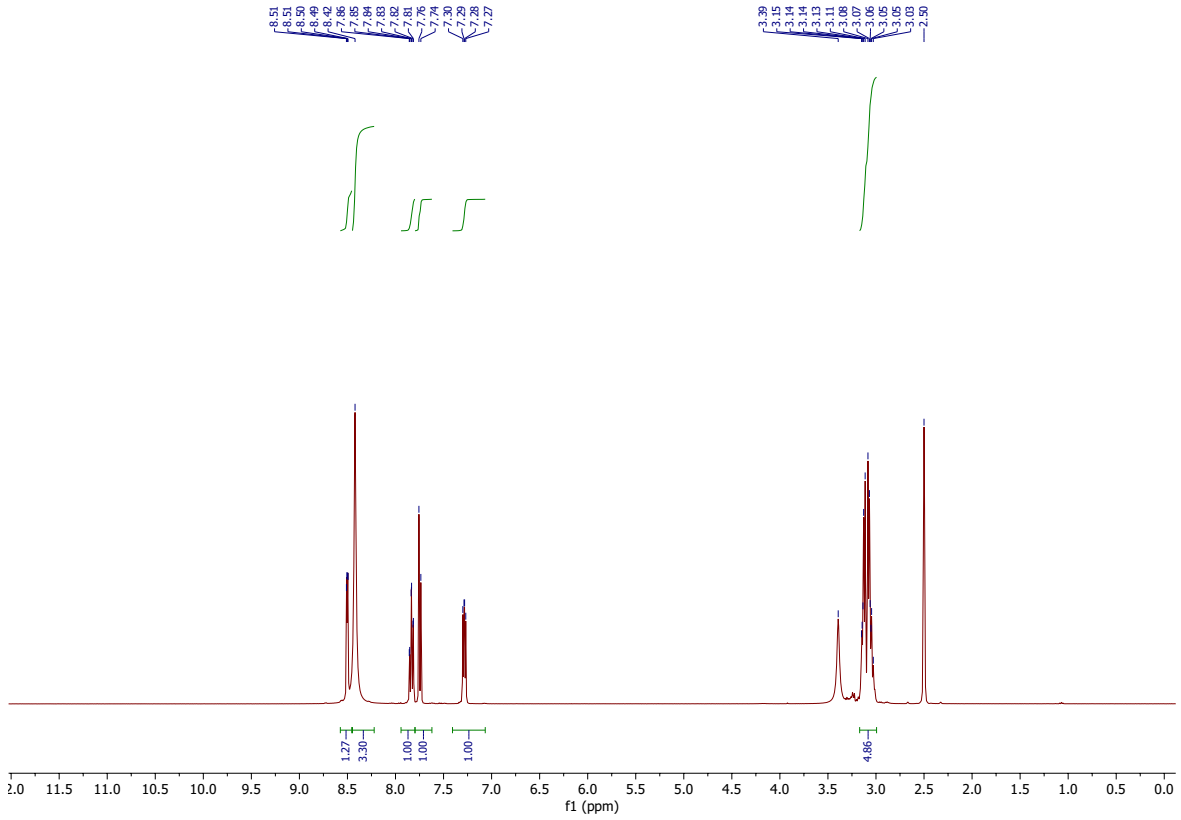

Appendix figure 28. ^{1}H NMR spectrum of compound **I**

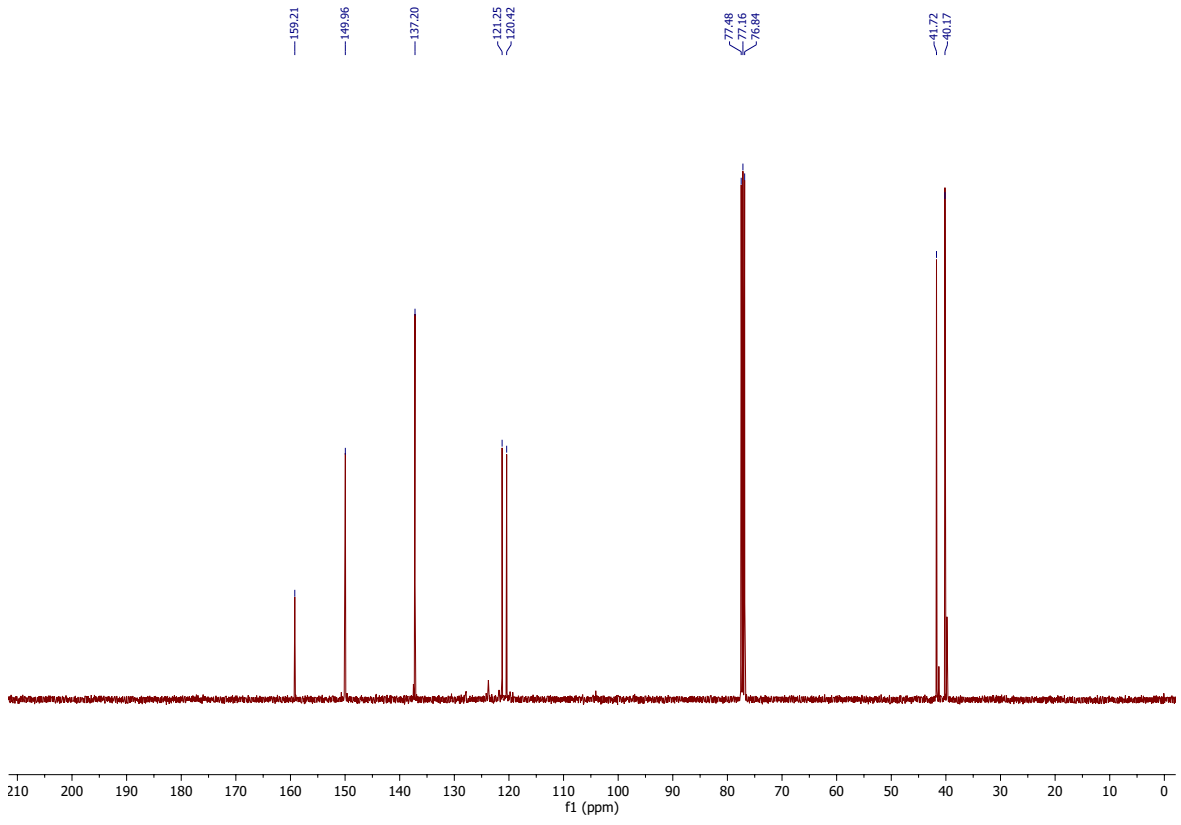

Appendix figure 29. ^{13}C NMR spectrum of compound **1**

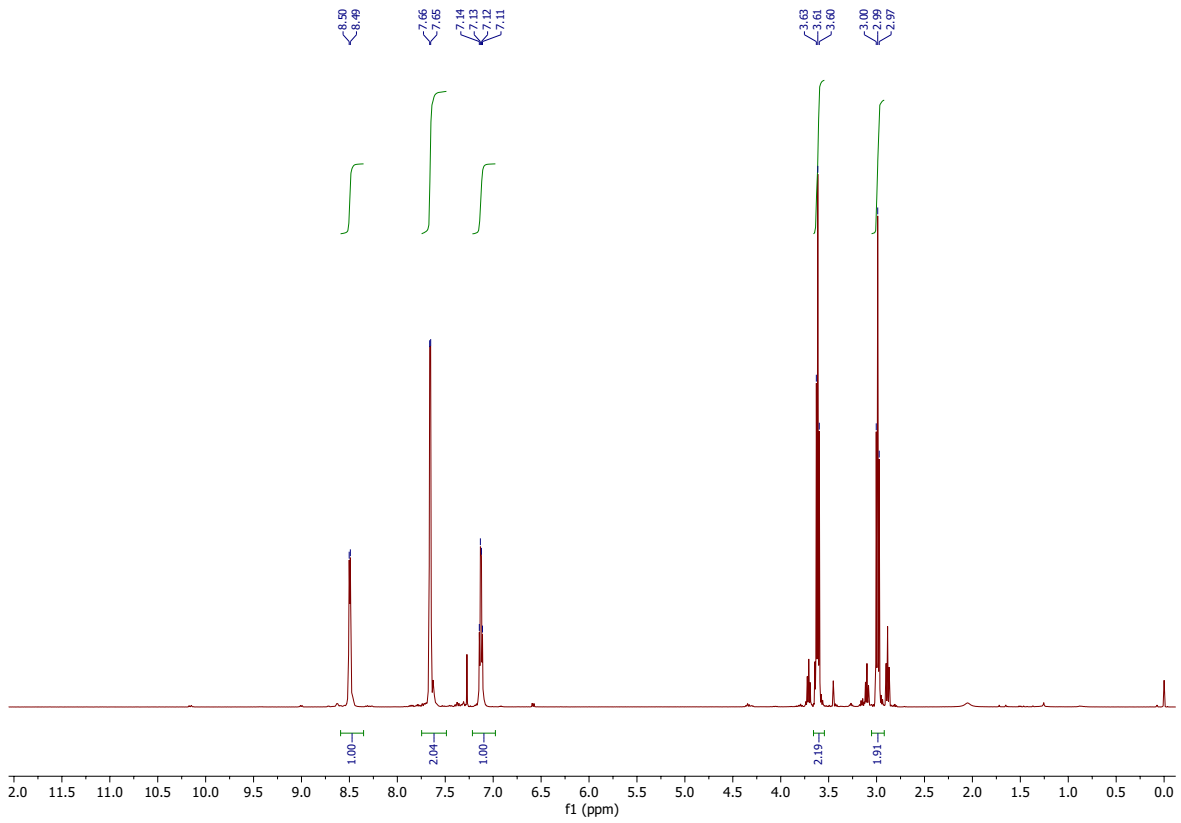

Appendix figure 30. ^{1}H NMR spectrum of compound **1**

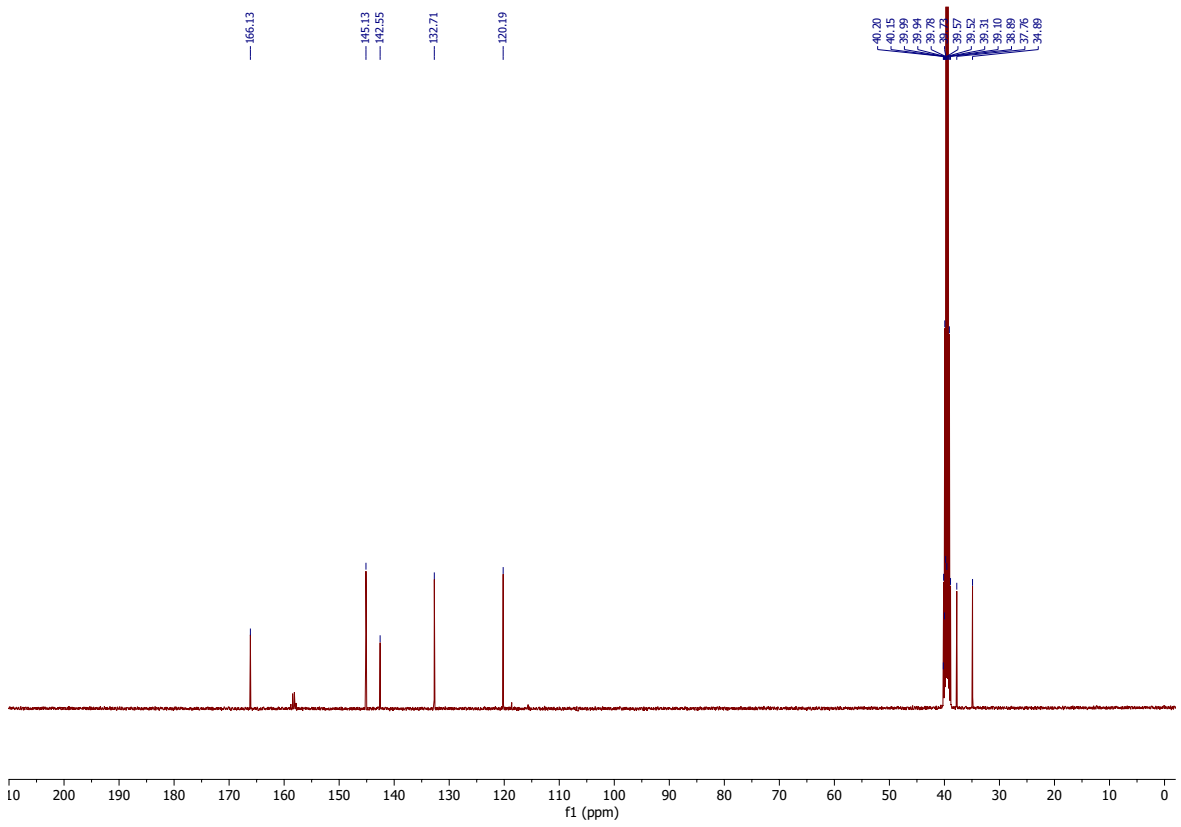

Appendix figure 31. ^{13}C NMR spectrum of compound **II**

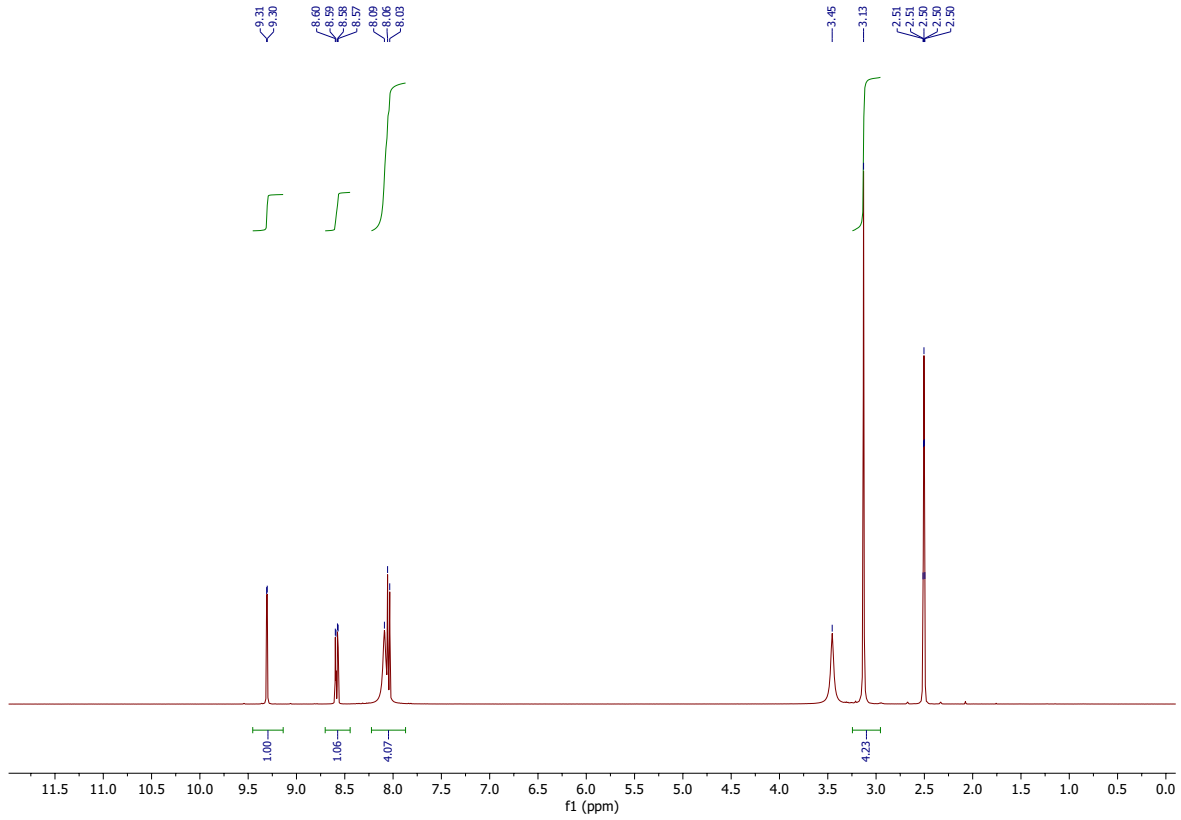

Appendix figure 32. ^{1}H NMR spectrum of compound **II**

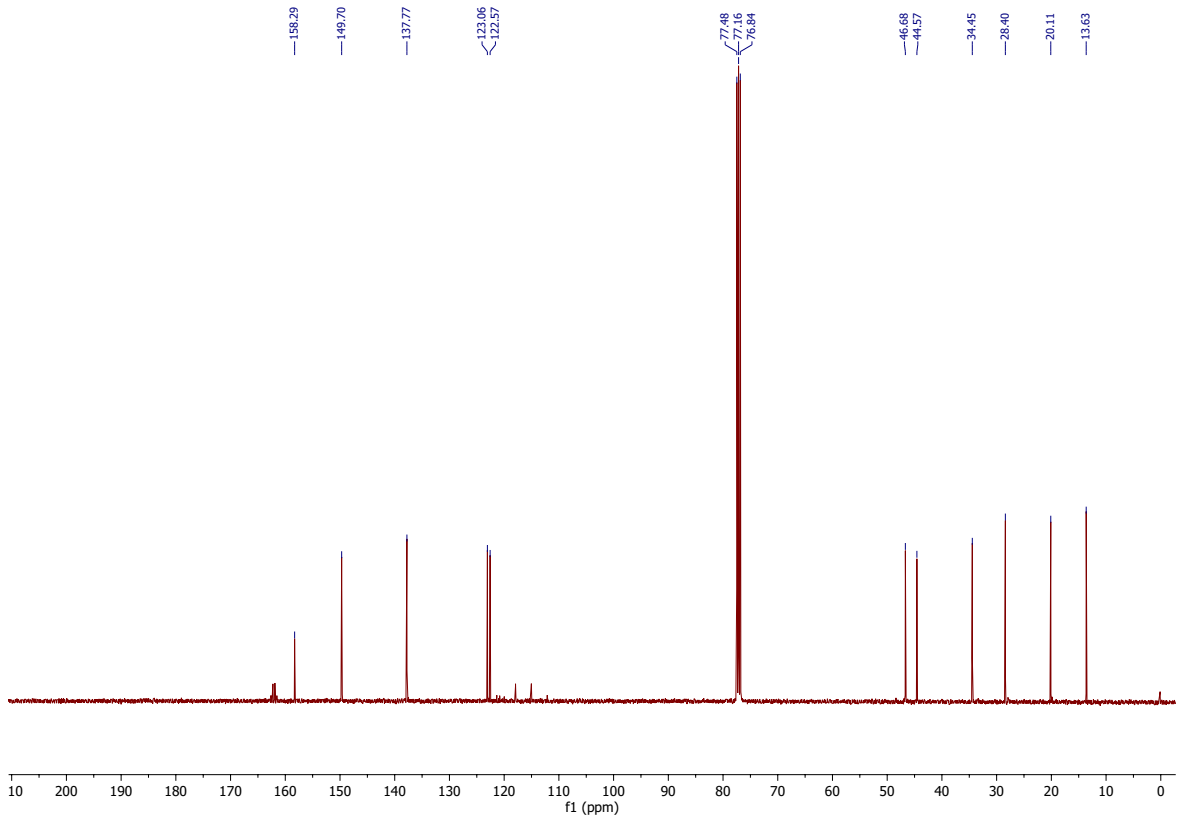

Appendix figure 33. ^{13}C NMR spectrum of compound **III**

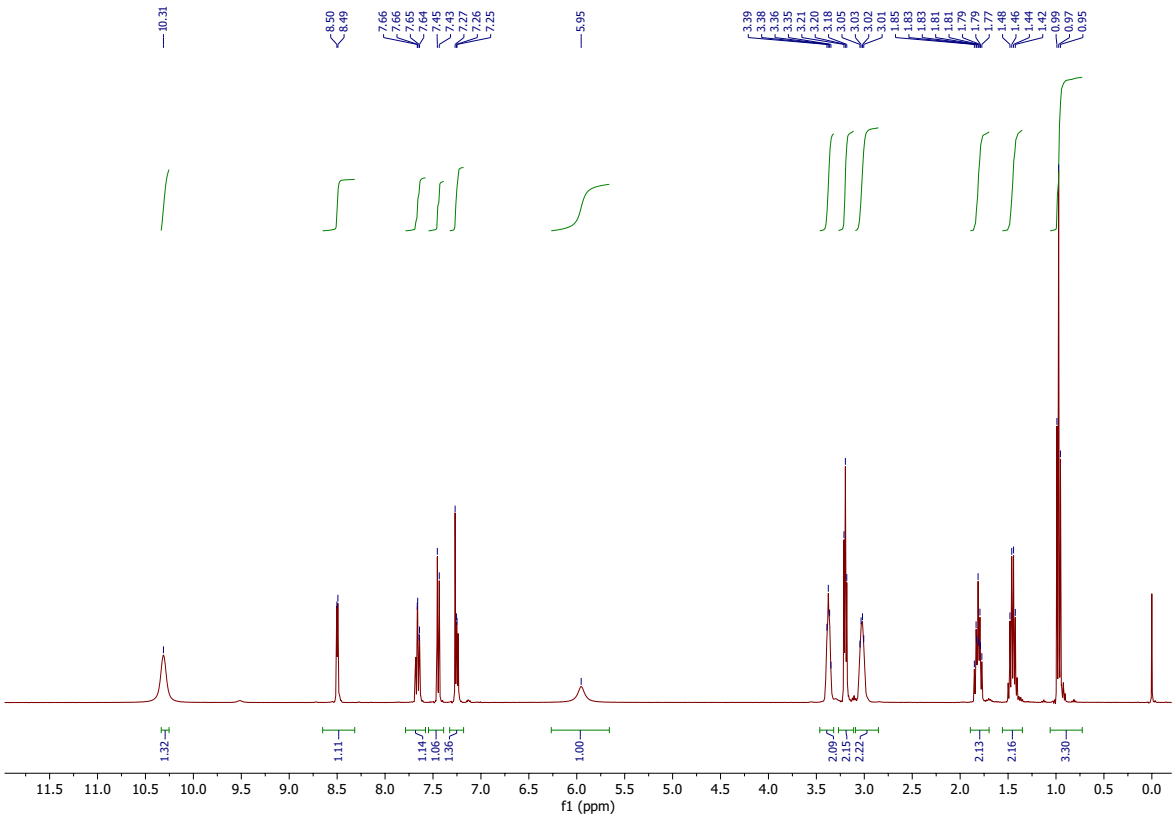

Appendix figure 34. ^{1}H NMR spectrum of compound **III**

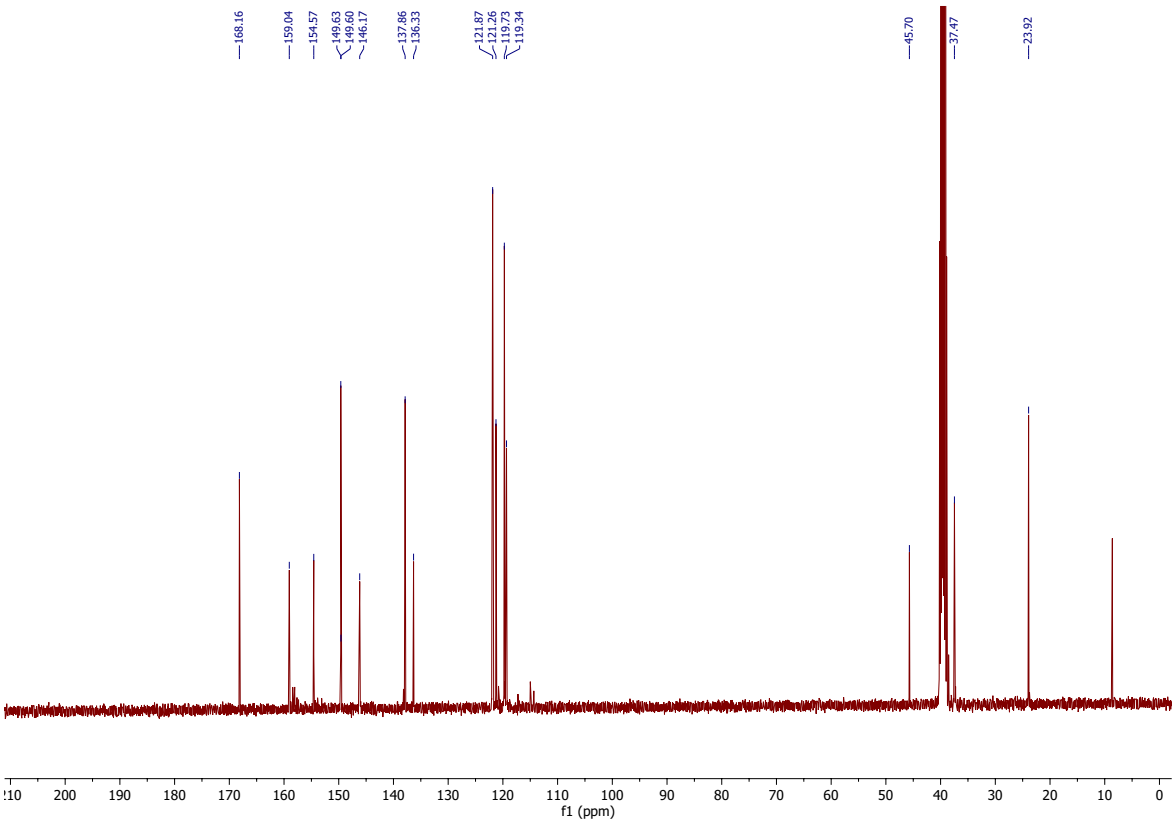

Appendix figure 35. ^{13}C NMR spectrum of compound **1A**

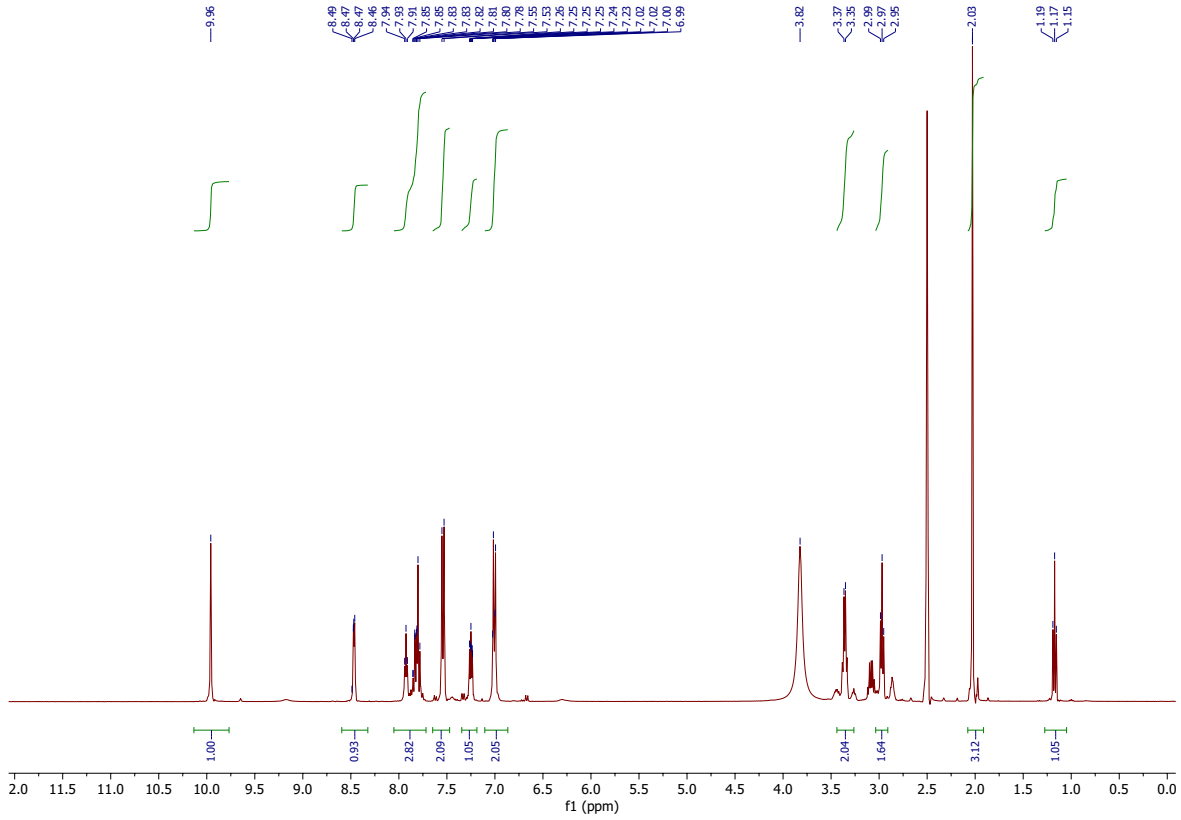

Appendix figure 36. ^{1}H NMR spectrum of compound **1A**

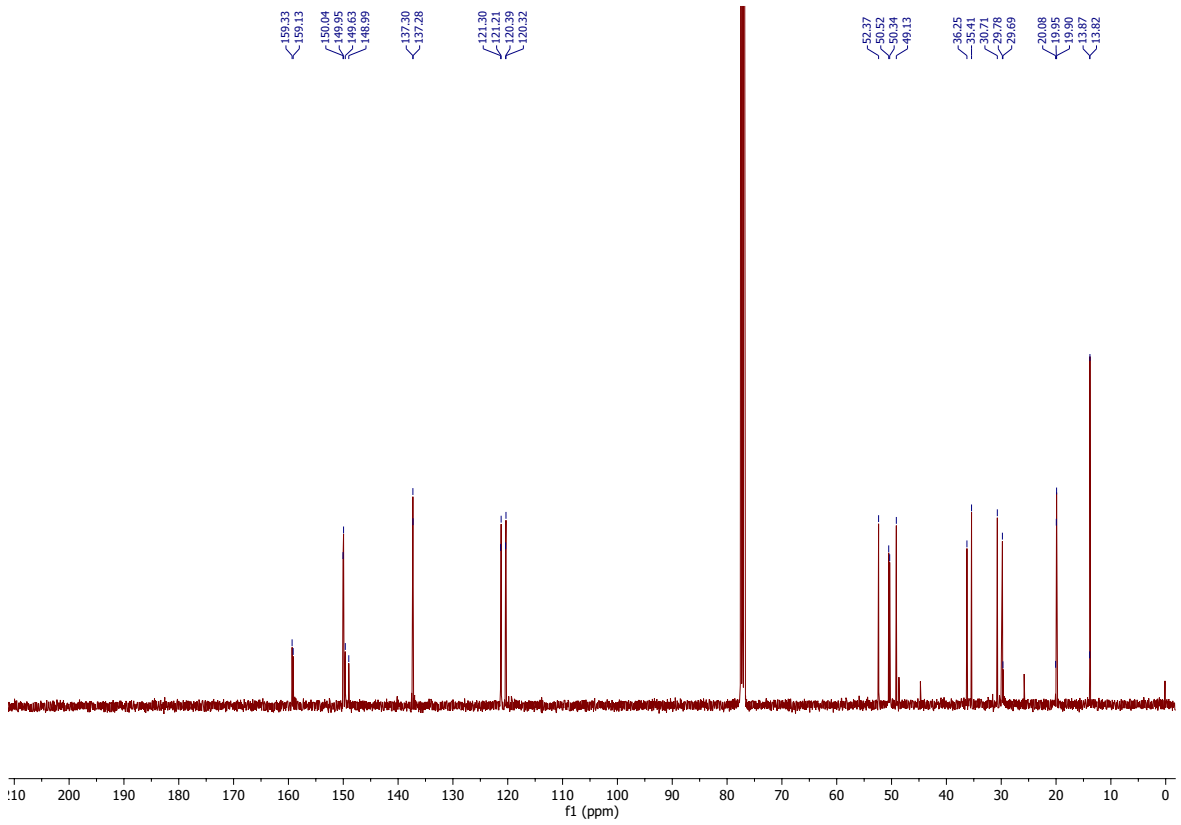

Appendix figure 37. ^{13}C NMR spectrum of compound **2**

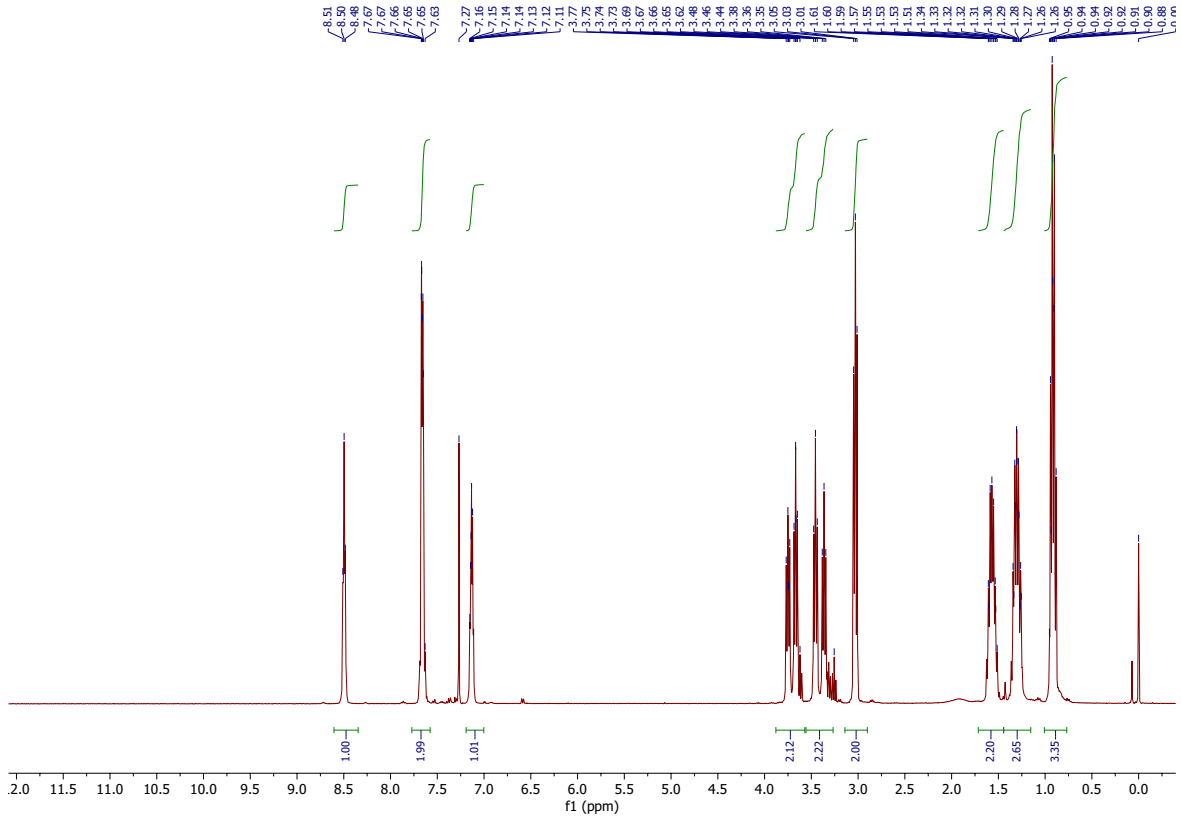

Appendix figure 38. ^{1}H NMR spectrum of compound **2**

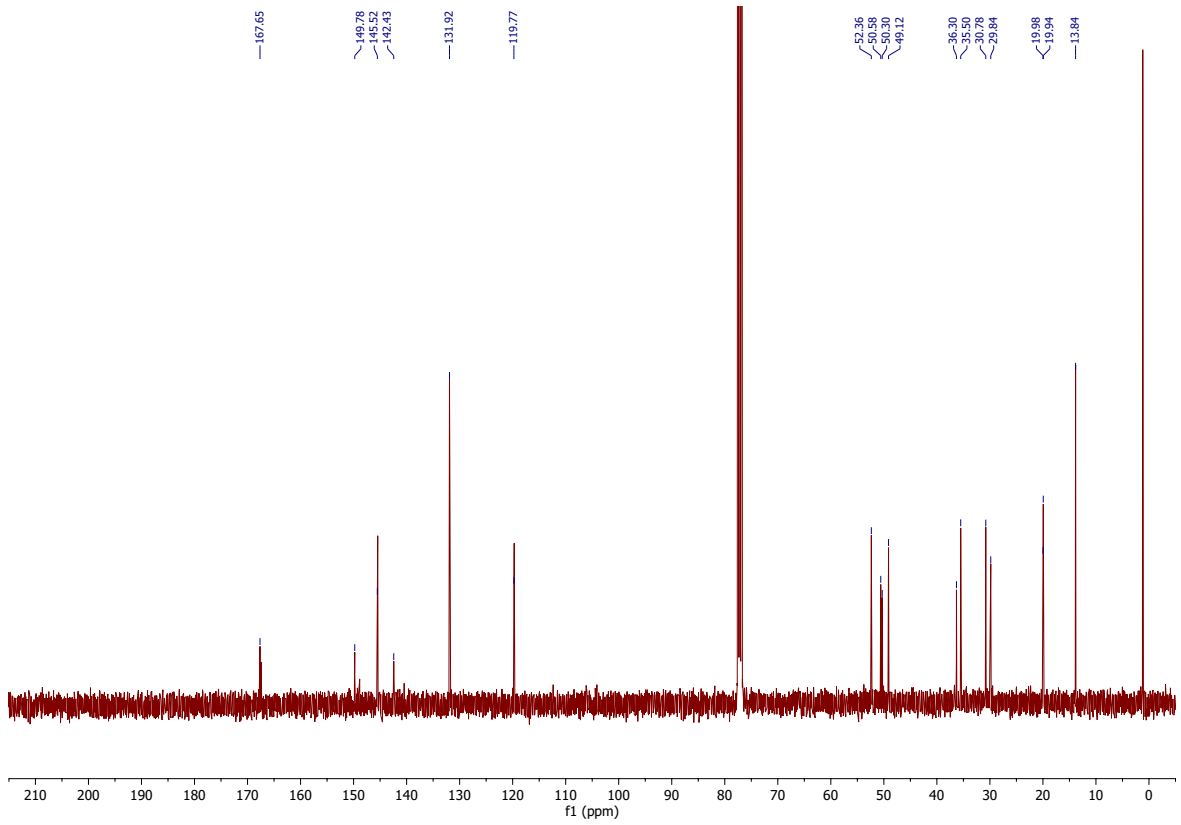

Appendix figure 39. ^{13}C NMR spectrum of compound **3**

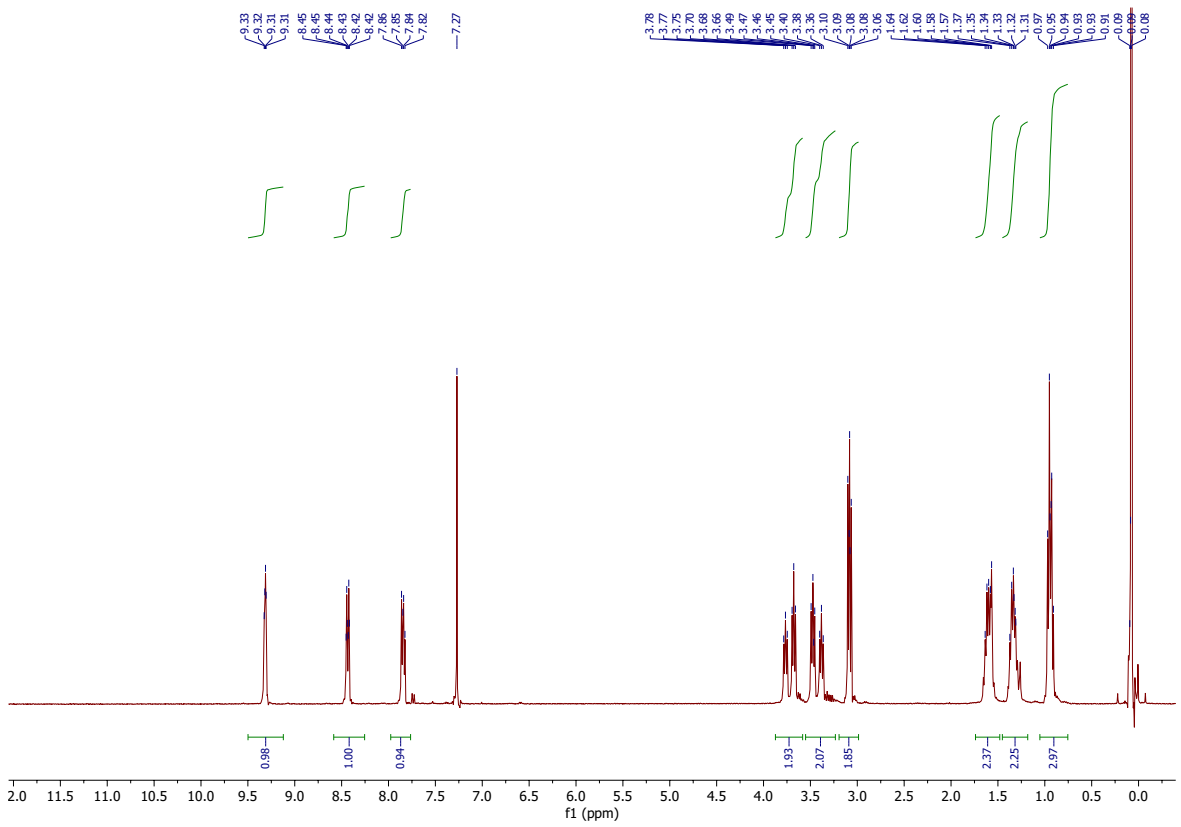

Appendix figure 40. ^{1}H NMR spectrum of compound **3**

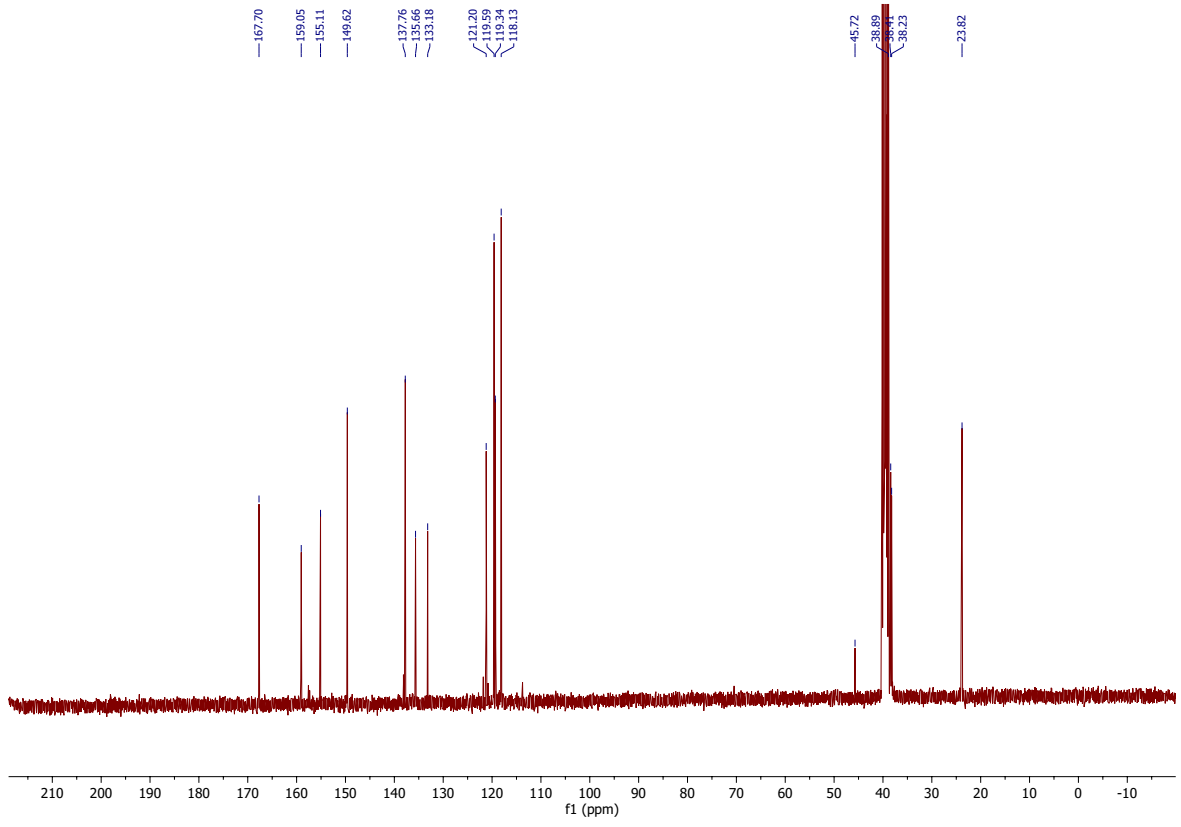

Appendix figure 41. ^{13}C NMR spectrum of compound **1B**

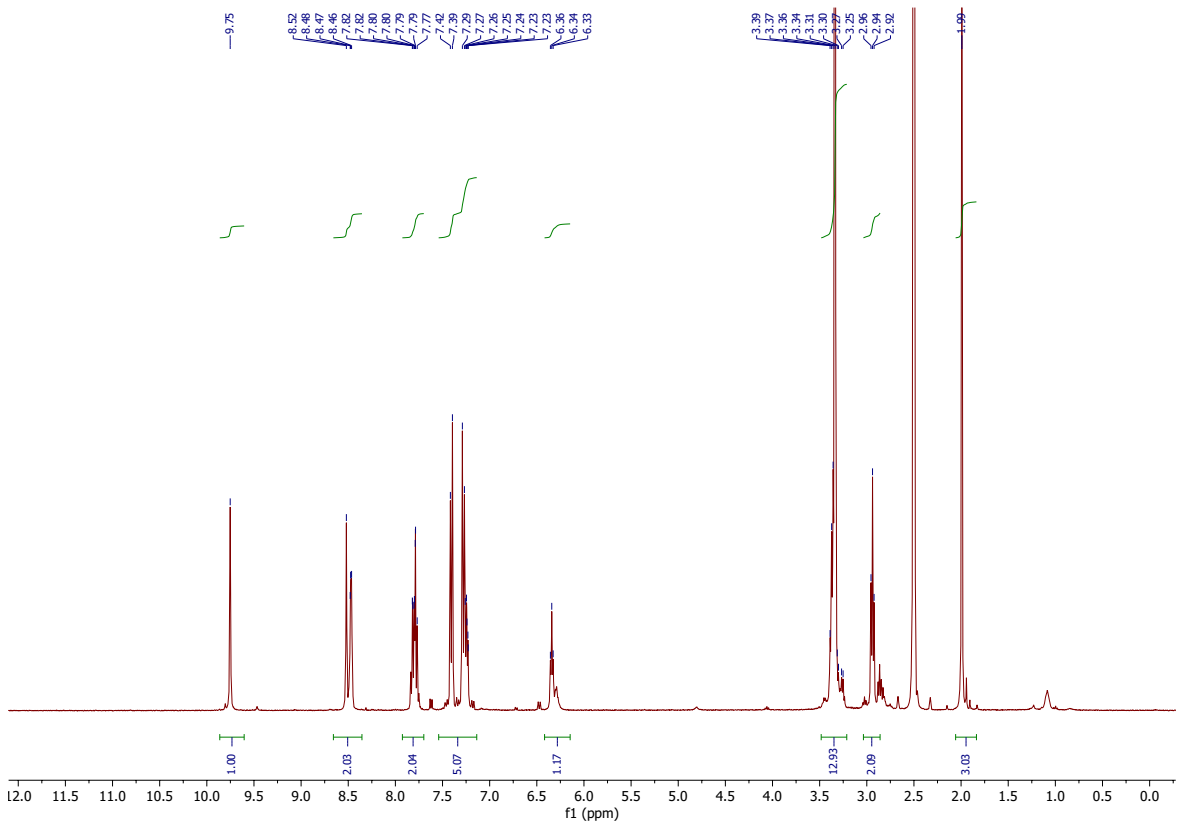

Appendix figure 42. ^{1}H NMR spectrum of compound **1B**

Primary data from kinetic analyses

Results of degradation analysis																	
Wavelength: 241 nm													Second addition of GSH/GSSG solution				
Pep-1A													(14 min)	(28 min)	(115 min)	(180 min)	(240 min)
Time (h)		0,23333333	0,46666667	0,93333333	1,5	2	3	4	7,83333333	20	27	34	44	44	45	47	48
		0,8	0,97	1,2	1,69	2,08	2,45	3,23	5,6	8,56	8,62	9,92	9,96	9,83	11,01	9,96	9,36
Drug (tr = 0.73)	%	2,58899676	3,30832196	4,18555982	5,81355349	7,13305898	8,62372404	11,0238908	19,8511166	30,8468468	32,6886614	34,6247818	33,6145798	33,5380416	37,3473541	35,1570773	35,2675207
		18,52	13,75	12,44	11,26	11,21	11,35	12,26	14,36	17,34	17,24	18,73	17,02	16,04	15,34	15,43	14,78
Drug-linker-glutation (tr = 2.77)	%	59,9352751	46,8963165	43,3903035	38,7340901	38,4430727	39,9507216	41,8430034	50,9039348	62,4864865	65,3773227	65,3752182	57,441782	54,7253497	52,0352782	54,4652312	55,6895252
		11,58	14,6	15,03	16,12	15,87	14,61	13,81	8,25	1,85	0,51	0	2,65	3,44	3,13	2,94	2,4
Drug-linker (tr = 3.06)	%	37,4757282	49,7953615	52,4241367	55,4523564	54,4238683	51,4255544	47,1331058	29,2449486	6,66666667	1,93401593	0	8,9436382	11,7366087	10,6173677	10,3776915	9,04295403
		30,9	29,32	28,67	29,07	29,16	28,41	29,3	28,21	27,75	26,37	28,65	29,63	29,31	29,48	28,33	26,54
Total	%	100	100	100	100	100	100	100	100	100	100	100	100	100	100	100	100

Appendix figure 43. Primary data from kinetic analysis with **Pep-1A** and GSH

Results of degradation analysis														
Wavelength: 241 nm								Second addition of GSH/GSSG solution						
Pep-2A								(14 min)	(56 min)	(175 min)	(220 min)	(27 h)	(53.5 h)	(117 h)
Time (h)		0,23333333	0,7	1,5	3,66666667	9,5	22,5	25	26	27,5	28,5	52	76	141
		0	0,51	0,94	3,01	4,35	5,02	6,17	6,48	7,57	8,43	8,67	8,89	10,06
Drug (tr = 0.93)	%	0	0,33799457	0,94	3,01	4,35	5,09696416	6,17	6,48	7,73633112	8,62051334	8,88866106	9,31085044	11,7468473
		36,62	56,59	58,81	65,09	71,47	77,57	63,22	58,23	58,65	59,8	63,12	68,71	75,58
Drug-linker-glutation (tr = 6.31)	%	77,6505513	37,5041421	58,81	65,09	71,47	78,7592649	63,22	58,23	59,9386817	61,151447	64,7119131	71,9627147	88,2531527
		10,54	93,79	40,25	31,9	24,18	15,9	30,61	35,29	31,63	29,56	25,75	17,88	0
Drug-linker (tr = 8.34)	%	22,3494487	62,1578633	40,25	31,9	24,18	16,1437709	30,61	35,29	32,3249872	30,2280397	26,3994259	18,7264349	0
		47,16	150,89	100,00	100,00	100,00	98,49	100,00	100,00	97,85	97,79	97,54	95,48	85,64
Total	%	100	100	100	100	100	100	100	100	100	100	100	100	100

Appendix figure 44. Primary data from kinetic analysis with **Pep-2A** and GSH